



## DIPLOMARBEIT

### Evaluation of Admittance Spectra of Resonant Piezoelectric Crystals

Ausgeführt am Institut für

Allgemeine Physik

der Technischen Universität Wien

unter der Anleitung von Ao.Univ.Prof. Dipl.-Ing. Dr.techn. Martin Gröschl und Dipl.-Ing. Dr. Reinhard Schnitzer als verantwortlich mitwirkendem Universitätsassistenten

durch

Thomas Kliche

Griesgasse 30-32/7  
2340 Mödling

6.10.2008

# Contents

Summary .....	1
Zusammenfassung .....	2
1 Introduction .....	4
2 Theory of resonance measurement .....	5
2.1 Admittance .....	5
2.2 Resonances of RPC .....	7
2.3 Resonance evaluation .....	9
3 Measurement system .....	10
3.1 Hardware .....	10
3.1.1 Computer system .....	11
3.1.2 Kernel electronics .....	17
3.1.3 Sensors .....	18
3.2 Signal processing .....	22
4 Resonance measurement .....	26
4.1 Signal transformation .....	26
4.1.1 Admittance calculation .....	27
4.1.2 Resonance evaluation .....	28
4.2 Measurement quality .....	30
4.2.1 Scan modes .....	30
4.2.2 DC offset compensation .....	33
4.2.3 Baseline compensation .....	35
4.2.4 Transient phenomena consideration .....	36
4.2.5 Signal-to-noise-ratio consideration .....	38
4.3 Measurement process description .....	40
4.3.1 Self organizing module .....	41
4.3.2 Initialization .....	42

4.3.3	Frequency scan .....	47
4.3.4	Applying the baseline compensation .....	55
4.3.5	Resonance evaluation .....	55
4.3.6	Display and save data .....	56
4.4	Software user interface .....	58
4.4.1	Program control .....	59
4.4.2	Scan parameters .....	60
4.4.3	System parameters .....	61
4.4.4	Kernel electronics parameters.....	61
4.4.5	Measurement quality parameters .....	62
4.4.6	File parameters.....	62
4.4.7	Baseline compensation parameters.....	63
4.4.8	Results.....	63
4.4.9	Error messages.....	64
4.5	Measurement results .....	64
4.5.1	QV sensor at 55 kHz.....	66
4.5.2	QV sensor at 2.7 MHz .....	70
4.5.3	QV sensor at 6 MHz .....	75
4.5.4	Standard quartz at 15 MHz.....	77
4.5.5	QT sensor at 29 MHz.....	78
5	Measurement applications .....	80
5.1	Peak Tracking Measurement(PTM).....	81
5.1.1	Auto Ranging Procedure (ARP) .....	85
5.1.2	Optimized Peak Search (OPS).....	87
5.2	Automatic system configuration.....	93
5.3	Temperature measurement with QT sensors .....	94
5.3.1	Configuration data .....	94
5.3.2	Measurement process.....	96
5.3.3	Software user interface .....	98

5.3.4	Measurement results .....	100
5.4	Viscosity measurement with QV sensors .....	100
5.4.1	Calibration .....	101
5.4.2	Configuration data .....	115
5.4.3	Measurement process.....	116
5.4.4	Software user interface .....	120
5.4.5	Measurement results .....	121
	List of figures .....	124
	List of tables.....	129
	List of references.....	130
	Curriculum vitae .....	132

# Summary

The aim of this diploma thesis is the development of evaluation processes for the *QxSens* measurement system developed within the GROWTH shared cost RTD funding scheme of the European Commission, project *QxSens* No. GRD1-2001-41816. The *QxSens* measurement system is a multi-purpose, multi-channel measurement system for RPC (Resonant Piezoelectric Crystals) based sensors.

In the second chapter a theoretical explanation of the admittance and its evaluation is given. The evaluation of the locus of admittance of RPC leads to the series resonance frequency and the quality factor. These values are used in further steps to calculate the desired measurement value.

There are three versions of the *QxSens* measurement system, the standard PC, the PXI and the external USB version. All versions contain kernel electronics, interface electronics and a DAQ device. The RPC based sensor is connected to the kernel electronics. The *QxSens* measurement system hardware is described in chapter three. At the end of chapter three a detailed description of the signal processing from the sensor to the digital value in the computer system is given.

In chapter 4 the resonance measurement process is described. Any *QxSens* measurement application is based on this resonance measurement. The admittance spectrum is calculated out of the digitized measured voltage signals. Accordingly, the series resonance frequency and the quality factor result from the evaluation of the locus of admittance. The second part of this chapter explains which parameters influence the measurement quality and how these parameters have to be set to improve measurement quality. Then the measurement process and the software interface, that implements this process, are shown. At the end of chapter 4 the measurement results obtained with the *QxSens* system are compared to the measurement results achieved with a commercial network/spectrum/impedance analyzer from Agilent Technologies (Agilent 4395A).

The temperature measurement and the viscosity measurement are documented in chapter 5. In both cases the desired measurement value is calculated out of the measured series resonance frequency. In order to enable continues measurement it is necessary to be able to track a resonance peak. Therefore the Peak Tracking Algorithm has been developed. The automatic *QxSens* system configuration enables the simple usage of the *QxSens* measurement system in experimental and industrial processes. The measurement process, the software interface and exemplary measurement results are given for both measurement applications.

# Zusammenfassung

Das Ziel dieser Diplomarbeit ist die Entwicklung von Auswertungsmethoden für das *QxSens* Messsystem. Dieses Messsystem wurde im *QxSens* Projekt (Nr. GRD1-2001-41816) im Rahmen des GROWTH shared cost RTD funding scheme der EU entwickelt. Es ist ein Mehrzweck- und Mehrkanalmesssystem für Ultraschall-Quarz-Sensoren.

Im zweiten Kapitel werden die Admittanz des Sensors und die Auswertung der Admittanzspektren theoretisch beschrieben. Die Auswertung der Ortskurve der Admittanz liefert die Serienresonanzfrequenz und den Gütefaktor. Aus diesen beiden Werten werden im Weiteren die gewünschten Messwerte berechnet.

Kapitel drei dokumentiert die Hardware-Komponenten des *QxSens* Messsystems. Es gibt drei unterschiedliche Versionen, die Standard PC Version, die PXI Version und die externe USB Version. Alle drei Versionen bestehen aus einer externen Kernel Elektronik, an die der Quarz-Sensor angeschlossen wird. Zwei in den Computer eingebaute Karten, die Interface Elektronik und der Analog-Digital-Wandler, bereiten die Messsignale für die softwaremäßige Verarbeitung auf. Am Ende des dritten Kapitels wird der gesamte Signaltransfer im Messsystem dargestellt.

Der Ablauf der Resonanzmessung wird im 4. Kapitel beschrieben. Die Resonanzmessung ist die Grundlage für jede *QxSens* Messanwendung. Das Admittanzspektrum wird aus den gemessenen, digitalisierten Spannungssignalen berechnet. Die Auswertung des Admittanzkreises liefert dann die Serienresonanzfrequenz und den Gütefaktor. Im zweiten Teil des Kapitels werden jene Parameter diskutiert, die die Messqualität beeinflussen. Zu jedem Parameter wird erklärt, wie dieser einzustellen ist um die Messqualität zu optimieren. Die folgenden Teile beinhalten eine Beschreibung des Messprozesses sowie des Software Interface. Am Schluss des Kapitels werden Messergebnisse des *QxSens* Messsystems mit Messergebnissen des kommerziellen Netzwerk-/Spektrum-/Impedanz-Analysators 4395A von Agilent Technologies verglichen.

Im 5. Kapitel werden die Temperaturmessung und die Viskositätsmessung beschrieben. In beiden Messanwendungen wird der gewünschte Messwert aus der gemessenen Serienresonanzfrequenz berechnet. Um kontinuierliche Messungen zu ermöglichen wurde eine Methode zur gleitenden Verfolgung eines Resonanzpeaks entwickelt. Das automatische Konfigurationssystem des *QxSens* Messsystems ermöglicht die einfache Anwendung dieses Messsystems im Labor sowie in Industrieprozessen. Die Beschreibung der Messprozesse, des Software Interface sowie beispielhafte Messergebnisse vervollständigen das Kapitel.

# 1 Introduction

Piezoelectric resonators have been used in technical applications since the beginning of the 20<sup>th</sup> century. The main advantage of crystal oscillators is the high acoustic quality factor and hence the high frequency stability. The usage of resonant piezoelectric crystals (RPC) in sensor applications is possible, because the anisotropy of the monocrystal allows the calculation of special cut angles, e.g. the temperature-sensitive NLC cut or the temperature-compensated AT-cut [1]. Such a specially cut crystal can be used in sensor applications, when the resonance behaviour changes with respect to one or more physical values. The aim of the *QxSens* project [2] is the development of a multi-purpose, multi-channel measurement system for RPC based sensors. The *QxSens* measurement system is based on standardized hardware and software and therefore allows a very flexible and wide-spread use in laboratory as well as industrial processes.

RPC based sensors show an influence of the physical measurand on the series resonance frequency and the quality factor. Therefore the measurement with such sensors is primarily based on resonance measurement. A series resonance can be measured by recording the admittance spectrum of a sensor and evaluating the series resonance peak. The hardware developed in the *QxSens* project is used to measure the admittance values of the sensor. The principle aim of this work is to develop an evaluation method for the measured admittance data. This evaluation method shall enable multi-purpose measurements with the *QxSens* measurement system. Additionally, special algorithms are developed to enable temperature and viscosity measurement, e.g. resonance peak tracking and viscosity sensor calibration. Virtual instruments created in LabVIEW are very flexible and used in laboratories and industry all over the world. Therefore LabVIEW is used to implement the software for the *QxSens* measurement system.

This work is organized in four parts. In chapter two the theoretical background of the resonance measurement is explained. The hardware and the signal processing of the *QxSens* measurement system are described in chapter 3. Chapter 4 contains the main part of this work and deals with the admittance measurement and the resonance evaluation. In chapter 5 the temperature and the viscosity measurement are presented.

## 2 Theory of resonance measurement

Measuring physical quantities like temperature or viscosity with RPC sensors is possible because some RPC change its resonance behaviour with respect to one or more physical quantities. Therefore the resonance measurement is the basis to all measurement applications using RPC sensors. In the *QxSens* system the resonance measurement is based on admittance measurement. In this chapter a theoretical description of the admittance, the resonances of an RPC and the evaluation of these resonances is given.

### 2.1 Admittance

The impedance ( $\underline{Z}$ ) is defined as the total opposition a device offers to the flow of an alternating current (AC) at a given frequency. It can be represented by a complex number. The impedance can be either expressed in Cartesian coordinates as  $\underline{Z} = R + iX$ , where the real part is the resistance ( $R$ ) and the imaginary part is the reactance ( $X$ ), or in polar coordinates as  $\underline{Z} = |\underline{Z}|e^{i\varphi_z}$  with the magnitude ( $|\underline{Z}|$ ) and phase angle ( $\varphi_z$ ). The conversion between polar coordinates and Cartesian coordinates is shown in (1). The SI unit of the impedance is Ohm.

$$\begin{aligned}\underline{Z} &= R + iX = |\underline{Z}|e^{i\varphi_z} \\ R &= |\underline{Z}|\cos(\varphi_z) \\ X &= |\underline{Z}|\sin(\varphi_z) \\ Z &= |\underline{Z}| = \sqrt{R^2 + X^2} \\ \varphi_z &= \arctan\left(\frac{X}{R}\right)\end{aligned}\tag{1}$$

The resistance ( $R$ ) is frequency independent and is calculated out of the ohmic resistances in an electrical circuit. The reactance ( $X$ ) depends on the frequency and can be capacitive or inductive. The impedance is the best parameter to describe resistances and reactances in series connections, because in series connections the impedance can be easily calculated as the sum of all  $R$  and  $X$  values. (2) shows how to calculate the impedance of a series connection of a resistance ( $R_1$ ), a capacitance ( $C_1$ ) and an inductance ( $L_1$ ). The angular frequency  $\omega$  is calculated out of the AC frequency  $f$  by using  $\omega = 2\pi f$ .

$$\begin{aligned}
\underline{Z} &= R_1 + iX \\
X &= X_L + X_C \\
X_L &= \omega \cdot L_1 \\
X_C &= \frac{1}{\omega \cdot C_1}
\end{aligned} \tag{2}$$

The reciprocal of the impedance is called the admittance ( $\underline{Y}$ ). In Cartesian coordinates it is given by the conductance ( $G$ ) as real part and the susceptance ( $B$ ) as imaginary part. The conductance is the inverse of the resistance and the susceptance is the inverse of the reactance. Like the impedance, the admittance can also be expressed in Cartesian or polar coordinates. The SI unit of the admittance is  $\text{Ohm}^{-1}$  or Siemens.

$$\begin{aligned}
\underline{Y} &= G + iB = |\underline{Y}| e^{i\varphi_Y} \\
G &= |\underline{Y}| \cos(\varphi_Y) \\
B &= |\underline{Y}| \sin(\varphi_Y) \\
Y &= |\underline{Y}| = \sqrt{G^2 + B^2} \\
\varphi_Y &= \arctan\left(\frac{B}{G}\right)
\end{aligned} \tag{3}$$

The mathematical conversion from impedance to admittance is shown in (4).

$$\begin{aligned}
\underline{Y} &= \frac{1}{\underline{Z}} = G + iB \\
G &= \frac{R}{R^2 + X^2} \\
B &= \frac{-X}{R^2 + X^2}
\end{aligned} \tag{4}$$

Just like the calculation of the impedance of series connections, the admittance of parallel connections of resistances, capacitances and inductances can be calculated as the sum of the conductances and susceptances of these components. So the admittance is the best parameter to describe parallel connections. (5) shows how to calculate the admittance of a parallel connection of a resistance ( $R_1$ ), a capacitance ( $C_1$ ) and an inductance ( $L_1$ ).

$$\begin{aligned}
\underline{Y} &= G + iB \\
G &= \frac{1}{R_1} \\
B &= B_L + B_C \\
B_L &= \frac{1}{\omega \cdot L_1} \\
B_C &= \omega \cdot C_1
\end{aligned} \tag{5}$$

An admittance value  $\underline{Y} = G + iB$  can be plotted into a vector plane with  $G$  and  $B$  as axes (see Figure 1). The curve that results from plotting admittance values with respect to frequency in the  $(G,B)$  vector plane is called the locus of admittance.

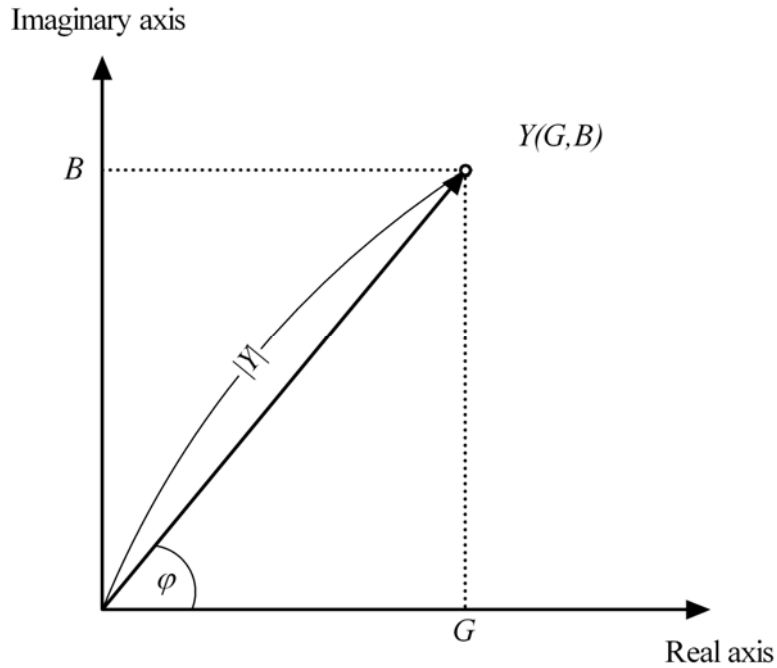


Figure 1: The graphical representation of a complex admittance value. The value can be expressed in Cartesian coordinates with the real axis as x-axis and the imaginary axis as y-axis,  $\underline{Y}=G+iB$  or in polar coordinates with the magnitude  $|\underline{Y}|$  and the phase angle  $\varphi$ ,  $\underline{Y}=|\underline{Y}|e^{i\varphi}$ .

## 2.2 Resonances of RPC

Applying a high-frequency (HF) voltage spectrum to an RPC leads to resonance effects in the piezoelectric response of the quartz crystal. The series resonance frequency is defined as the frequency where the conductance is a relative maximum. Besides the main (fundamental) resonance every RPC has also harmonic resonances. It is important to note, that in this work only the fundamental resonance of an RPC is considered.

The electrical behaviour of a lightly damped RPC in the range of its series resonance frequency can be described by the Van Dyke equivalent circuit shown in Figure 2 [3]. The so called motional branch consists of the motional resistance  $R_1$ , the motional capacitance  $C_1$ , and the motional inductance  $L_1$ . The motional resistance  $R_1$  comprises the losses. The capacitance  $C_0$ , shunted by the motional branch, includes the capacitive effects of the electrodes, enclosure and cable.

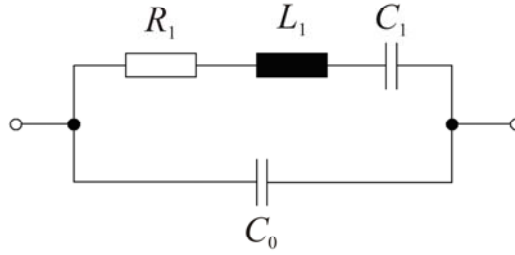


Figure 2: Van Dyke equivalent circuit of a piezoelectric crystal sensor.

In the admittance locus plot of an RPC, that can be described by the Van Dyke equivalent circuit, the resonance is represented by a circle (Figure 3). This circle passes clockwise with increasing frequency. On this circle several characteristic frequencies can be identified. The series resonance frequency  $f_s$  is the frequency where the conductance has its maximum.  $f_{y-}$  and  $f_{y+}$  are the frequencies at the maximum and the minimum susceptance, respectively. The maximum of the absolute value of the admittance corresponds to  $f_m$ . The frequency  $f_r$  is only defined, when the locus circle crosses the conductance axis. It is given by the frequency where the susceptance is zero.

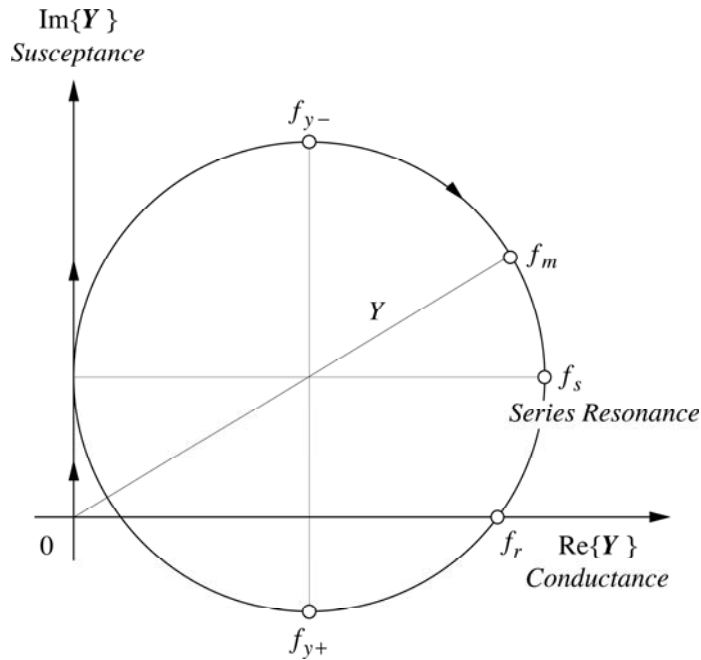


Figure 3: Locus of admittance of a resonance of a piezoelectric resonator with the characteristic frequencies marked.

The resonance of an RPC is determined by the series resonance frequency  $f_s$  and the half width  $HW$  or the quality factor  $Q$ . The half width is defined as the difference between the frequencies, higher and lower than the series resonance frequency, where the input power in the RPC has decreased to half of the input power at the series resonance frequency. The quality factor is defined as the ratio of the mean stored energy and the dissipated energy per oscillation period. (6) shows how to calculate  $f_s$ ,  $Q$  and  $HW$  out of the components of the Van Dyke equivalent circuit.

$$\begin{aligned}
f_s &= \frac{1}{2\pi\sqrt{L_1 C_1}} \\
HW &= f_{y+} - f_{y-} \\
Q &= \frac{\omega_s L_1}{R_1} = \frac{1}{\omega_s C_1 R_1} = \frac{1}{R_1} \sqrt{\frac{L_1}{C_1}} \cong \frac{f_s}{HW} \\
\omega_s &= 2\pi f_s
\end{aligned} \tag{6}$$

## 2.3 Resonance evaluation

When measuring physical quantities, measuring the series resonance frequency  $f_s$  and the quality factor  $Q$  of the main resonance of an RPC based sensor goes ahead of calculating the desired physical quantity out of these values. In order to get  $f_s$  and  $Q$ , the conductances  $G_S$  and the susceptances  $B_S$  are measured stepwise over the considered frequency range and stored digitally. The measured values can be plotted as locus circle which has to be evaluated. When choosing an appropriate evaluation method, it has to be taken into account that depending on the value of  $C_0$  the circle in the locus of admittance can be shifted towards higher susceptance. It can be shown mathematically that this shift does neither distort the circular form of the resonance locus nor the resonance behaviour. A suitable resonance evaluation method has to be insensitive to this shift.

There are several iterative approaches to calculate  $f_s$  and  $Q$  out of the measured admittance values [4]. The disadvantage of these iterative calculation methods is, that they require much computational effort. The non-iterative method used in the *QxSens* system is a better choice as it is a fast and precise algorithm that is able to find and evaluate all resonances of an RPC. It consists of two parts. In the first part the centre, represented by  $G_C$  and  $B_C$ , and the radius  $Y_r$  of the admittance circle are calculated from the raw admittance data  $G_S$  and  $B_S$  with a circle fit algorithm [5]. Out of this the resistance  $R_1$  is obtained using  $R_1 = 1/(2Y_r)$ . In the second part a least square fit method is used to calculate the capacitance  $C_1$  and the inductance  $L_1$  out of the raw admittance data,  $G_S$  and  $B_S$ , and the values resulting from the first part,  $G_C$ ,  $B_C$  and  $Y_r$ . It has to be noted, that the described non-iterative algorithm is only working properly when the condition

$$Q^2 \gg \frac{C_0}{C_1} \tag{7}$$

is fulfilled [6]. That means, the locus circle is not distorted by the admittance of the parallel capacitance  $C_0$ .

# 3 Measurement system

The *QxSens* system is a low cost measurement system that is designed to operate over a wide range of electrical sensor specifications in terms of series resonance frequency, quality factor and resonance resistance. In the first part of this chapter the hardware of the *QxSens* system is described. The second part deals with the signal processing in the measurement system.

## 3.1 Hardware

The *QxSens* system consists of a sensor, the kernel electronics and a computer system, including a synthesizer card, a multifunction I/O card and the interface electronics. The sensor consists of an RPC contacted with two electrodes. One electrode is connected to the kernel electronics with a triaxial cable, the other electrode is grounded. A PT100 temperature sensor can be included in the sensor housing optionally. This PT100 is also connected to the kernel electronics. The kernel electronics transform the measurement signal from the RPC into 4 DC signals  $S1..S4$  and loop through the 4 PT100 wires directly to the computer interface. The kernel electronics are connected to the interface electronics with the so called *QxSens* cable, a standard VGA cable. It is possible to connect up to three kernel electronics to one interface electronic unit. That means three measurements can be done quasi simultaneously. A simultaneous PT100 measurement is only implemented on the first channel. The interface electronics transfer all signals to the multifunctional I/O card, where they are digitized. The digitized signals are then evaluated by the measurement software.

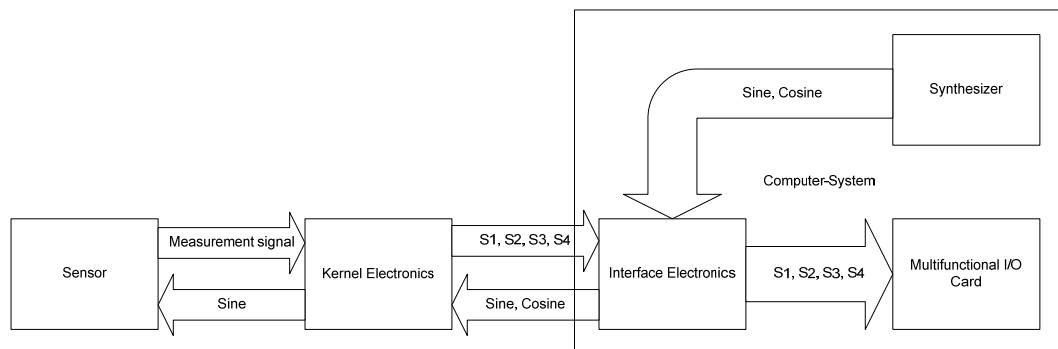


Figure 4: Schematic description of the *QxSens* system. The different parts and the signal-flow between them is displayed.

### 3.1.1 Computer system

There are three different versions of the computer system. One is based on a standard desktop PC and another one on an industrial PXI system. In these two systems the measurement components are mounted in the computer system's case. Therefore they are called internal systems. The third version is an external measurement box with a USB connector. It can be used with any standard PC based computer system that supports USB 1.0 or higher. All three computer systems include a synthesizer, a multifunction I/O card and interface electronics which have been designed specifically for the QxSens system.

#### 3.1.1.1 General description of the computer system's components

##### 3.1.1.1.1 Multifunctional I/O card

The multifunctional I/O card contains a 12 or 16 bit AD converter. This AD converter is the interface between the analog measurement signals and the software evaluation based on digital values. In the *QxSens* system multifunctional I/O cards from National Instruments (NI DAQ boards) are used.

The low resolution of a 12 bit AD converter can lead to quantization errors. To minimize this type of error, 12-bit DAQ boards from NI can improve their resolution with a hardware technique called dithering [7]. It adds approximately  $0.5 \text{ LSB}_{\text{rms}}$  of Gaussian white noise to the input signal. This noise is added to the signal before it is fed to the input of the AD converter. Averaging can then improve the resolution of the measurement results. 16 bit AD converters do not support dithering as it is not required because the resolution of a 16 bit AD converter is a priori much better [8].

##### 3.1.1.1.2 Synthesizer

The synthesizer is a 100 MHz quadrature signal generator. It generates the generator signal  $V_G$  (sine HF signal) and the reference signal  $V_0$  (cosine HF signal). These HF signals are used in the kernel electronics to generate the measurement signals,  $S1..S4$ .

The absolute frequency accuracy of the synthesizer was measured using an HP 5372A device. This is a high performance frequency and time interval analyzer. Figure 5 shows the absolute error of the synthesizer. It can be seen that the absolute error is a linear function of the frequency.

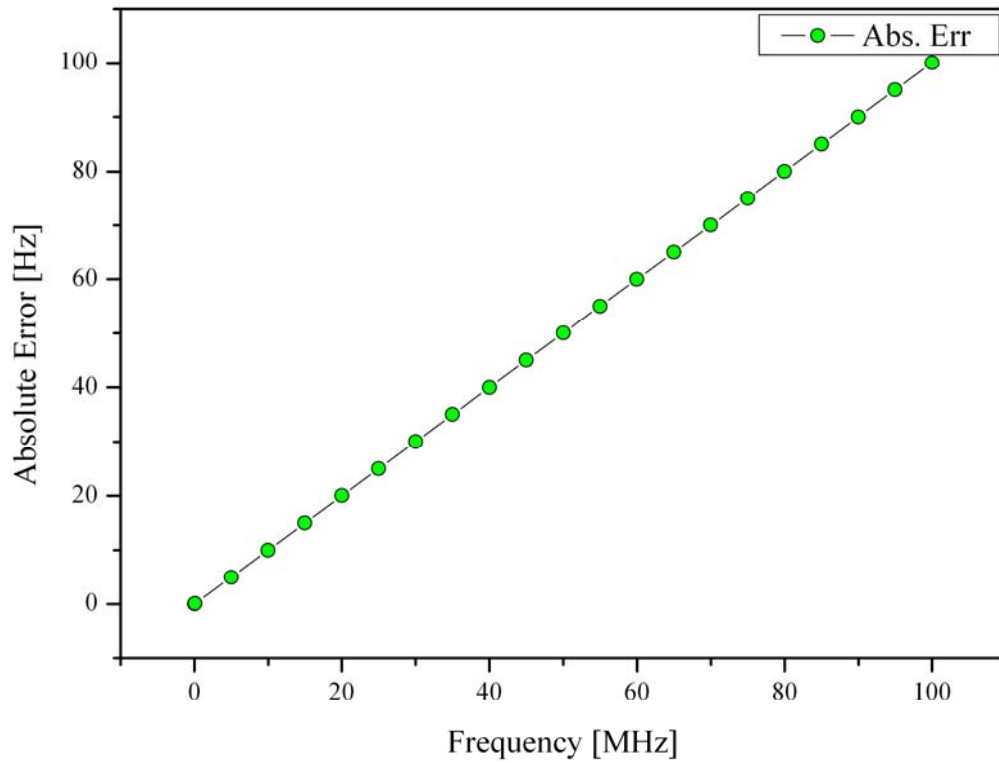


Figure 5: Absolute error of the output frequency of the synthesizer used in the *QxSens* system. The absolute frequency error depends on the output frequency. The output frequency of the synthesizer was measured with a HP 5372A high performance frequency and time analyzer.

### 3.1.1.1.3 Interface electronics

The interface electronic unit is the interface between the kernel electronics and the computer system. There are different versions for the internal and the external systems. Both versions consist of four main parts. The first part applies two high frequency signals  $V_G$  and  $V_0$  to the kernel electronics. The second part provides the necessary power for the kernel electronics. The third part transfers the signals  $S1..S4$  from the VGA connectors to the multifunctional I/O card. And the last part is a PT100 measurement module. In addition the external version has two BNC connectors for monitoring the sine and cosine signals generated by the synthesizer.

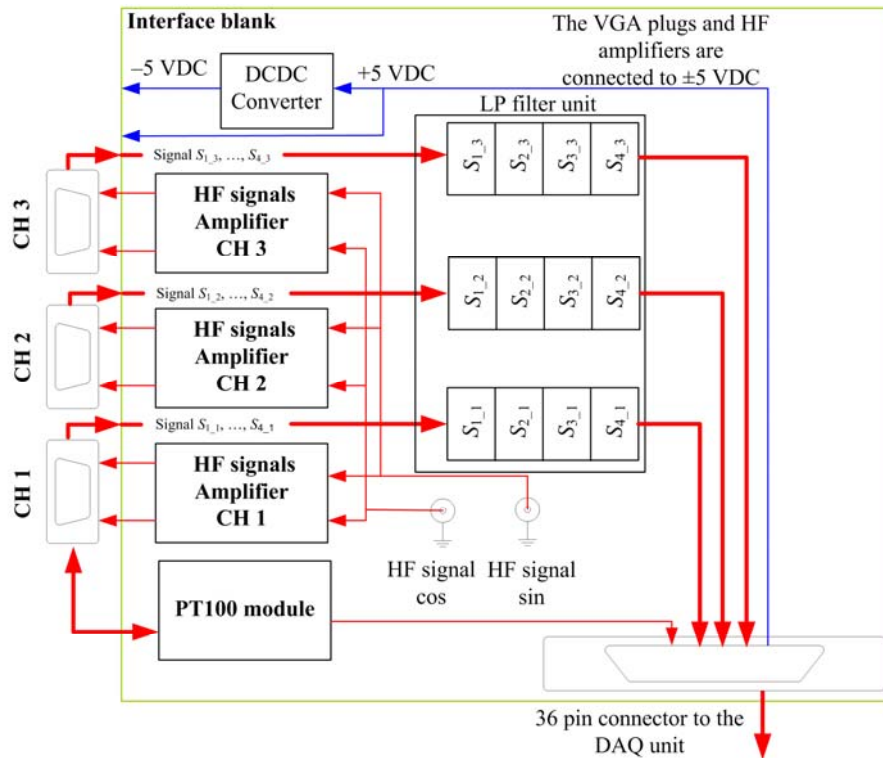


Figure 6: Block diagram of the signal processing in the interface electronics.

The high frequency sine and cosine signals are amplified by an AD8056 op-amp. This op-amp drives the signals taken from the synthesizer card along the *QxSens* cable to the kernel electronics.

The power for the kernel electronics is taken from the multifunctional I/O card. This brings up the limitation of a maximum current of 1 A (fused). This fact should be considered when connecting three sensors with low resistance.

The sensor signals  $S_{1..4}$  pass a low-pass filter in order to remove possible high frequency voltage from the signals before they are further processed in the multifunctional I/O card. These parasitic effects are caused by possible EMC sources outside the measurement system. The radiation can influence the signals during the transmission through the *QxSens* cable.

The PT100 measurement module used here is the SCM5B35 from Dataforth. There are two types with different temperature ranges used in the *QxSens* systems, 0 to 100 °C and -100 to +200 °C. The module linearizes the given temperature range to a voltage from 0 to +5 V.

### 3.1.1.2 The 3 versions of the computer system

#### 3.1.1.2.1 Desktop PC version

A standard desktop PC is used as base for this computer system. The advantage of this version of the *QxSens* system is that any standard PC can easily be equipped with the *QxSens* system's components.

The standard PC used in this work is equipped with the following components:

- Mainboard: MSI 865PE Neo 2
- CPU: Intel P4 2.8 GHz
- RAM: 1024 MB
- Graphic card: ATI Radeon 9200 Series
- Hard disc capacity: 2 \* 150 GB
- Synthesizer: Team Solutions, Inc. TE 5100
- Multifunctional I/O card: NI PCI-6024E (12 bit analog input) or NI PCI-6036E (16 bit analog input)
- Interface electronics

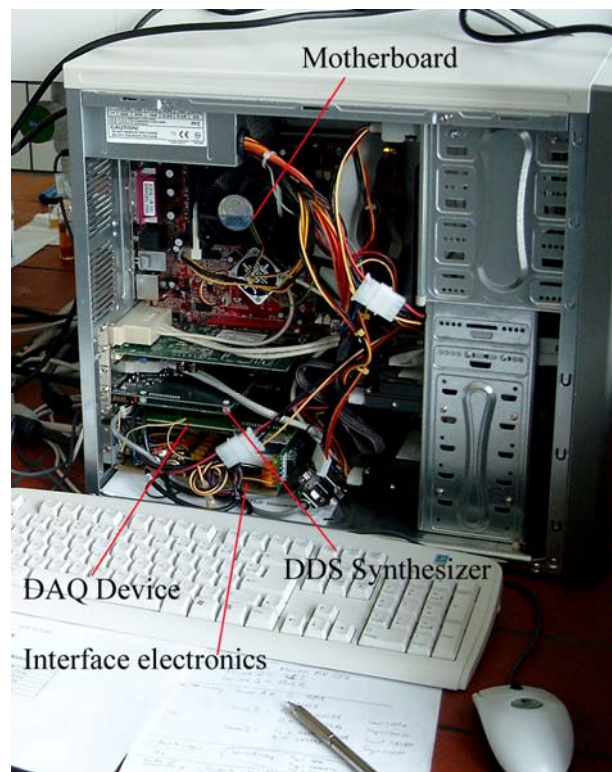


Figure 7: Picture of the PC version of the *QxSens* system. The important parts for the *QxSens* system are marked.

### 3.1.1.2.2 Industrial PXI version

PXI (PCI eXtensions for Instrumentation) is a rugged, PC-based platform for measurement and automation systems. This *QxSens* version can be attached to any other PXI system in any industrial process.

The PXI system used in this work is equipped with the following components:

- Chassis: NI PXI-1002
- PXI system controller: NI PXI-8174
- RAM: 128 MB
- Synthesizer: Team Solutions, Inc. TE 5100
- Multifunctional I/O card: NI PXI-6025E (12 bit analog input)
- External chassis with interface electronics



Figure 8: Picture of the PXI version of the *QxSens* system. The interface electronics are mounted on the right side of the chassis.

### 3.1.1.2.3 External USB version

The two versions described above can be used very flexibly, but they are not really portable. The external USB version of the *QxSens* system is easily portable and can be connected to any standard PC based computer system supporting USB 1.0 or higher.

The external USB version is mounted in an external case. It is equipped with the following components:

- Multifunctional I/O card: NI DAQPad – 6016 (USB)
- Synthesizer: DDS8m, Novatech Instruments
- USB Serial Adapter from Keyspan
- Interface electronics
- 12 V DC Power supply 25 W: Traco TXL 025 – 12S
- USB – Hub: 4 Port HI – Speed Hub



Figure 9: Picture of the open housing of the external USB version of the *QxSens* system.

### 3.1.2 Kernel electronics

Three types of kernel electronics have been developed during the *QxSens* project. Two types use a voltage divider principle (VDP) and the third one uses the compensated current principle (CCP). In this work, only kernel electronics based on the VDP have been used, and therefore only these types are described here. In the VDP version two voltages,  $V_C$  and  $V_S$ , can be used alternatively for the evaluation of the measurement. These two types of kernel electronics are referred to as VDP- $V_C$  and VDP- $V_S$ , respectively.

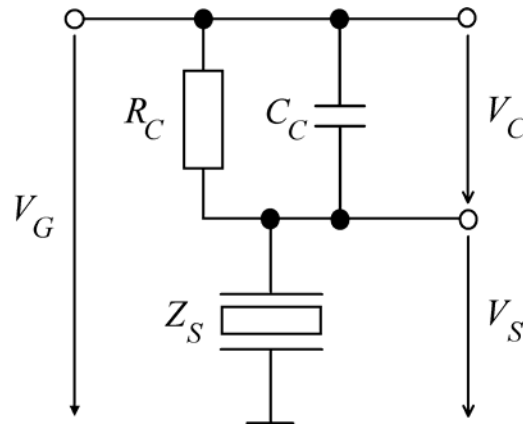


Figure 10: The voltage divider principle used in the VDP kernel electronics. The generator voltage  $V_G$  is applied to the voltage divider consisting of the sensor  $Z_S$  and the resistor  $R_C$  shunted by a capacitor  $C_C$ .  $V_S$  is the sensor signal, that is used as measurement signal in the VDP- $V_S$  version.  $V_C$  is used as measurement signal in the VDP- $V_C$  version.

The kernel electronics have three tasks to perform. The first task is to transfer the generator signal  $V_G$  and the reference signal  $V_0$  to the sensor. The second task is to compensate the cable capacitance of the triaxial cable between the sensor and the kernel electronics. The third task is to transform the measurement signal into 4 DC signals and then transfer them to the interface electronics.

The input signals  $V_G$  and  $V_0$  in the kernel electronics are DC-decoupled and 75 $\Omega$  line terminated. This is necessary to remove possible DC offsets and to avoid signal reflections from the *QxSens* cable which has a characteristic impedance of 75 Ohm. The sensor (represented here by its impedance  $Z_S$ ) is connected in series to an impedance  $Z_C$ , consisting of a resistor  $R_C$  that can be shunted with a capacitor  $C_C$ . This voltage divider is shown in Figure 10.

The signal  $V_S$  (or  $V_C$ ) is transferred to the sensor with a triaxial cable. Usually coaxial cables are used for transferring HF signals. But a coaxial cable has a capacitance between the inner wire and the shielding. This capacitance depends on the length of the cable and increases the parallel capacitance of the sensor. Therefore the resolution of the measurement signal decreases, especially when evaluating sensors with low quality factor. To avoid this effect, a triaxial cable is used here. The kernel electronics make the

potential on the centre wire and the inner shielding of the triaxial cable the same and therefore compensates this capacitance.

In the VDP- $V_C$  version the floating measurement signal  $V_C$  is converted into a grounded voltage by a differential receiver amplifier AD8130. The grounded voltage  $V_C$  is then multiplied with the generator signal  $V_G$  and the reference signal  $V_0$ , respectively. The generator signal  $V_G$  and the reference signal  $V_0$  are also squared. These operations are done by 4 multipliers AD835. The multiplier output signals are converted into 4 DC signals,  $S1..S4$ , by passing low-pass filters. After decoupling these DC signals, they are transferred to the interface electronics through the QxSens cable.

In the VDP- $V_S$  version the signal  $V_S$  on the sensor is taken as measurement value instead of  $V_C$ . As  $V_S$  is already a voltage against ground the differential receiver amplifier AD8130 is not used in this version. The multiplications and DC conversions are the same as in the VDP- $V_C$  version.

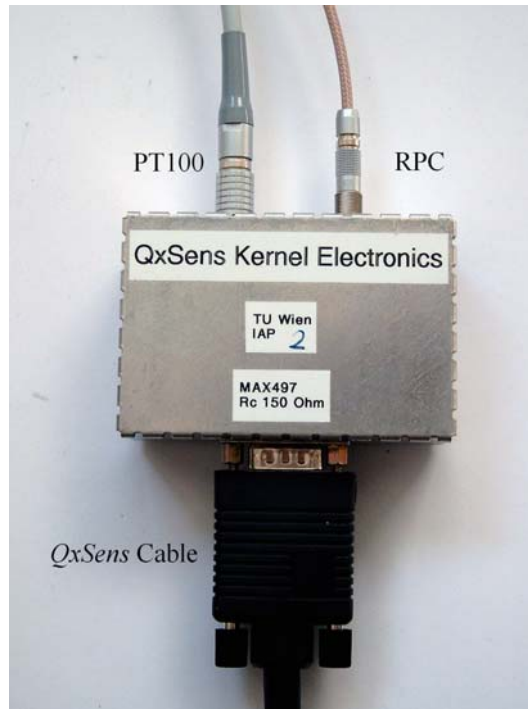


Figure 11: Picture of the kernel electronics.

### 3.1.3 Sensors

The sensors used in the *QxSens* system are based on resonant piezoelectric crystals. Depending on the material and the cut of the RPC these sensors are sensitive to different physical quantities. That means that one or more properties of the crystal, like series resonance frequency, quality factor or motional resistance, change with respect to one or more physical values of the surrounding, like e.g. temperature, viscosity or

pressure. In this work sensors for temperature measurement and viscosity have been used.

### 3.1.3.1 Temperature sensors

The basis for thermometry with RPC based sensors is the fact, that the series resonance frequency of some cuts of resonant piezoelectric crystals strongly changes with temperature. Different materials can be used to build an RPC temperature sensor. The Institute of Solid State Physics at the Bulgarian Academy of Sciences in Sofia developed RPC sensors based on quartz crystals [9]. The so called QT sensors are NLC-cut quartz crystal thickness-shear resonators embedded in a standard HC-49/U package. These QT sensors have a series resonance frequency of about 29 MHz, and a very low motional resistance of less than 20  $\Omega$ . The sensor function (8) is given by a polynomial of third order. A one-point calibration can be used to calibrate the complete measurement system with the QT sensor attached. The calibration data are a temperature value  $T_0$  and the corresponding measured frequency  $f_0$ . The variables  $k_1$ ,  $k_2$  and  $k_3$  are the fit parameters of the polynomial.

$$T(f_s) = T_0 + k_1 \frac{(f_s - f_0)}{f_0} + k_2 \left( \frac{(f_s - f_0)}{f_0} \right)^2 + k_3 \left( \frac{(f_s - f_0)}{f_0} \right)^3 \quad (8)$$

A second type of temperature sensors have been developed at Piezocryst GmbH in Graz, Austria [10]. These sensors are based on GaPO<sub>4</sub> and therefore called GT sensors. The temperature sensitive part of the sensor is a gallium-orthophosphate crystal oscillating in thickness-shear mode. Its series resonance frequency is between 6 and 8 MHz, and its motional resistance is about 100  $\Omega$ . The sensor function is also a polynomial of third order. Therefore both sensor types can be used with the same measurement algorithms.

The sensors of both sensor types have been calibrated in a temperature calibrator at Piezocryst. The difference between the QT and GT sensors is the temperature range. While quartz sensors only work below 200°C, GT sensors can be used to measure temperatures up to 900°C.

### 3.1.3.2 QV sensors

The basis for viscosity measurement with RPC sensors is the interaction of the oscillating quartz crystal with the viscous fluid. When the quartz crystal is excited with an HF voltage, it performs shear oscillations and therefore radiates shear waves into the fluid that surrounds the sensor. The decay length of these waves is only a few micrometers. The fluid layer on the quartz surface decreases the series resonance frequency as well as the quality factor compared to the unperturbed dry crystal.

As viscosity is highly correlated with temperature, measuring viscosity with RPC sensors requires simultaneous temperature measurement. There are two different approaches to this subject. On the one hand there are sensors with two RPCs in the same housing. One of these RPCs is sensitive to the viscosity, the other one is sensitive to temperature. The problem with this solution is, that the two quartz crystals must not have resonances in the same frequency range. Even if the fundamental resonance frequency ranges of the two crystals do not overlap, there can still be interactions due to overlapping of a resonance with overtones of the other resonance. The advantage of this solution is that both measurement signals can be transferred through one triaxial cable. On the other hand there are sensors that combine a viscosity-sensitive RPC with a PT100. The PT100 in these sensors is connected to the kernel electronics with a 4-way cable.

In this work two different types of viscosity sensors have been used for measurement. The first sensor was made of a thin temperature compensated AT-cut quartz plate, which oscillates in thickness-shear mode [11]. This type is therefore called QV-shear (Figure 12). The AT-cut is a temperature compensated cut with standardized cut angle of (YXI)  $-35^\circ$  [12]. Additionally, a quartz temperature (QT) sensor was attached beneath the QV-shear sensor plate for temperature measurement. The QV-shear sensor function is given as follows [13].

$$\eta \cdot \rho = \frac{n^2 \pi z_Q'^2}{4} \frac{1}{Q_{nL}^2 f_{n0}} = n^2 \pi z_Q'^2 \frac{\Delta f_n^2}{f_{n0}^3} \quad (9)$$

Thereby  $n$  is the mode number of the considered resonance,  $z_Q'$  the acoustic impedance (real part) of the quartz,  $\Delta f_n = f_n - f_{n0}$  the frequency shift due to the viscous load of the quartz,  $f_n, f_{n0}$  are the series resonance frequencies of the loaded and unloaded resonator, respectively.  $Q_{nL}$  is the acoustic quality factor of the fluid that can be derived from the quality factors of the loaded and unloaded crystal, respectively:

$$\frac{1}{Q_{nL}} = \frac{1}{Q_n} - \frac{1}{Q_{n0}} \quad (10)$$

The quality factor and the series resonance frequency of the crystal's resonance (loaded and unloaded case, respectively) can be determined out of the measured locus of admittance curves.

A big problem with the sensor function is, that the theoretical predictions of the sensor function do not fit satisfactorily to the real measured data. This was shown by Schnitzer [14]. Therefore a calibration is needed in order to get accurate measurement results.

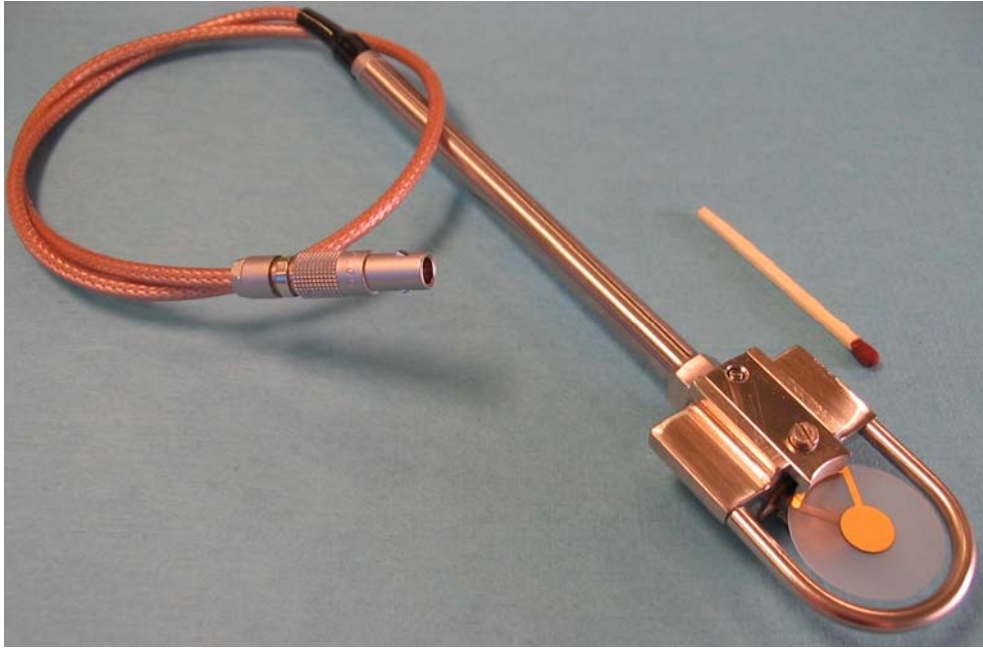


Figure 12: Picture of the QV-shear sensor.

The viscosity-sensitive part of the other sensor used in this work is a quartz rod that performs torsional vibrations. The quartz rod is clamped in the middle where the oscillation amplitude theoretically vanishes. Inside the housing the quartz crystal is contacted with electrodes applied in four strips along half of the quartz crystal's rod length. Applying an HF voltage to the quartz crystal contacted in this way leads to torsional vibrations [15]. Therefore this type of sensor is called QV-torsion (Figure 13). The part outside the housing is in contact with the viscous fluid. Its torsional vibrations induce cylindrical shear waves in the fluid. Concerning the sensor function the QV-torsion sensor qualitatively shows the same behaviour as the QV-shear sensor. It can be seen from the sensor function of the QV-shear sensor (9), that the square of the frequency change caused by Newtonian liquids is proportional to the viscosity-density product of the liquid. This relation is also true for the QV-torsion sensor [16]. But, as Bode has shown in [17], a calibration is required to get correct absolute values.



Figure 13: Picture of the QV-torsion sensor.

## 3.2 Signal processing

In the computer system the synthesizer generates two HF signals, the generator signal  $V_G$  and the reference signal  $V_0$ , which has a  $90^\circ$  phase shift to the generator signal. Then the signals are transferred from the synthesizer to the interface electronics. The interface electronics amplify the signals in order to drive the signals through the *QxSens* cable to the kernel electronics. It also decouples the signals from the computer system.

The HF inputs of the kernel electronics are DC-decoupled in order to get rid of parasitic DC offsets. To avoid signal reflections caused by the characteristic impedance of the *QxSens* cable the HF inputs have also a  $75 \Omega$  line termination. After this decoupling the generator signal  $V_G$  is contacted to the voltage divider and hence the HF signal is applied to the sensor.

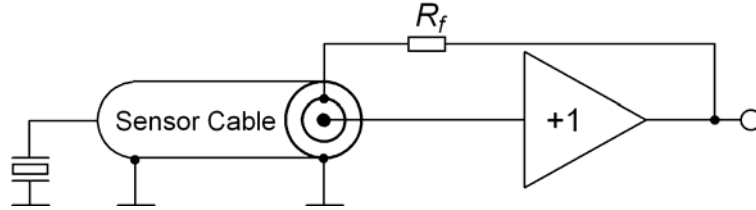


Figure 14: Diagram of the working principle of the cable compensation. The sensor signal is decoupled and applied to the inner shielding over a resistor  $R_f$ .

The capacitance of the triaxial cable, which connects the sensor to the kernel electronics, is connected in parallel to the sensor. This leads to a significantly higher total parallel capacitance and therefore, especially when using sensors with low quality factors, the signal-to-noise ratio is getting worse. The compensation of the capacitance of the triaxial cable is done by decoupling the sensor signal  $V_S$  and applying the decoupled signal to the inner shielding of the triaxial cable (Figure 14). This procedure equalizes the potentials of the inner shielding and the centre wire, and therefore reduces the capacitance of the cable. It can be shown that the maximum cable length  $l_{Cable}$ , at which the cable compensation is working properly, is given by (11).  $C_{r\_Cable}$  is the relative cable capacitance between the inner and the outer shielding and is  $250 \text{ pF/m}$ ,  $X_{Cable\_min}=200 \Omega$  [18] and  $\omega$  is the angular frequency of the HF voltage.

$$l_{Cable} = \frac{1}{\omega C_r X_{Cable\_min}} \quad (11)$$

At 3 MHz the maximum length of the cable can be calculated to 1 m. If a longer cable is used, a phase shift between the signals at the inner connector and the first shielding leads to parasitic effects, like negative conductances, and therefore reduces the compensation effect.

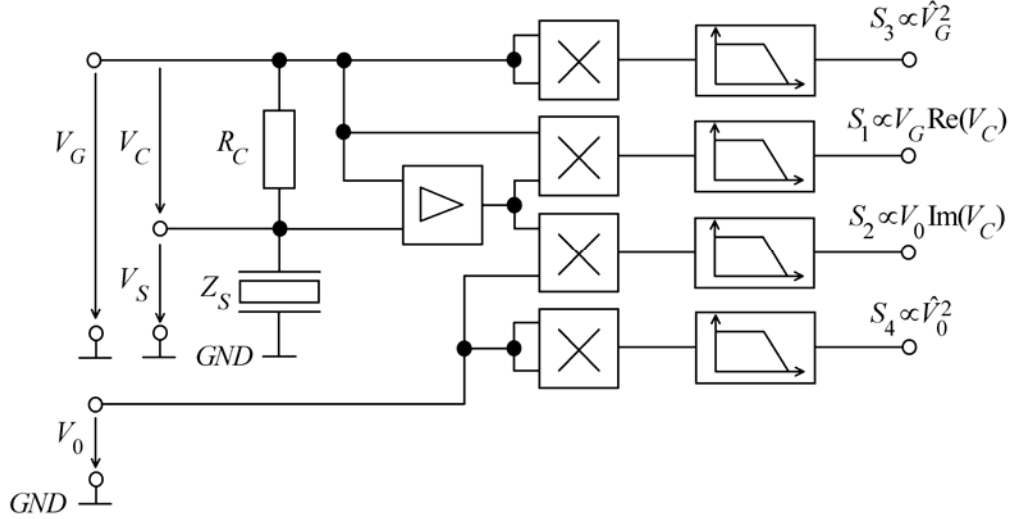


Figure 15: Block diagram of the signal processing in the VDP- $V_C$  kernel electronics. The voltage divider is shown without the capacitance  $C_C$ . The voltage across  $R_C$  is converted by the differential receiver amplifier ( $\Delta$ ). The signal  $S_1$  to  $S_4$  are the DC signals used in the computer system to calculate the measured admittance value. To change the block diagram to VDP- $V_S$  only the differential receiver amplifier has to be removed and the sensor is then directly connected to the multipliers.

As DC signal transmissions are less error-prone than HF signal transmissions the HF measurement signal is transformed into 4 DC signals before being transferred to the computer system. Figure 15 shows a block diagram of this transformation process in the VDP- $V_C$  version. The VDP- $V_S$  version does the same, but without the differential receiver amplifier and hence multiplies  $V_S$  instead of  $V_C$ . The generated DC signals,  $S_1..S_4$ , are proportional to the measurement signal and thus the measurement signal can be calculated out of these values in the computer system.

In the VDP- $V_C$  version the voltage  $V_C$  across the resistor  $R_C$  is used as measurement signal. As  $V_C$  is a floating voltage (not referred to ground), a differential receiver amplifier is used to convert this floating voltage to a voltage against ground. After that  $V_C$  is multiplied with the generator voltage  $V_G$  and the reference signal  $V_0$ , respectively. Low-pass filters applied to the multiplier output signals give the DC signals  $S_1$  and  $S_2$  which are proportional to the real and the imaginary part of  $V_C$ , respectively. The mathematical representation of this multiplication and filtering is shown in (12), where  $\omega$  is the angular frequency of the HF signals  $V_G$  and  $V_0$ .

$$S_1 = \frac{\omega}{2\pi} \int_0^{\frac{2\pi}{\omega}} V_C(t) \cdot V_G(t) dt = V_G \frac{\text{Re}(V_C)}{2}$$

$$S_2 = \frac{\omega}{2\pi} \int_0^{\frac{2\pi}{\omega}} V_C(t) \cdot V_0(t) dt = V_0 \frac{\text{Im}(V_C)}{2}$$
(12)

The calculation of  $S_1$  and  $S_2$  in the VDP- $V_S$  version can be deduced by taking (12) and replacing  $V_C$  by  $V_S$ .

Like all analog electronic devices the analog multipliers have internal offset errors. Furthermore the amplitudes of the two output signals on the synthesizer are generally not exactly the same. These two points would lead to wrong conductance and susceptance values calculated out of  $S_1$  and  $S_2$ . To avoid these errors the mathematical formalism used in the computer system for calculating the conductance and susceptance is based on ratios of  $S_1/S_3$  and  $S_2/S_4$ , where  $S_3$  and  $S_4$  are the squared generator voltage  $V_G$  and reference voltage  $V_0$ , respectively.

$$S_3 = \frac{\omega}{2\pi} \int_0^{\frac{2\pi}{\omega}} V_G^2(t) dt = \frac{V_G^2}{2} \quad (13)$$

$$S_4 = \frac{\omega}{2\pi} \int_0^{\frac{2\pi}{\omega}} V_0^2(t) dt = \frac{V_0^2}{2}$$

Before transferring the 4 DC signals over the QxSens cable to the interface electronics in the computer system the signals are decoupled from the rest of the kernel electronics. A low-pass filter in the interface electronics only lets the DC (low frequency) component of the transferred signals pass. Parasitic effects, caused by possible EMC sources outside the measurement system, are removed.

The DC signals  $S_1$  to  $S_4$  are digitized by the NI DAQ board in the computer system. In a *QxSens* system two different NI DAQ boards can be used. One contains a 16-bit and the other a 12-bit AD converter. The advantage of the 12-bit version is that it is much cheaper than the 16-bit version. The only problem with 12-bit AD conversion is, that there are only  $2^{12}=4096$  possible values to represent a physical voltage in comparison with a 16-bit AD converter that provides  $2^{16}=65536$  values for the same task. That leads to quantization errors when digitizing small voltages with 12-bit AD converters. The smallest detectable voltage difference is given by the least significant bit (LSB) of the AD converter. The LSB depends on the selected input voltage range, the selected gain and the given resolution of the DAQ board. Therefore a 16-bit AD converter provides a 16 times smaller LSB than a 12-bit AD converter under the same conditions.

The 12-bit NI DAQ boards provide a technique called dithering to improve the theoretical resolution. By adding about 0.5 LSB of Gaussian white noise to the input signal before digitizing and averaging over at least 50 so prepared digitized measurement values the theoretical resolution is like the resolution of a 14-bit AD converter [7]. Figure 16 shows the significant improvement of the measurement resolution when dithering is turned on.

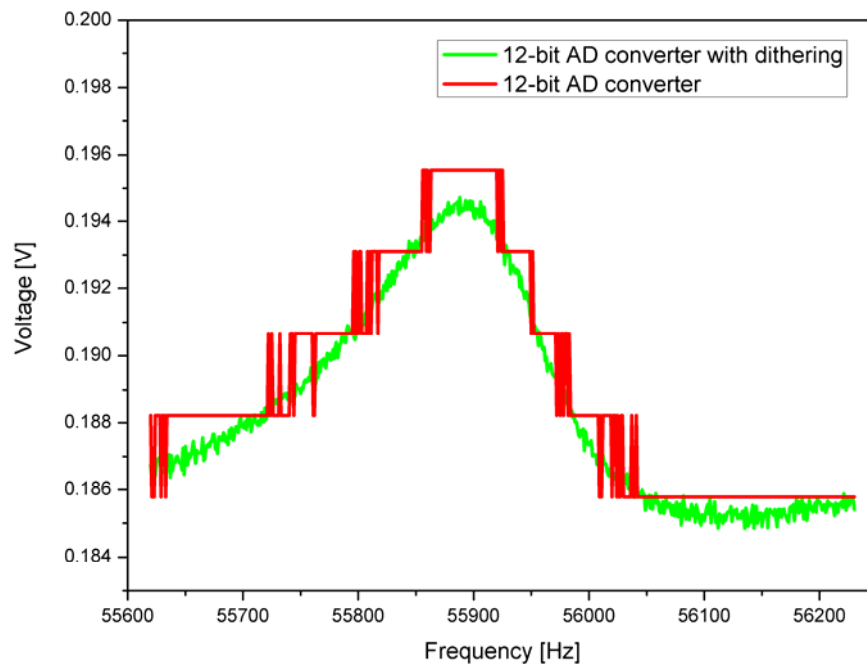


Figure 16: Comparison of a resonance voltage signal digitized with a 12-bit AD converter with and without dithering. Without dithering (red line) the voltage curve cannot be resolved, which results in steps in the digitized signal. With dithering (green line) the 12-bit AD converter has an increased resolution.

The 4 digitized values  $S_1..S_4$  can be used with an evaluation software to calculate the conductance and susceptance values of the sensor over frequency. The evaluation software used in the *QxSens* system is described in the next chapter.

# 4 Resonance measurement

Measuring physical quantities with RPC based sensors can be done, because at least one of the resonance values of the RPC, these are the series resonance frequency, the quality factor and the equivalent circuit parameters, change with respect to the physical quantity. Therefore it was necessary to develop a fast and precise resonance measurement process. The resonance measurement is done by stepwise scanning a given frequency range and measuring the admittance at each frequency step. The measured admittance curve is then checked for possible resonances. If resonances are found, the resonance with the highest conductance value (peak) is evaluated using the method described in section 2.3. The series resonance frequency, the quality factor and the equivalent circuit parameters are the output values of this evaluation.

In the development of a resonance measurement system many criterions have to be concerned. When measuring viscosity the quality factor undergoes changes of the factor 1000 and more, depending on the viscosity of the sample liquid. Also the height of the conductance peak can be between 100 mS and a few  $\mu$ S. The system must therefore be able to detect resonances of different quality factors and conductance peak values. In some measurement applications the measured physical quantity changes very fast. Measurement speed is therefore also an important point. The precision of the measurement results is influenced by the measurement hardware and the compensation techniques used to compensate parasitic effects, the transient phenomena and the signal-to-noise ratio. It is important to note that there is always a compromise between measurement speed and measurement precision. So the system has to be developed in a way, that the user can adapt the system's parameters to the actual requirements. From this it follows that easy operating of the measurement system has also to be taken into account.

## 4.1 Signal transformation

After initializing the measurement system, a frequency scan is performed. At each frequency step the signals  $S_1..S_4$  coming from the kernel electronics are digitized. The aim of the resonance measurement is to find, analyse and evaluate a resonance. Therefore in a first step, the admittance values have to be calculated out of the measured signals. In the following step the admittance spectrum is analysed and a possibly found

resonance is evaluated. The results of this process are the equivalent circuit parameters, the series resonance frequency and the resonance quality factor.

### 4.1.1 Admittance calculation

It can be seen in 3.2 that the measurement signals  $S_1$  and  $S_2$  carry the admittance information of the connected sensor. The reference signals  $S_3$  and  $S_4$  contain only the information of the generator voltage and the reference voltage, respectively. In the calculation of the conductance  $G$  and the susceptance  $B$  out of these measurement signals the ratios

$$\begin{aligned} K_1 &= \frac{S_1}{S_3} \\ K_2 &= \frac{S_2}{\sqrt{S_3 \cdot S_4}} \end{aligned} \quad (14)$$

are used. There are two reasons for this calculation method. Firstly, the divisions normalize the measurement signals and therefore make the calculated  $G$  and  $B$  values independent from the driving voltage. And secondly, possible common mode errors, caused by electronic devices as well as the *QxSens* cable resistance, are compensated. These errors are represented by constant multiplication factors. As the kernel electronics are symmetrical with respect to the signals generation, these multiplication factors affect all 4 signals in essentially the same way. That is why the divisions of the measurement signals cancel out the error effects.

Regarding the VDP- $V_C$  version of the kernel electronics, the admittance values  $G_S$  and  $B_S$  are calculated using

$$\begin{aligned} G_S &= \frac{K_1 - K_1^2 - K_2^2 - \omega C_C R_C K_2}{R_C (K_2^2 + (K_1 - 1)^2)} \\ B_S &= \frac{K_2 - \omega C_C R_C (K_1^2 + K_2^2 - K_1)}{R_C (K_2^2 + (K_1 - 1)^2)} \end{aligned} \quad (15)$$

If a sensor with high capacitance is used, the impedance of the sensor changes highly with the frequency. A capacity  $C_C$  parallel to a resistor  $R_C$  is used in this case to ensure good signal quality in the whole measured frequency range. But in most cases kernel electronics without  $C_C$  are used. Then the calculation of  $G_S$  and  $B_S$  simplifies to

$$G_s = \frac{K_1 - K_1^2 - K_2^2}{R_c (K_2^2 + (K_1 - 1)^2)}$$

$$B_s = \frac{K_2}{R_c (K_2^2 + (K_1 - 1)^2)}$$
(16)

Using a VDP-V<sub>S</sub> version, the calculation of the conductance and susceptance changes to

$$G_s = \frac{K_1 - K_1^2 - K_2^2 + \omega C_c R_c K_2}{R_c (K_2^2 + K_1^2)}$$

$$B_s = -\frac{K_2 + \omega C_c R_c (K_1^2 + K_2^2 - K_1)}{R_c (K_2^2 + K_1^2)}$$
(17)

Without  $C_c$  this calculation simplifies to

$$G_s = \frac{K_1 - K_1^2 - K_2^2}{R_c (K_2^2 + K_1^2)}$$

$$B_s = \frac{K_2}{R_c (K_2^2 + K_1^2)}$$
(18)

### 4.1.2 Resonance evaluation

After the admittance scan in the desired frequency range has been performed, the measurement data has to be evaluated with regard to possible resonances. The search algorithm scans the conductance spectrum for resonances with a maximum conductance peak value of at least 70% of the difference between the maximum and the minimum measured conductance. This is an experimentally determined suitable value. A requirement for the resonance analysis is that there is only one such resonance within the measured frequency range. If there is more than one such resonance, the search cannot distinguish between the resonances. In this case the search algorithm takes always the resonance with the lowest resonance frequency as search result. The main condition for the resonance evaluation method used is (7). It means, that the locus circle is not distorted by the admittance of the parallel capacitance  $C_0$ . This condition is fulfilled in most cases. When using long cables,  $C_0$  can be very high because of the parallel capacitance of the cable. In this case the resonance analysis would not give correct results.  $C_0$  can be reduced using the cable compensation, and therefore the

resonance analysis method used will work properly in almost any measurement applications.

If a resonance is found, this resonance is evaluated using the non-iterative evaluation method described in 2.3. The results of this evaluation are the equivalent circuit parameters  $R_1$ ,  $C_1$ ,  $L_1$  and  $C_0$ . These parameters contain all information on the resonance required for the analysis of physical measurands. The series resonance frequency  $f_s$  and the quality factor  $Q$  are calculated using

$$f_s = \frac{1}{2\pi\sqrt{L_1 C_1}} \quad (19)$$

$$Q = \frac{1}{R_1} \sqrt{\frac{L_1}{C_1}}$$

The success of the resonance evaluation is mainly dependent on the number of measurement points within the half width of the resonance ( $N_{HW}$ ). If there are too less points, the detected series resonance frequency may be incorrect.  $N_{HW}$  is determined by the scanned frequency range and the used step width.

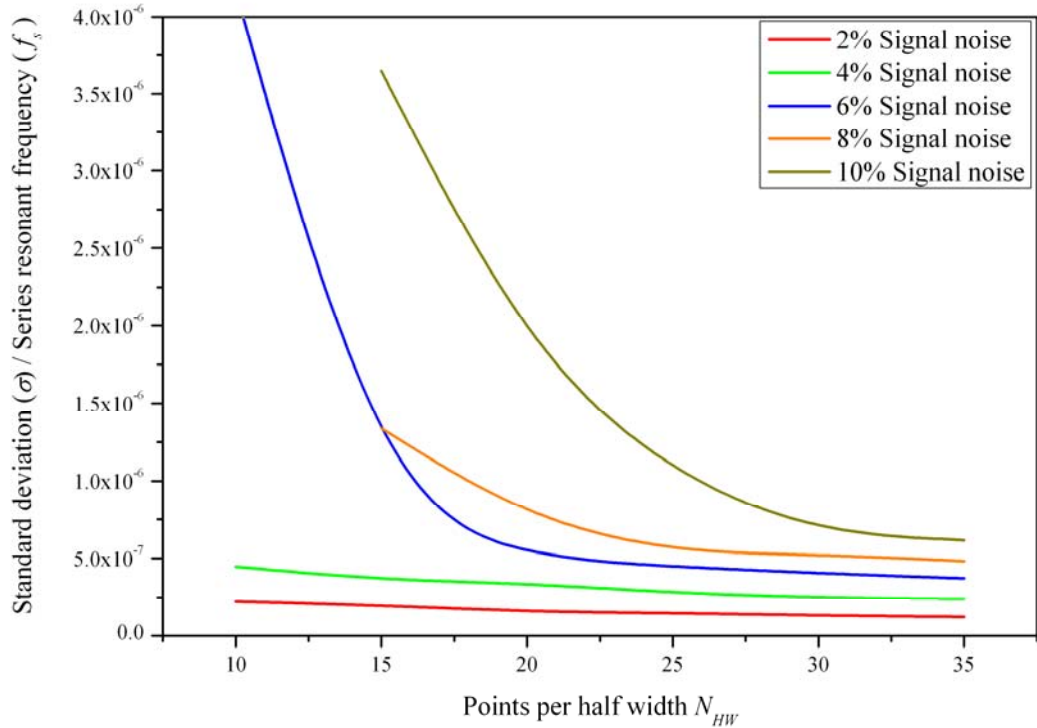


Figure 17: Simulation of different point densities measured as points within a resonance half width. The standard deviation of the series resonance frequency depends on the number of points measured in a half width and the signal noise. The graph shows simulated data for noise levels of 2 to 10%. In many measurement application, the noise is less than 4%. This means, that about 15 points per half width are enough for precise measurements. Increasing the number does not improve measurement results.

Figure 17 shows the precision of the series resonance frequency  $f_s$  versus the number of measured admittance points in the half width of the resonance. The data for this plot was generated in a simulation that adds variable noise to the measurement signal and then evaluates the series resonance frequency. As for many measurement applications the noise is less than 4%, it can be derived from the results of the simulation that setting the number of points per half width to a value of 15 is sufficient for the measurement purposes considered here. A higher  $N_{HW}$  would only lead to an increase in measurement time. The minimum frequency step width is therefore calculated using

$$stepwidth \leq \frac{halfwidth}{15} \quad (20)$$

## 4.2 Measurement quality

The quality of the measurement result is influenced by many different parameters. The number of measured points in the range of a resonance determines the precision of the measurement result. The scan mode and its parameters define the number of points used in a measurement. A DC offset coming from offset errors in the kernel electronics can disturb the measurement result. A compensation that cancels out the errors coming from this DC offset is implemented in the *QxSens* system. In some measurement applications the cable compensation leads to a reduction of the admittance signal. This effect generates an offset in the conductance and susceptance values. The offset is nearly linear and can therefore be compensated with a baseline compensation method. Besides the described offset problems, one of the most important points when dealing with high frequency RPCs is the problem of transient phenomena. And finally, the signal-to-noise ratio is also very important for the accuracy of the measurement results.

### 4.2.1 Scan modes

Resonance measurement is based on a stepwise admittance scan over a given frequency range, where the admittance spectrum of the sensor is measured. In the *QxSens* system there are two modes for an admittance scan. The linear mode divides the measurement range given by the start and the stop frequency into equal parts. Each frequency step has a constant width. The second mode uses dynamically calculated step widths. That means, the actual-step width is calculated for each measurement interval using the noise of the conductance as parameter.

In the linear mode the frequency range is scanned linearly using constant frequency steps. This is the easiest and most common method to scan a given frequency range. It is a very fast method, as long as the frequency range is small. The reason for this is that as the step width is constant, no computation concerning the step width is necessary during the admittance scan. Another advantage follows from the fact, that the step width must be small in order to give precise resonance measurement results. It is shown in 4.1.2 that the step width must satisfy the expression (20). Hence, with a constant small step width the admittance change from one frequency step to the next is small and therefore no or at least very small transient phenomena occur. Scanning wide frequency ranges with the linear mode increases measurement time significantly because also many admittance values outside the range of the series resonance frequency are measured. These measurement points do not improve measurement accuracy, but increase measurement time. That means the linear mode is the best choice, if the resonance parameters  $f_s$  and  $Q$  are known approximately, for example in sensor applications.

In the dynamic non-linear scan mode the actual frequency step width is calculated depending on the noise of the last 15 conductance values. The conductance is used because it is not influenced by the parallel capacitance of the sensor and therefore it is sensitive to find even small resonances of sensors with a high parallel capacitance. Taking 15 points was an experimentally determined value. It is a good choice to calculate the signal-to-noise ratio of the conductance out of the last 15 points. This means that the first 15 points have to be measured without using this dynamic approach. Hence, the linear mode is used for the first 15 points with the minimum step width. Out of this the signal-to-noise ratio of the measured conductance values can be derived. Every further measured conductance value is compared to the calculated noise-level. If the conductance is outside the noise-level, the step width is reduced by 20% and the measurement continues at the last measured frequency. The measured conductance and susceptance values are stored separately, in order not to disturb the step width calculation. The reduction of the step width is done until a minimum step width, given as a parameter, is reached. The minimum step width determines the measurement precision. In order to get precise measurement results, the minimum step width has to satisfy the same relation (20) as in the linear mode. This means that the point-density and hence the measurement precision in the range of a resonance is the same in the non-linear and the linear mode. In the non-linear scan mode the point-density can even be increased. The separately stored conductance and susceptance values can be used in the resonance analysis as additional points. This gives a higher point density and therefore a better basis for the resonance analysis. If the measured conductance value is in the range of 20% of the calculated noise-level, the step width is increased by 20%. This speeds up the measurement without decreasing the measurement result's accuracy. The maximum

of the step width is a multiple of the minimum step width. The multiplication factor is given as a parameter called max-factor. The higher the max-factor the higher is the measurement speed. But if the maximum step width is too large, small peaks may be skipped. Another problem with large step widths is, that transient phenomena have to be considered. This partly reduces the possible speeding-up of the measurement, as an artificial wait after setting the next frequency point has to be applied. The possibility of fast and still precise measurements makes the non-linear scan mode the best choice when scanning large frequency ranges for unknown resonances or analysing unknown admittance spectra. The high computational effort of calculating the new frequency values where the conductance changes rapidly, makes the non-linear mode slower than the linear mode when scanning small frequency ranges in the vicinity of a resonance.

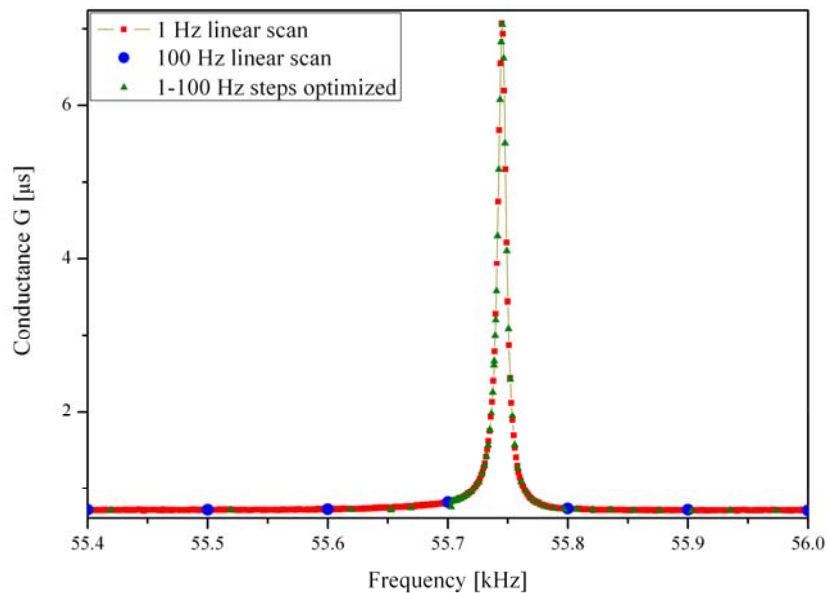


Figure 18: Comparison between the linear and the non-linear scan mode. This figure shows measurements using the linear scan mode with low resolution (100 Hz step width) and high resolution (1 Hz step width) and the non-linear scan with dynamically adapted step width. It can be seen that the low resolution linear scan skips the peak. The high resolution linear scan measures the peak with a very high resolution but also measures many points besides the peak, that do not give more information. The non-linear scan adjusts the step width dynamically and therefore scans only the peak with high resolution, which leads to an increase in measurement speed.

Three measurements have been done to demonstrate the different functionalities of the scan modes. The results are displayed in Figure 18 and Figure 19. Two frequency scans have been recorded using the linear mode. The first one uses a step width of 1 Hz, which gives a very good resolution of the admittance circle. But it also measures a lot of useless<sup>1</sup> points besides the series resonance frequency, which makes the measurement

---

<sup>1</sup> “useless” in terms of not improving the results of the resonance analysis.

very time-consuming (about 5 minutes). The second linear scan is done with a step width of 100 Hz. This speeds up the measurement to less than 1 s, but it skips the resonance and therefore this settings lead to useless measurement results. The non-linear scan is done with a minimum step width of 1 Hz. This gives at least the same resolution as in the first linear scan especially in the range of interest, near the series resonance frequency. The max-factor is set to 100, so the maximum step width is 100 Hz. This speeds up the measurement in frequency ranges where the conductance is changing only lightly. The result of the non-linear scan shows that the point density is optimized. In the range of the series resonance frequency the point density is even higher than in the linear mode. Besides the resonance the point density is decreased. From this it follows that the measurement results are as good as in the linear mode, but the measurement time is about 100 times faster shorter.

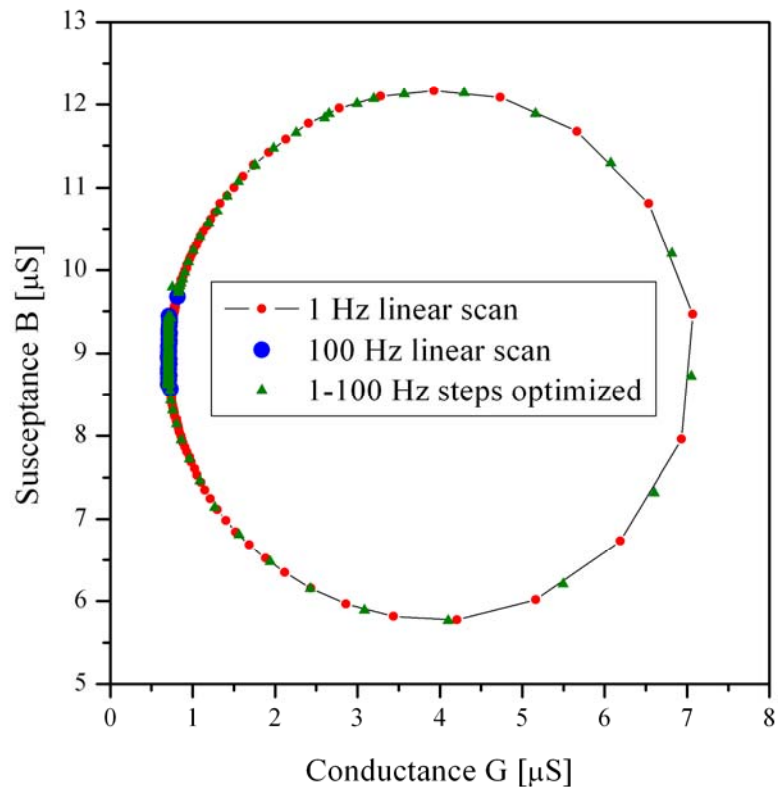


Figure 19: Locus of admittance of the comparison between the linear and the non-linear scan mode (see Figure 18).

#### 4.2.2 DC offset compensation

When the output voltage of the synthesizer is turned off, the four signals  $S_1..S_4$  should theoretically be zero. But measuring the four signals shows that there are still

signals of up to 30 mV. These remaining potentials are caused by offset errors of the electronic components and its different ground potentials. This DC offset leads to disturbance of the measured admittance values.

The DC offset can be compensated by measuring the DC offset signals prior to the resonance scan and subtracting these DC compensation signals from the measurement signals before the admittance calculation is performed. Thus the DC offset compensation needs an initialization before the resonance scan is started. For that reason, the output voltage of the synthesizer is set to zero and the remaining DC offset signals coming from the kernel electronics are measured. This initialization has to be done before each resonance scan, to avoid drift of the offset voltages between two subsequent resonance scans which could be more than 50%. During the resonance scan every measured signal from the kernel electronics is corrected by subtracting the corresponding DC compensation signal.

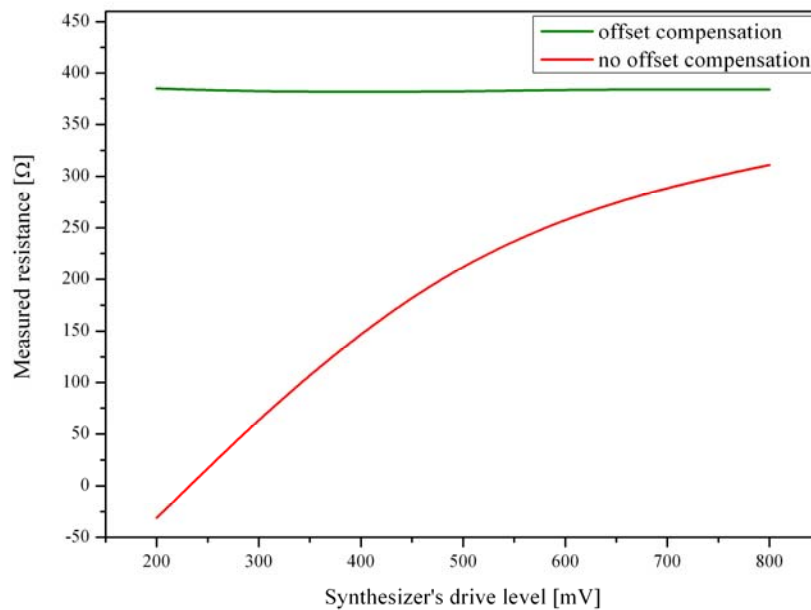


Figure 20: shows the effect of the DC offset compensation. A resistor with a nominal value of 390  $\Omega$  was measured with the DC offset compensation turned on and off. The non-compensated measurement shows a strong drive level dependency, which is associated with a signal distortion during the admittance scans of RPC sensors.

The effect of the DC offset compensation can be demonstrated most impressively by varying the drive level of the synthesizer. To ensure well defined conditions a resistor of 390  $\Omega$  was used instead of an RPC. A reference measurement with the impedance network analyzer Agilent 4395A gives a nominal value of 384  $\Omega$  at 100 kHz. The same resistor was measured with the *QxSens* system with a constant frequency of 100 kHz and a varying drive level. Figure 20 shows the measurement results. It can be seen that without compensating the DC offset the measured resistance

changes very strongly with the drive level. This is an effect that is totally unphysical. Theoretically the resistance of a resistor must be independent from the drive level. This is only true if the DC offset compensation is turned on.

### **4.2.3 Baseline compensation**

A main problem of the cable compensation of the kernel electronics described in section 3.2 is the limitation of the length of the triaxial cable. The length depends on the frequency and its limit is given in (11). When using longer cables, the cable compensation causes spurious effects. These effects can be seen in a baseline that distorts the measurement results and in some cases makes the resonance analysis impossible. The main reason for this baseline is a small phase shift between the voltages at the inner conductor and the first shielding. It reduces the compensation effect. In addition, a parasitic voltage from the signal of the first shielding is coupled to the inner conductor. This results in a reduction of the measured admittance and can be seen as an offset (baseline) in the conductance and susceptance spectra. This is not a problem as long as the changes of the admittance in the resonance range are large. But strongly damped oscillators (sensors) show only small changes of the admittance. Therefore the data analysis of such oscillators is distorted by the effects of the non-perfect cable compensation. To overcome this problem it is possible to compensate this baseline by subtracting the baseline from the admittance measurement result before the resonance analysis is started. A linear approach can be used, because the offset coming from the cable compensation is approximately linearly increasing with frequency in the small frequency range that is commonly used for resonance measurement.

The baseline compensation is initialized before the resonance scan is started. First the conductance and susceptance values at the start and the stop frequency are measured. Then the respective measurement points are used to fit a straight line function in the conductance and the susceptance values, respectively. In many measurement applications where fast continuous resonance scans must be done, only a small part of the resonance peak, near the series resonance frequency, is scanned. Initializing the baseline at the start and the stop frequency would lead to a wrong baseline compensation in these cases because the baseline must be placed under the whole peak. To overcome this problem there is a possibility to expand the frequency range used for the baseline initialization. Prior to the resonance evaluation the measured conductance and susceptance values are baseline-corrected. The conductance and susceptance compensation values are calculated by evaluating the respective straight line function at the corresponding frequencies. These compensation values are then subtracted from the respective measured values giving a compensated admittance

spectrum. The compensated spectrum is shifted to zero, but this shift does not affect the results of the resonance evaluation.

Figure 20 shows the functionality of the baseline compensation for the conductance. The red line is the measured conductance. The blue line is the baseline under the resonance peak that is created in the initialization of the baseline compensation. The green line shows the compensated conductance spectrum.

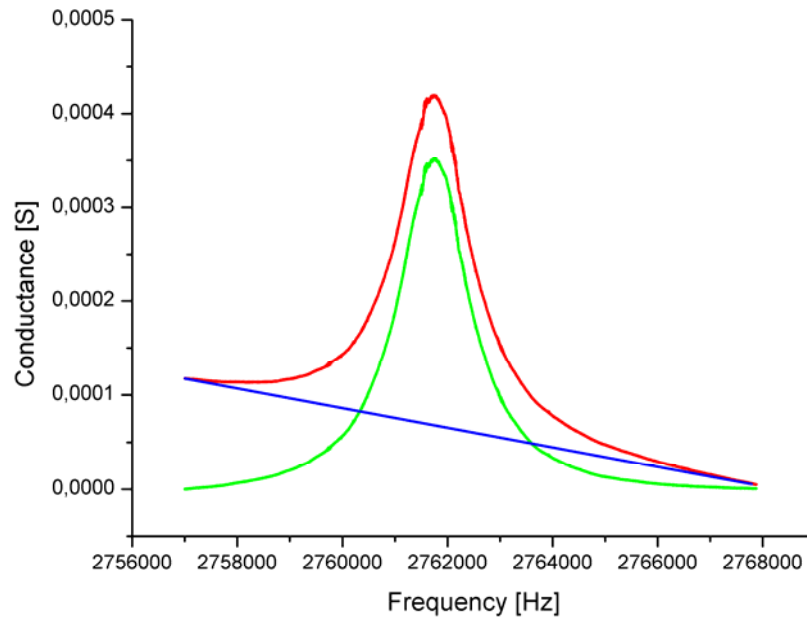


Figure 21: shows the functionality of the baseline compensation. The red line shows the raw measurement data without any compensation. The baseline (blue line) is calculated out of the conductance values at the start and the stop frequency of the measurement. The green line shows the compensated conductance curve.

As stated above, the baseline compensation should be used when measuring highly damped oscillators connected with longer triaxial cables. Viscosity measurements of high-viscosity fluids in industrial processes are a good example for such a measurement application.

#### 4.2.4 Transient phenomena consideration

When measuring oscillating systems in a step-wise frequency scan, transient phenomena occur after each discrete frequency step. It can be shown that the transient time is a function of the frequency and the damping and it is also influenced by the resistor in the kernel electronics' voltage divider [14]. The amplitudes of the transient phenomena are small when measuring frequencies far away from or exactly at the series resonance frequency. Transient phenomena can then be neglected. The problem is, that especially in the frequency range commonly used in resonance measurements, that is, a

few half-width lengths besides the series resonance frequency, transient phenomena show a noticeable effect. The disturbing effect is even worse, if a big frequency step precedes the actual measurement. An important parameter to describe the influence of transient phenomena is the time constant  $\tau$ . It describes how fast the amplitudes of the transient phenomena decrease. More precisely, it is the time when the amplitude has decreased by  $1/e$ .

In the *QxSens* system, the transient time of the kernel electronics itself as well as the transient time of the kernel-electronics plus the sensor have to be regarded. The transient time of the kernel electronics is constant and smaller than 1 ms [14]. The runtime of the *QxSens* software, which is about 1 ms, gives this delay automatically. The time constant  $\tau$  of the kernel electronics plus the sensor depends on the kernel electronics' reference impedance  $R_C$  and the values  $R_1$  and  $L_1$  of the sensor and can be calculated to

$$\tau = \frac{2L_1}{R_1 + R_C} \quad (21)$$

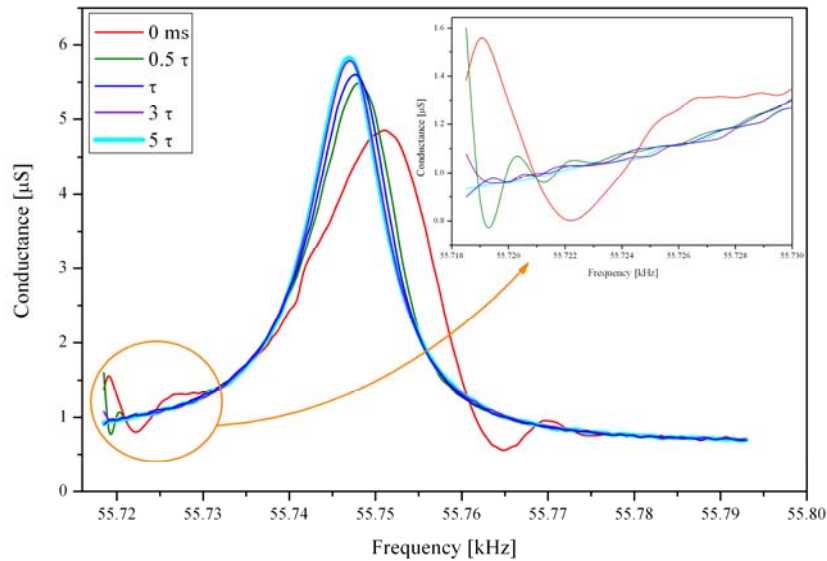


Figure 22 shows the disturbing effect of the transient phenomena. The transient phenomena influence the measurement results of the series resonance frequency and the quality factor. Only after a time delay at least  $3\tau$  the measurement results of the series resonance frequency and the quality factor are quite correct.

An artificial delay between each change of the output frequency of the synthesizer and the subsequent recording of the measurement values can reduce the effects of transient phenomena in the *QxSens* system. The delay is controlled by the “wait” parameter. Figure 22 shows the relation between wait and  $\tau$ . It can be seen that if wait is greater than or equal to  $3\tau$ , the precision of the measurement result is a maximum. After  $3\tau$  setting time the amplitude of the transient oscillation has decreased

by approximately 95 %. The remaining 5 % amplitude is not distorting the measurement result. It has to be noted that when using a delay time of  $3 \tau$ , transient oscillations still occur at the beginning of the frequency scan. Only if the delay is set to a value greater than or equal to  $5 \tau$ , the amplitude of the transient oscillation has essentially vanished before the measurement signal is recorded. In general it can be stated, that after big frequency steps a delay of  $5 \tau$  is necessary, but between the small frequency steps in a resonance scan a delay of  $3 \tau$  is sufficient.

#### 4.2.5 Signal-to-noise-ratio consideration

The precision of a measurement result depends on the signal-to-noise ratio (S/N) of the measurement signal. In the *QxSens* system the S/N is above all dependent on the level of the measurement signal. The measurement signal  $V_C$ , respectively  $V_S$ , is on the one hand correlated to the output voltage of the synthesizer and on the other hand determined by the ratio of the impedances in the voltage divider of the kernel electronics (see Figure 10).

If the impedance  $Z_C$  in the kernel electronics is about the same size as the impedance of the sensor at the considered series resonance frequency, the S/N is high and therefore the most precise measurement results can be achieved. That means the kernel electronics have to be dimensioned with respect to  $Z_C$  according to the resonance resistance  $R_1$  of the utilized sensor. When the resistance of the sensor is unknown, any (practicable)  $Z_C$  value may be used for the first measurement. To get more precise results the kernel electronics should then be adapted for further measurements.

The output voltage amplitude of the synthesizer determines the maximum level of the measurement signal and therefore the maximum of the S/N. The higher the output voltage the better is the S/N. It has to be noted that the output voltage and thus the generator voltage that is applied to the sensor in the kernel electronics may lead to self-warming of the sensor. This effect becomes important especially when using temperature sensors, because consequently the self-warming results in incorrect temperature measurement values. When the external USB measurement system is used, another limiting point for the synthesizer output voltage is, that the maximum output voltage of the synthesizer mounted in the external USB version drives the analog multipliers in the kernel electronics into saturation. That means the HF signals are cut at its maximum and minimum values when passing the analog multipliers. From this it follows that the DC signals  $S_1..S_4$  and hence the calculated admittance values are wrong. To avoid this effects the output voltage of the synthesizer in the external USB version must not be greater than 80 % of the possible maximum value.

In every measurement procedure systematic and stochastic errors occur. Systematic errors are caused only by the measurement hardware and therefore are not influenced by measurement parameters. The only thing the *QxSens* user can influence to decrease systematic errors is the appropriate choice of the kernel electronics with respect to the impedance  $Z_C$ . In order to minimize stochastic errors of the measurement result it is necessary to repeat a measurement many times and calculate the mean value as the final measurement result. Therefore in the *QxSens* system at each single frequency point a finite sampling number greater than 2 for each voltage signal  $S_1..S_4$  is applied. In the *QxSens* software the number of samples acquired is also called “average value”. The measurement value is calculated by averaging over the measured number of samples. The higher the number of samples the lower is the noise in the measured signals  $S_1..S_4$ , but the longer is the total measurement time. Measurement time is also a factor that has to be taken into account especially when concerning industrial usage of the measurement system. Therefore the optimal number of samples is always a compromise between measurement speed and measurement accuracy.

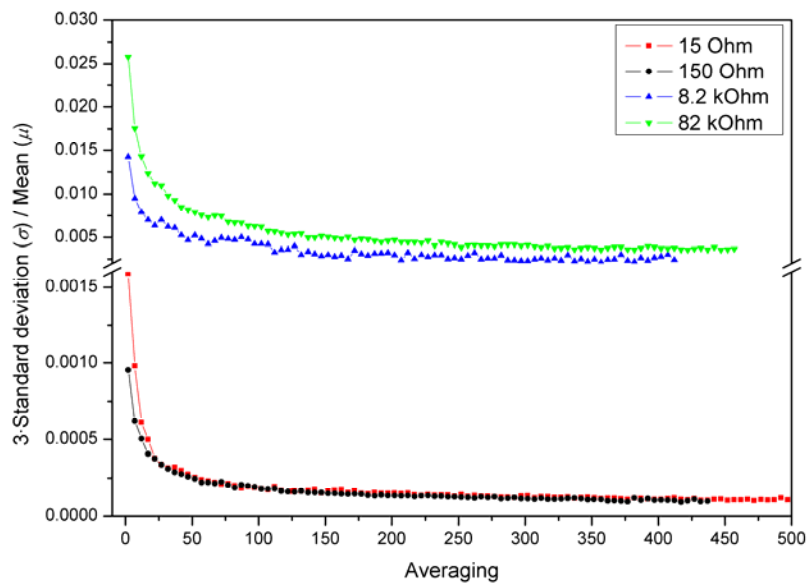


Figure 23: The noise of the admittance measurement results depends on the level of the measurement signal and the averaging value. To get different signal levels, four different resistors have been measured with the same kernel electronics. Each resistor has been measured with an increasing averaging value. At each averaging value the mean value ( $\mu$ ) and the standard deviation ( $\sigma$ ) of the admittance have been calculated out of 1000 measurements.  $3\sigma/\mu$  is then the uncertainty of the admittance measurement results. Firstly, it can be seen that matching kernel electronics (match here for 150 Ohm) produce much less noise in the measurement results than mismatched kernel electronics. Secondly, the measurement results show that an averaging value greater than 100 does not further improve measurement accuracy.

Figure 23 shows the correlation between the stochastic error of an admittance measurement result and the number of samples that has been averaged. The measurement was done at a fixed frequency of 1 MHz. At each averaging value 1000

admittance measurement values have been acquired. The stochastic error was obtained by calculating the mean value  $\mu$  and the standard deviation  $\sigma$  of these 1000 measurement results and taking  $3\cdot\sigma/\mu$  as the uncertainty of the final admittance measurement result. Using  $3\cdot\sigma$  takes approximately all (99.7%) measured values into account. In order to show the dependency of the precision of the measurement result on the appropriate choice (dimensioning) of the kernel electronics, four different resistors (15 Ohm, 150 Ohm, 8.2 kOhm and 82 kOhm) have been measured with the same kernel electronics. The kernel electronics used were of VDP- $V_C$  version with an internal resistor  $R_C$  of 150 Ohm and without a shunted capacitor  $C_C$ . It can be seen that if the measured resistor has about the same value as the kernel electronics' internal resistor, in this case 15 Ohm or 150 Ohm, the stochastic error of the measured admittance value is smaller than 0.2 % for a single point measurement and even less for higher averaging values. When measuring with mismatched impedances of the kernel electronics and the measured resistor, here 8.2 kOhm and 82 kOhm, the stochastic error is between 0.5 and 3 % of the measurement result. As a conclusion from the measurement results plotted in Figure 23 it can be stated that choosing impedance-matched kernel electronics is the main issue that determines the accuracy of the admittance measurement. As second parameter the choice of the averaging value influences the fine tuning of the accuracy. It can be seen that in all cases using an averaging value greater than 100 does not further improve measurement results. A good compromise between measurement accuracy and measurement speed is to use an averaging value of 20 to 30. This speeds up the measurement while giving measurement results with an error less than 0.05 %, anyhow.

### 4.3 Measurement process description

The resonance measurement process is divided into five steps (Figure 24). The self organizing module finds out which hardware components are used in the given measurement system. At the initialization the hardware components are reset and the compensation algorithms are initialized. After the initialization the measurement of the conductance and susceptance is performed in the frequency scan. In the next steps the resonance characteristics are calculated out of these values and the results are displayed and optionally saved to disk.

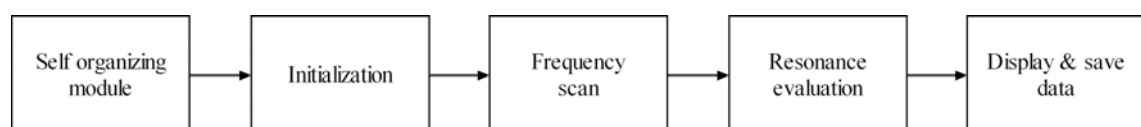


Figure 24: Schematic overview of the resonance measurement process.

### 4.3.1 Self organizing module

As explained in chapter 3.1.1, there are three different versions of the computer system used for the *QxSens* system. There are two reasons why it is necessary to find out which hardware components are used in a given computer system. When a device, like a DAQ (data acquisition) device or a synthesizer board, is installed in a computer system an identifier is assigned to this device. This identifier is unique within the computer system but can differ between computer systems. Software, that uses the device, needs this identifier to control it. In the *QxSens* system it is necessary to find out the identifier of the NI DAQ device and the synthesizer installed. It is also necessary to find out exactly which type of NI DAQ device is installed because some DAQ properties are only available on certain types of NI DAQ devices, e.g. dithering. The detection of the identifier and the type of the NI DAQ device is done automatically. The only decision the user has to make is whether an internal or an external version should be used for measurement. This decision cannot be made automatically, because it is possible to connect the external USB version to an internal PC/PXI *QxSens* system. In this case the system cannot know which DAQ device and sensor should be used in the current measurement.

The detection of the NI DAQ device is the same in the internal and the external computer systems. The identifier is found out by checking the device name of every installed NI DAQ device. If the device name of the checked NI DAQ device matches a name in Table 1, this device is used for the measurement. The type of the device is corresponding to its device name. If no device corresponding to one of the devices in Table 1 can be found, an error message is displayed.

<b>NI DAQ device name</b>	<b>System Type</b>	<b>Resolution</b>
PCI-6024E	PC	12 bit
PXI-6025E	PXI	12 bit
PCI-6036E	PC	16 bit
DAQPad-6016	USB	16 bit

Table 1: Device names used in the automatic NI DAQ device detection.

The synthesizer detection is different for the internal and the external version. In the internal version (PC/PXI) up to 4 synthesizers (TE 5100 boards) can be installed. Each installed TE 5100 board has a unique ID from 0 to 3. For each ID a check is done to find out, whether a board is present on this ID, starting with ID 0. The first board found is used for the measurement. The external version contains a USB-to-COM converter for the programming of the synthesizer board (DDS8m). When the converter is installed in the PC/PXI, an arbitrary, free serial port number is assigned to the COM

port. Therefore, it is necessary first to find out which COM ports are installed. Then initialization commands<sup>2</sup> are sent to each COM port. The replies of the devices connected to the COM ports are analysed. If the reply from a device matches the expected reply from the DDS8m board, it is assumed that the external USB version is found on that COM port.

### 4.3.2 Initialization

The initialization process starts with a hardware reset. Then a DAQ task for the measurement is created. After that the DC-compensation is initialized. The DC-compensation is necessary for the compensation of a DC-offset caused by the kernel electronics. Optionally a baseline in the conductance/susceptance spectrum that affects the results of the resonance measurement can be compensated by the *QxSens* system. The initialization of this compensation is done in the next step. Finally the scan direction is detected and the start values for the admittance scan are set.

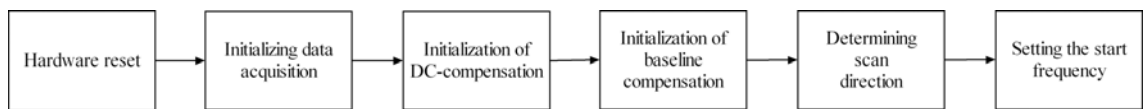


Figure 25: Schematic overview of the initialization of the resonance measurement.

#### 4.3.2.1 Hardware reset

Each hardware component used in a measurement system has to be reset to its factory default settings before a measurement is started. This is done in order to avoid effects from previous uses of the hardware components. The hardware reset is done once every time the *QxSens* software is launched.

The internal synthesizer is reset by calling the function `te51_Initialize_DDS` from the `te5100sg.dll`. The external synthesizer is reset by sending a reset command "R" via the COM port. By default the DDS8m board sends each command back as an echo. As this behaviour would lead to a loss of time in the measurement process, the echo function is turned off by sending the "E D" command via COM. A detailed description of the programming is given in the TE5100 Programming Manual [19].

The DAQ devices are reset by using the reset function from the NI DAQ drivers.

---

<sup>2</sup> The initialization of the DDS8m board is done by sending a reset command "R" and an echo disable command "E D" to the DDS8m board. The reply to these commands has to be "E D" and "OK".

### 4.3.2.2 Initializing the data acquisition

The DAQ concept of NI is based on DAQ tasks. A DAQ task represents a measurement to be performed by a DAQ based measurement system. Based on the physical input channels used in a measurement, virtual channels are created. Virtual channels are software entities that encapsulate a physical channel along with other channel specific information. A DAQ task is a collection of one or more virtual channels. The DAQ task used in the *QxSens* system as well as its properties are described in detail in the next paragraphs.

#### 4.3.2.2.1 Physical channels

The input pins on the DAQ device are called physical channels. The *QxSens* system uses 4 input voltages  $S_1..S_4$  for each evaluated sensor. Depending on the channel number used for a measurement, different physical input channels are used (Table 2).

Channel Number	DAQ Input Channel
1	AI0, AI1, AI2, AI3
2	AI4, AI5, AI6, AI7
3	AI8, AI9, AI10, AI11

Table 2: Analog Input channels (AI)

#### 4.3.2.2.2 Virtual channels

Based on the 4 physical input channels used for a given channel number, 4 virtual channels are created. These virtual channels are named in the following way:  $SA\_B$ , where  $A$  is the signal number 1 to 4 and  $B$  is the channel number. For example, the virtual channel  $S2\_1$  stands for the signal  $S2$  of the channel number 1. It is therefore connected with the physical input channel AI1.

#### 4.3.2.2.3 Units

The DAQ task can handle different units of the digitized input voltages. The resonance measurement process uses Volts as unit for all calculations. Therefore this property is set to Volts.

#### 4.3.2.2.4 Input terminal configuration

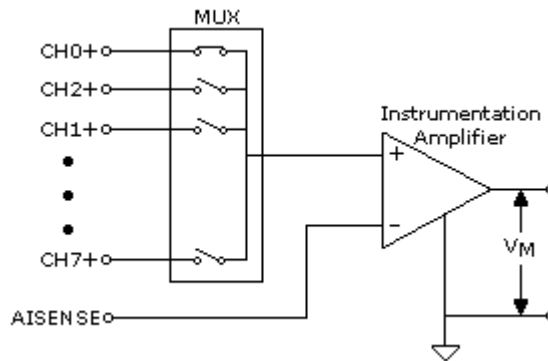


Figure 26: Schematic drawing of the non-referenced single-ended mode of the DAQ device [20]. The input channels are signals referenced to AISENSE.

The input terminal configuration determines how the DAQ device measures input voltages. There are several possible types of input terminal configuration. In the kernel electronics the signals  $S_1..S_4$  are DC voltages measured against ground. Therefore the non-referenced single-ended mode (NRSE) of the DAQ device is the best choice for this measurement task. Figure 26 shows how an NRSE system works. In the *QxSens* system the kernel electronics' ground is connected to the single-node analog input sense pin (AISENSE). The wires for the signals  $S_1..S_4$  are connected as described in the section Physical channels.

#### 4.3.2.2.5 Input limits

The input limits determine how the DAQ device processes the input signals. Different input limits lead to different gain settings of the amplifier used in the DAQ device. To get the best measurement results, the input limits should be adapted to the used voltage range in the measurement. In the *QxSens* system a minimum value of -5 V and a maximum value of +5 V have approved to return good measurement results.

#### 4.3.2.2.6 Sample mode and averaging

Any NI DAQ device can perform single point measurements, continuous measurements or measurements of a certain number of samples. As described in chapter 4.2.5 the *QxSens* system measures a finite number of samples at each frequency step (averaging). The number of samples is defined by the averaging value. The averaging reduces the statistical errors of the measurement results.

#### 4.3.2.2.7 Dithering

The low resolution of a 12 bit AD converter may create noise, known as quantization error. To minimize this type of error, 12-bit DAQ boards from NI can improve resolution with a hardware technique called dithering (see 3.2). So, first it has to be found out, if a 12 bit DAQ device is used. Table 1 shows which device names are

associated with a 12 bit DAQ device. In the self organizing module described in 4.3.1 the device name of the DAQ board is detected at program start. This device name is compared with Table 1 and if the DAQ board is a 12-bit AD converter dithering may be enabled.

In the NI DAQ documentation it is stated that dithering only should be used when sampling at least 50 values at one measuring point [7]. Therefore, dithering is automatically enabled when the averaging value is greater than or equal to 50 and a 12 bit DAQ device is used. In all other cases dithering is disabled.

### 4.3.2.3 Initialization of the DC-compensation

The signals  $S_1..S_4$  can have a DC offset of up to 30 mV, when the output voltage of the synthesizer is set to zero. Compensating this DC offset with the DC offset compensation described in 4.2.2 reduces the negative effects of the DC offset on the measurement results.

The compensation of the DC offset is done by measuring the offset values  $S_{10}..S_{40}$  at drive level zero and subtracting these offset values from the measurement signals  $S_1..S_4$  before calculating the conductance and the susceptance out of the measured signals. The initialization of this compensation is done by setting the output voltage of the synthesizer to zero and measuring the 4 offset signals  $S_{10}..S_{40}$  at the start frequency. The measured signals are stored for further processing during the frequency scan. The initialization of the DC offset has to be done before each resonance scan, because the drift of the offset voltages between two subsequent resonance scans can be more than 50% during a log operation time. After the measurement of the offset signals the amplitude of the output voltage of the synthesizer is reset to the value that will be used for the frequency scan. As explained in 4.2.4 the precision of the admittance measurement depends amongst others on the transient phenomena after a frequency change. During the frequency scan, where the frequency steps are small, the transient oscillations have decayed after about  $3\tau$ , hence the wait parameter should be set to this value. The problem with this recommendation is that  $\tau$  is not known before a measurement, as it can only be estimated from the equivalent circuit parameters after the measurement using (21). Therefore the wait parameter is usually set to a value, where the measurement results appeared to be good and the locus of admittance is not distorted. This is an empirical value to be set by the user of the measurement system. If a big frequency jump is done between two measurements, as being the case during the initialization procedure, the actual transient time is unknown. And also the actual transient time is unknown. It may be much longer due to resonances between the two frequency points. To ensure, that all transient phenomena have vanished before the actual measurement starts, the system waits 5 times longer as in the normal frequency scan. This value is fixed pragmatically based on experiences from many experimental

investigations. It ensures that the following measurements are not distorted by transient phenomena caused by a preceding big frequency jump. The disadvantage of the longer measurement time is overbalanced by the advantage of accurate measurement results in all measurement applications, especially because this long break occurs only during initialization once in a measurement.

#### 4.3.2.4 Initialization of the baseline compensation

As described in 4.2.3 the cable compensation may in some cases lead to an admittance baseline that affects the measurement results. The baseline compensation, that compensates this effect, can be switched on depending on the particular measurement application. By default the compensation is disabled.

For the initialization of the baseline compensation two admittance values are measured at two different frequencies,  $f_{C1}$  and  $f_{C2}$ . By default the start and the stop frequency are used as  $f_{C1}$  and  $f_{C2}$ , respectively. In some cases the approximation of the physical baseline by the compensation line can be improved by expanding the frequency range between  $f_{C1}$  and  $f_{C2}$ . This expansion is controlled by the parameter expand-frequency-range (*EFR*).  $f_{C1}$  and  $f_{C2}$  are then given as follows.

$$\begin{aligned}
 f_{C1} &= f_{Min} - EFR \\
 f_{C2} &= f_{Max} + EFR \\
 f_{Min} &= \text{Min}(f_{Start}, f_{Stop}) \\
 f_{Max} &= \text{Max}(f_{Start}, f_{Stop})
 \end{aligned}
 \tag{22}$$

In 4.3.2.3 it was explained that after a big frequency step the transient phenomena are enhanced and therefore the artificial wait after a big frequency step has to be prolonged. Hence, in the initialization of the baseline compensation the system pauses a time in milliseconds that corresponds to 5 times the value of (1+wait parameter) after setting the frequencies  $f_{C1}$  and  $f_{C2}$ .

The connection line between the two measured admittances is called the compensation line. The compensation lines for the conductance  $G_{CL}$  and the susceptance  $B_{CL}$  are calculated separately by fitting linear functions into the measured conductance and susceptance values.

$$\begin{aligned}
 G_{CL}(f) &= k_G \cdot f + d_G \\
 B_{CL}(f) &= k_B \cdot f + d_B
 \end{aligned}
 \tag{23}$$

Formula (24) shows the calculation of the parameters of these linear functions. The calculated values  $k_G$ ,  $d_G$ ,  $k_B$ ,  $d_B$  are stored in memory for further processing.

$$\begin{aligned}
k_G &= \frac{G_{C2} - G_{C1}}{f_{C2} - f_{C1}} \\
d_G &= G_{C2} - k_G f_{C2} \\
k_B &= \frac{B_{C2} - B_{C1}}{f_{C2} - f_{C1}} \\
d_B &= B_{C2} - k_B f_{C2}
\end{aligned} \tag{24}$$

#### 4.3.2.5 Determining the scan direction

The frequency range can be scanned upwards or downwards. The ability of scanning in two directions is necessary for some search algorithms. It is important to note that the scan direction does not influence the measurement result but the direction of the frequency scan must be known when calculating the frequency of the next measuring point. Therefore the scan direction is detected in this process step. The scan direction is upwards if the stop frequency is higher than the start frequency and the step width parameter is greater than zero. The frequency range is scanned downwards if the start frequency is higher than the stop frequency and the step width is negative. If the start frequency, the stop frequency and the step width as entered by the user do not match one of these conditions, an error is raised.

#### 4.3.2.6 Setting the start frequency

The output signal frequency of the synthesizer is set to the start frequency and the output amplitude is set to the value given in the V\_RMS parameter. It is assumed that the difference between the last frequency set on the synthesizer and the start frequency is big (initialization). Therefore the system waits 1 ms for the transient time of the kernel electronics and additional 5 times the time given in the wait parameter to ensure that the transient phenomena have vanished before the frequency scan is started.

### 4.3.3 Frequency scan

In the frequency scan the chosen frequency range given by the start and the stop frequency is scanned stepwise in a loop. At each frequency step the measurement signals  $S_1..S_4$  are acquired and the admittance is calculated out of these values. The measured data triples, frequency, conductance and susceptance, are stored in a measurement data array. Depending on the STEP WIDTH parameter the frequency for the next measuring point is calculated.

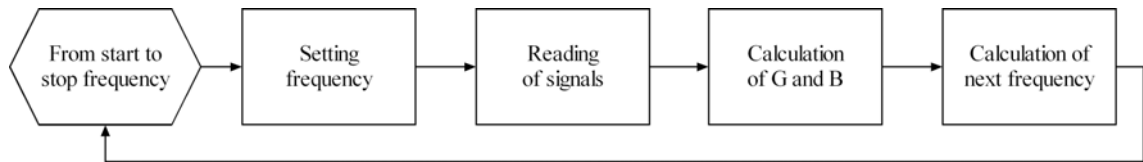


Figure 27: Schematic overview of the frequency scan loop in the resonance measurement process.

### 4.3.3.1 Setting the frequency

When the loop is entered, the output frequency of the synthesizer is already set to the start frequency and therefore this step is skipped. At every further pass of the loop the frequency calculated as the frequency of the next measuring point is set as output frequency. After each frequency setting of the synthesizer the system waits in order to avoid transient phenomena. The wait time is given in the wait parameter. A minimum wait of 1 ms is included for the transient time of the kernel electronics.

### 4.3.3.2 Reading of signals

The measurement signals  $S_1..S_4$  coming from the kernel electronics are digitized by the A/D converter on the DAQ board in the computer system. As described in 4.3.2.2 the NI DAQ measurement concept is based on DAQ tasks. In this process step the actual data acquisition is done using the DAQ task defined earlier in the initialization process. The measurement values are read using the NI DAQ multi-channel multi-sample data reading function. This function reads a given number of samples on several channels at once. In the QxSens system the number of samples is given by the averaging value. The number of channels is 4 according to the 4 measurement signals  $S_1..S_4$ . The result of this measurement is an array. Only if the averaging value is smaller than 6, the measurement is faster when several single point measurements are done instead of multiple samples. In this case the NI DAQ multi-channel single-point data reading function is used and after each measurement the acquired data is put into an array. In both cases the resulting array of measurement values has two dimensions. The first dimension stands for the signal number, 1 to 4, and the second dimension contains the measured values. Averaging over the values in the second dimension results in the 4 measurement signals  $S_1..S_4$ .

Before the measurement signals are evaluated, a consistency check is performed. If one consistency rule is not fulfilled, an error is raised. Possible errors are the following. The normalizing signals  $S_3$  and  $S_4$  must be of nearly the same level. A defect in the QxSens cable can cause differences between these two values. An error occurs if the difference between  $S_3$  and  $S_4$  is greater than 10% of the maximum of  $S_3$  and  $S_4$ . If the values  $S_3$  and  $S_4$  are about the same but approximately zero<sup>3</sup>, the kernel electronics may

---

<sup>3</sup> Approximately zero is defined here as smaller than 0.1.

be faulty or not connected properly to the computer system. The measuring signals  $S_1$  and  $S_2$  are related to the connected sensor. Therefore if  $S_3$  and  $S_4$  are correct but  $S_1$  or  $S_2$  are nearly zero<sup>3</sup>, it can be deduced that the sensor is faulty or not connected properly to the kernel electronics.

### 4.3.3.3 Calculation of G and B

The measurement signals  $S_1..S_4$  still include the DC offset voltages that are caused by offset errors coming from the kernel electronics. The DC-compensation that compensates these effects has been initialized in 4.3.2.3. The result of the initialization are the 4 DC-compensation signals  $S_{10}..S_{40}$ . Before calculating the conductance  $G$  and the susceptance  $B$  the measurement signals  $S_1..S_4$  must be corrected by subtracting the DC-compensation values  $S_{10}..S_{40}$  from the measurement signals  $S_1..S_4$ .

$$S_i = S_i - S_{i0} \quad i = 1..4 \quad (25)$$

It can be seen in 3.2 that the measurement signals  $S_1$  and  $S_2$  carry the admittance information of the connected sensor. The reference signals  $S_3$  and  $S_4$  contain only the information of the generator voltage and the reference voltage. In the calculation of the conductance  $G$  and the susceptance  $B$  out of these measurement signals the ratios

$$K_1 = \frac{S_1}{S_3} \quad (26)$$

$$K_2 = \frac{S_2}{\sqrt{S_3 \cdot S_4}}$$

are used.

Depending on the employed type of kernel electronics, different formulas are used to calculate the admittance values  $G$  and  $B$ .

VDP- $V_C$  type:

$$G = \frac{K_1 - K_1^2 - K_2^2 - \omega C_C R_C K_2}{R_C (K_2^2 + (K_1 - 1)^2)} \quad (27)$$

$$B = \frac{K_2 - \omega C_C R_C (K_1^2 + K_2^2 - K_1)}{R_C (K_2^2 + (K_1 - 1)^2)}$$

VDP- $V_S$  type:

$$G = \frac{K_1 - K_1^2 - K_2^2 + \omega C_C R_C K_2}{R_C (K_2^2 + K_1^2)} \quad (28)$$

$$B = -\frac{K_2 + \omega C_C R_C (K_1^2 + K_2^2 - K_1)}{R_C (K_2^2 + K_1^2)}$$

For each measuring point, the measured data triple, frequency, conductance and susceptance, is added to the measurement data array.

#### 4.3.3.4 Calculation of the next frequency

In the frequency scan the frequency range from start to stop frequency is scanned stepwise. That means that admittance values are measured at several frequency points between the start and the stop frequency. The calculation of the next frequency where the next admittance value will be measured is controlled by the given frequency scan parameters. The frequency scan parameters define the mode that is used for the calculation of frequency steps, linear or non-linear. Depending on the chosen mode different additional parameters influence the actual calculation. The scan direction detected in 4.3.2.5 is also important for the calculation.

In the linear mode the frequency range is scanned linearly using constant equal steps determined by the step width parameter  $f_{step}$ . If the frequency range is scanned upwards, the next frequency  $f_{Next}$  is calculated using

$$f_{Next} = f_{Current} + f_{step} \quad (29)$$

The loop is terminated if  $f_{Next}$  is greater than the stop frequency. Formula (30) gives the next frequency if the scan direction is downwards. In this case the loop is terminated if  $f_{Next}$  is smaller than the stop frequency.

$$f_{Next} = f_{Current} - f_{step} \quad (30)$$

The non-linear mode uses dynamically adapted step widths. The actual step width is calculated after each measurement point. It depends on the noise of the conductance and the change of the actual conductance with respect to the last measured value. The noise is calculated out of the change of the conductance from one frequency point to another. If this change is increasing significantly, the step width is decreased in order to get precise measurement results. If the change decreases significantly, the step width is increased to speed up the measurement. Figure 29 shows the Nassi-Shneiderman diagram of the CalculateNextFrequency function. This function calculates the next frequency that will be used for the next admittance measurement. It takes the array with the already measured conductances ( $G[]$ ) as well as the *stop frequency*, the *current step width*, the *minimum step width* and the *maximum factor* as input parameters. The *current frequency* is the frequency at which the current admittance measurement has been done. When the loop is passed for the first time, the *current step width* is the initial step width given by the user. After the first calculation of the next frequency has been performed, the *current step width* is the last calculated step width. The sign of the step width depends on the scan direction. If the scan direction is upwards, the step width is positive. If the scan direction is downwards, the step width is

negative. The calculated new step width is bounded at the lower limit using the value given in *minimum step width*. The higher limit is given by the product of the *minimum step width* with the *maximum factor*. The output values of the CalculateNextFrequency function are the *next frequency* and the *next step width*. The *next frequency* is the frequency that will be used for the next admittance measurement. The *next step width* gives the difference between the *next frequency* and the *current frequency*. In addition the function has also two output flags. The *step with reduced* flag indicates if the step width was reduced. The *stop condition* flag is true, if the end of the frequency range has been reached.

In the first 15 passes of the frequency scan loop, the *next frequency* is calculated out of the *current frequency* and the *minimum step width* in the same way as in the linear scan mode. This is done because the dynamic step width calculation used in the non-linear scan mode does only work properly if more than 15 conductance values have been measured. That follows from the fact that in the non-linear mode the calculation is based on the comparison of conductance changes with the mean value of the pairwise differences of the last conductance values. It can be shown that this mean value is not convincing before at least 15 values can be used for the calculation of the mean value. In the first 15 passes of the loop the *next frequency* is calculated like in the linear mode by adding the *minimum step width* to the *current frequency*. The flag *step width reduced* is set to false, as the step width is constant.

When at least 15 conductance values have been measured, only the last 15 values of the conductance array  $G[]$  are taken. All other array elements are ignored. The last two conductance values, with index 15 and 14, are used to calculate the change between the conductance measured at the last frequency and at the current frequency,  $\Delta G = |G[15] - G[14]|$ . The CalcMeanDifference function first creates an array out of the pairwise absolute differences of the conductance values given in  $G[]$ . The array elements  $G_{Diff}[]$  are calculated as follows:

$$G_{Diff}[i] = |G[i+1] - G[i]| \quad i = 1..15 \quad (31)$$

The return value of the CalcMeanDifference function is then the mean value of the  $G_{Diff}[]$  array, the so called mean conductance difference (*MCD*). It represents the noise of the conductance. Now the two parameters on which the calculation of the next frequency depends are available,  $\Delta G$  and *MCD*.

A measured conductance change being significantly above the calculated noise-level indicates an actual measuring frequency in the vicinity of a resonance. In this case the step width is decreased in order to get precise measurement results. Comparing the last conductance change  $\Delta G$  with 4 times the mean conductance difference (*MCD*) has proven to be a good indication for a significant change in the conductance. Thus, if the

last conductance difference  $\Delta G$  is greater than 4 times the  $MCD$  and the step width has not yet reached its lower limit, the step width is reduced and re-calculated by dividing the current step width by 1.2. The resonance scan has to continue with the measurement at the last frequency instead of the *current frequency*. Therefore the variable *Freq.* is set to the last measured frequency by subtracting the *current step width* from the *current frequency*. The variable *Freq.* is used to calculate the *next frequency* later in this function. The flag, indicating that the step width has been reduced, is set to true. Also a check is performed ensuring that the *next step width* is not lower than the *minimum step width*. If the *current step width* is already the *minimum step width* or  $\Delta G \leq 4 MCD$ , the measurement can continue at the *current frequency* with the same or an increased step width. Therefore the variable *Freq.* is set to the *current frequency* and the flag *step width reduced* is set to false. Further, it has to be checked, if the measured conductance is again within the calculated noise level. Then the step width would be increased in order to speed up the measurement. The noise level to compare to is defined as  $2 MCD$  and therefore the condition for an increase of the step width is given as  $\Delta G < 2 MCD$ . If this is true, the step width is increased by 20%. Otherwise it is not changed. If the step width is increased, a check is performed that ensures that the step width does not exceed the allowed *maximum step width* defined by the *minimum step width* multiplied with the *maximum factor*. The *next frequency* is then calculated by adding the calculated *next step width* to the variable *Freq.*

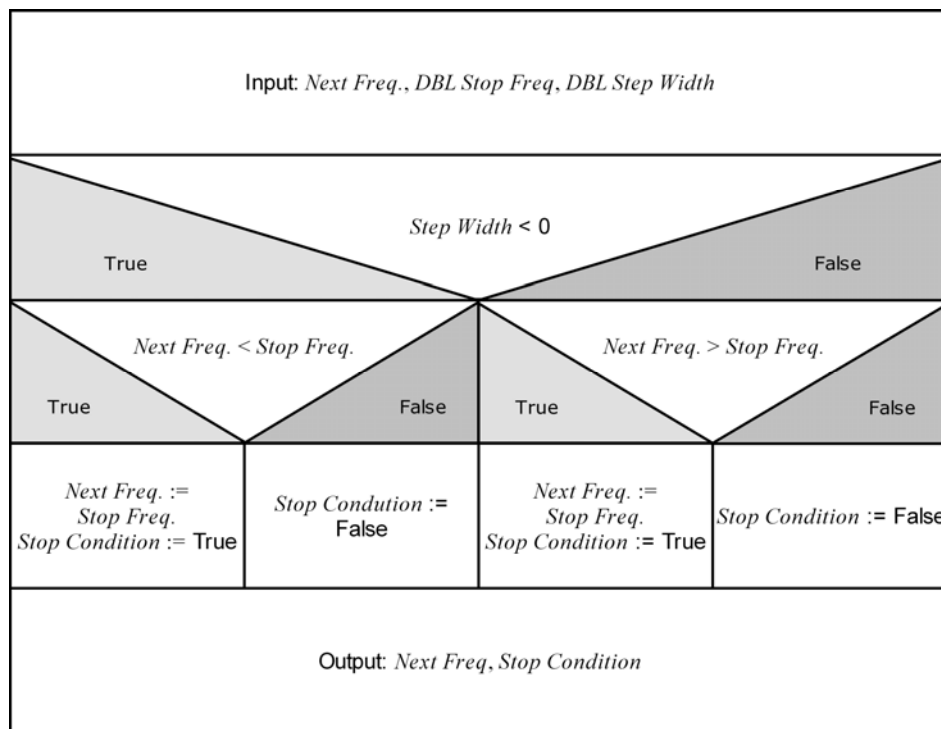


Figure 28: Nassi-Shneiderman diagram of the stop condition for the dynamic step width calculation algorithm. The stop condition is true if the frequency scan has reached the stop frequency. The scan direction is also taken into account. The output is either a true stop condition or the next frequency value.

At this point the *next frequency* and the *next step width* have been calculated. It must now be checked if a stop condition for the frequency scan is true. The frequency scan is terminated when the *next frequency* is out of the range defined by the *start* and the *stop frequency*. The Nassi-Shneiderman diagram given in Figure 28 shows the flow of the CheckStopCondition function. The function takes the calculated *next frequency*, the *stop frequency* and the *next step width* as input parameters and returns the *next frequency*, that is set in the first step of the frequency scan loop, and a flag indicating if the stop condition has been reached and therefore the frequency scan is terminated.

Depending on the direction of the frequency scan, determined by the sign of the step width, it is checked if the calculated next frequency is smaller or greater than the *stop frequency*. If yes, the *next frequency* is set to the *stop frequency* and the *stop condition* flag is set to true. Otherwise the *next frequency* is not changed and the *stop condition* flag is false.

Now the CaculateNextFrequency function is finished and returns the *next frequency*, the *next step width* and the two flags *step width reduced* and *stop condition*.

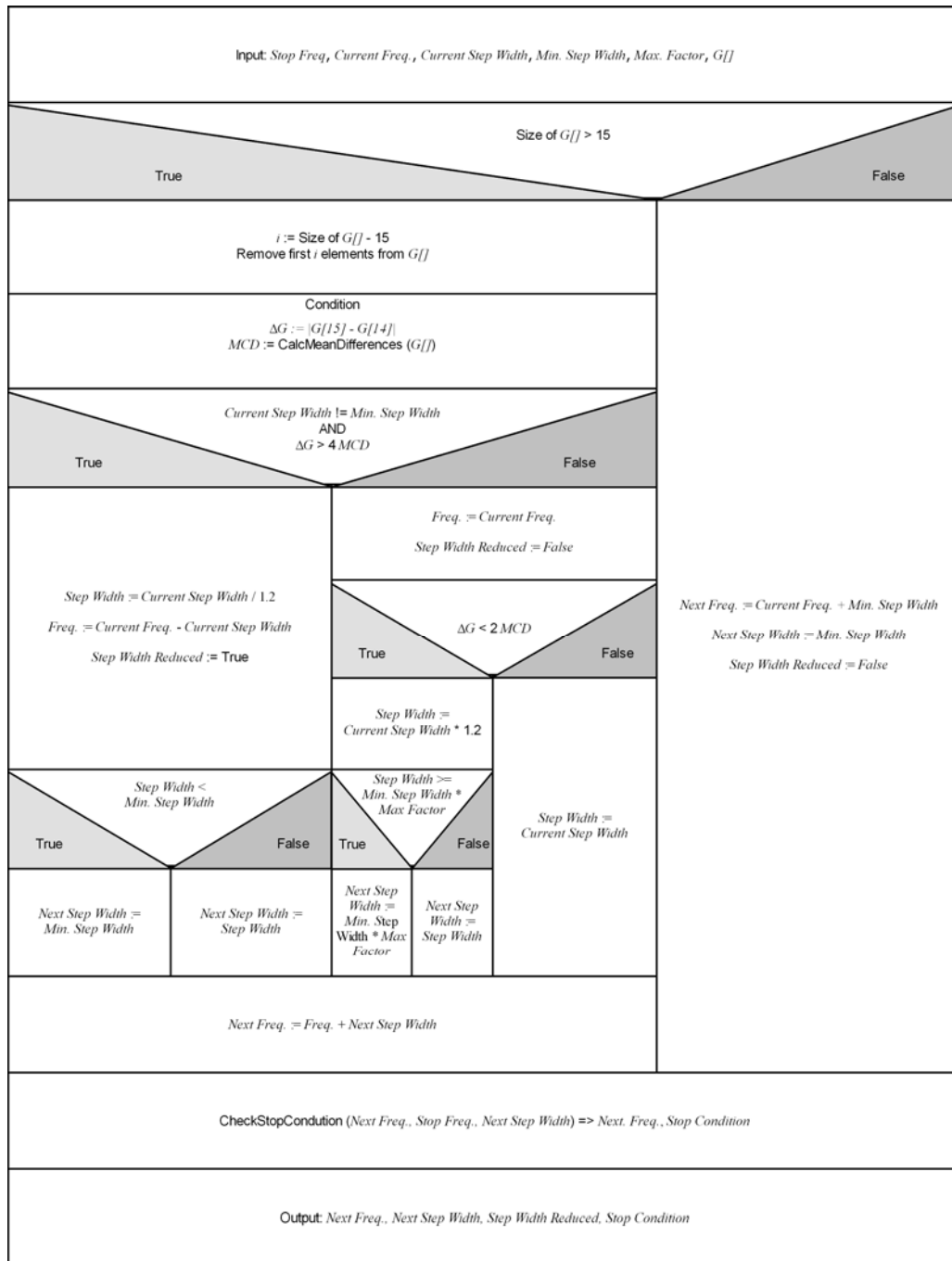


Figure 29: Nassi-Shneiderman diagram of the dynamic step width calculation algorithm. In the first 15 runs of the frequency scan loop the step width calculation is done linearly. If more than 15 previous measurement values are available, the conductance noise is calculated as mean value of the last 15 conductance changes. The conductance difference from the last to the current measurement is then compared to this noise level. If the conductance difference exceeds four times the noise level, the step width is reduced to improve measurement precision. Otherwise, if the conductance is still within the noise level, the step width is increased to speed up the measurement. After checking if the stop condition is already fulfilled, the output values are the parameters for the next admittance data acquisition.

If the flag *step width reduced* is true, the current data triple frequency, conductance and susceptance is stored separately and removed from the measurement data array. This is necessary because unless this separate storage, the conductance measured at a frequency, where the step width was too large, and was therefore reduced, would lead to a wrong noise level calculation. The separately stored data is inserted

again in the measurement data array after the frequency scan is finished. This is done to increase the point density in the measurement data array and hence increase the accuracy of the resonance evaluation.

### 4.3.4 Applying the baseline compensation

If the baseline compensation is turned on the baseline compensation is applied to the measured admittance values in this process step. The compensated admittance values are calculated in a loop that runs once for each measured frequency point. The compensation line functions  $G_{CL}$  and  $B_{CL}$  given in (23) are used to calculate the compensated conductance and susceptance values,  $G_{Comp}$  and  $B_{Comp}$  respectively. For each measured frequency  $f$ ,  $G_{Comp}$  and  $B_{Comp}$  are calculated out of the measured conductance  $G$  and susceptance  $B$  using

$$\begin{aligned} G_{Comp} &= G - G_{CL}(f) \\ B_{Comp} &= B - B_{CL}(f) \end{aligned} \quad (32)$$

The compensated admittance spectrum is then used in the resonance evaluation.

### 4.3.5 Resonance evaluation

In this process step the measured admittance values are scanned for a resonance. If a resonance is found, the series resonance frequency, the quality factor and the equivalent circuit parameters of the sensor are calculated. The algorithms used in this process step are based on the resonance evaluation described in 4.1.2. The search for a resonance and the evaluation of the characteristic values are implemented in the CMAEval.dll. This is a C-based software library, that originally was written for the Computer-controlled Measurement system for Admittance spectra (CMA) [6].

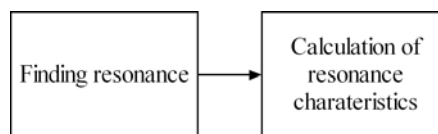


Figure 30: Schematic overview of the resonance evaluation in the resonance measurement process.

#### 4.3.5.1 Finding a resonance

The FindFrequencies function in the CMAEval.dll is used to search for a resonance in the measurement data array. The input parameters of the function are an array of conductance values, an array of susceptance values and a recognition level. A resonance is only detected by the function if the conductance at the series resonance frequency is at least as great as the recognition level. The recognition level in the

*QxSens* system is set by definition to 70% of the maximum value of the conductance array by definition. The value of 70% was chosen as it enables resonance detection even if the resonance peak is placed on top of an underground spectrum where the maximum conductance may be higher than the resonance peak. But this does not detect possibly measured harmonic overtones as resonances, as they generally have lower conductance levels. The recognition level defines a requirement in the *QxSens* system. If a specific resonance should be identified in a spectrum containing several resonances, the detection parameters must be set properly so that this resonance is the only resonance with a conductance level at its series resonance frequency being higher than 70% of the maximum conductance value measured. If the FindFrequencies function detects a resonance, the output values of the function are indices of the input conductance and susceptance arrays. These indices define the array elements that contain the characteristic frequencies of the resonance,  $f_s$ ,  $f_+$ ,  $f_-$ ,  $f_m$  and  $f_r$  (see 2.2), as a good approximation of the real resonance curve.

#### **4.3.5.2 Calculation of resonance characteristics**

The frequencies corresponding to the array indices returned from the FindFrequencies function in the previous process step can only approximate the real characteristic frequencies. This approximation is the better, the higher the density is of measurement points on the locus of admittance. The frequencies corresponding to the indices are called raw resonance characteristic frequencies. This indicates that they are not exactly the characteristic resonance frequencies. The quality factor calculated out of these raw frequencies is called raw quality factor  $Q_{raw}$ . In order to get precise measurement results, a circle is fit into the locus of admittance (see 2.3). This fit is implemented in the CMAEval.dll in the function CalcLSFQuality. The function's input parameters are the measured data triple, frequency, conductance and susceptance, and the array indices of the characteristic frequencies of the resonance that should be evaluated. The return values of the CalcLSFQuality function are the series resonance frequency  $f_s$ , the quality factor  $Q$ , and the equivalent circuit parameters  $R_1, C_1, L_1$  and  $C_0$ . In the next steps, the data are displayed to the user and can optionally be saved.

#### **4.3.6 Display and save data**

The last process step in a measurement is the displaying of the measurement results. The measurement results of the resonance detection are displayed as follows. The series resonance frequency and quality factor and the equivalent circuit parameters are displayed as numerical values. The measured admittance spectra are displayed in three graphs. One graph shows the conductance versus frequency. The second one shows the susceptance versus frequency. And the third one shows the locus of

admittance with the conductance as abscissa and the susceptance as ordinate. All three graphs display in addition to the measured data, the result of the RPC simulation calculated out of the equivalent circuit parameters (33). These simulated data can be used to compare the measured real data with their theoretical values.

$$\begin{aligned}\omega &= 2\pi f \\ G &= \frac{C_1^2 R_1 \omega^2}{(C_1 R_1 \omega)^2 + (C_1 L_1 \omega^2 - 1)^2} \\ B &= \omega \frac{C_0 + C_1 - (C_1 \omega)^2 L_1}{1 + C_1 \omega^2 (C_1 R_1^2 + L_1 (C_1 L_1 \omega^2 - 2))}\end{aligned}\tag{33}$$

When considering the expressiveness of a graph, the scaling of the axis is an important point. The scales on the x- and y-axis of the two graphs showing the conductance and susceptance, respectively, versus frequency are adjusted to the measured data automatically. The locus of admittance, displayed in the third graph, is a circle and should therefore also be displayed as a circle. From this it follows that the graph has to be quadratic and the scaling on the x- and y-axis has to be the same. LabVIEW cannot do this scaling automatically. That is why the calculation of the scaling is done in a function called CalculateAspectRatio (see Figure 31). This function calculates the maximum and minimum values of the scaling. First it searches for the smallest and the greatest value to be displayed. Out of this the range that must at least be displayed (maxRange) is calculated. It is possible to extend this range by a percentage of maxRange given in the input parameter Border. The parameter has a default value of 10%. This ensures a better readability of the displayed data. The calculated axes scaling limits X-Min, X-Max, Y-Min and Y-Max on the respective axes are then applied to the graph.

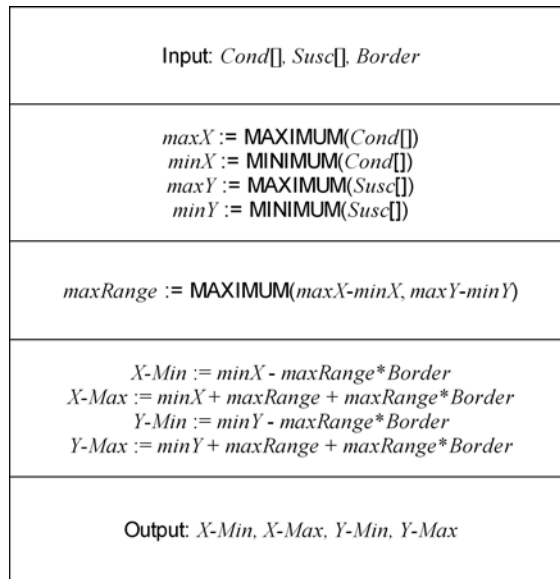


Figure 31: Nassi-Shneiderman diagram of the Calculate Aspect Ratio function. This function calculates the scaling for the graph, that displays the locus of admittance. For the locus of admittance being displayed as a circle, the graph must be quadratic and both axes must have the same scaling. The *Border* parameter determines the border around the locus-circle (in percent of the calculated scaling range).

Optionally it is possible to save the measured admittance spectrum to disk. A detailed description of the file format used is given in 4.4.6.

## 4.4 Software user interface

The user interface is divided into 8 sections, 6 parameter sections, the “Program Control” and the “Results”. The measurement is controlled by using the buttons in the “Program Control” section. 3 of the 6 parameter sections contain required fields. These parameters must be entered before the measurement may start. The required parameters are the “Scan Parameters”, the “System Parameters” and the “Kernel Electronics Parameters”. The 3 optional parameter sections, namely “Measurement Quality Parameters”, “File Parameters” and “Baseline Compensation Parameters”, contain fields with default values that can be changed optionally.

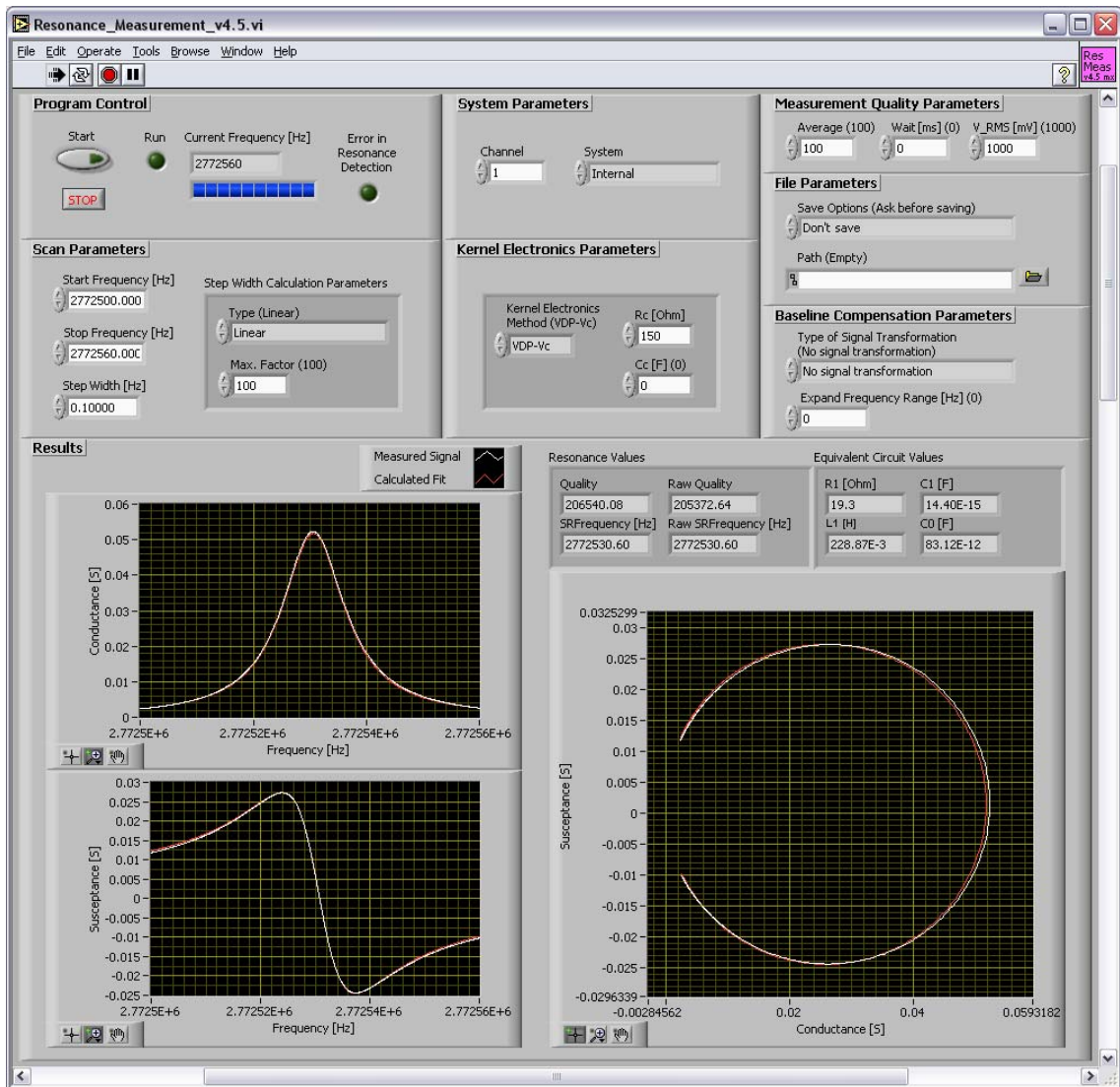


Figure 32: Screenshot of the user interface of the QxSens resonance measurement program.

Each control in the user interface has a unique label. The label of a field contains the name and in square brackets the unit. The labels of optional input fields contain also the default values written in parentheses, e.g. Wait [ms] (0). That means that the parameter Wait is given in ms and has a default value of 0 ms.

#### 4.4.1 Program control

At the program start-up the system detects the hardware installed in the computer system. If the hardware detection is successful the “Start” button is displayed. In case of a hardware detection failure, an error message indicates which hardware part could not be found or shows a defect.

Pressing the “Start” button starts the measurement. The “Run” LED lights up green and indicates that the measurement is in progress. The LED goes out after the measurement is finished and a resonance has been detected. If no resonance can be

found in the measurement results, the “Error in Resonance Detection” LED lights up red. The progress of the measurement is displayed in the “Current Frequency” field, which is updated every second. Pressing the “Stop” button during the measurement stops the current measurement.

#### **4.4.2 Scan parameters**

The “Scan Parameters” determine the frequency range of the measurement. The frequency range is given by the “Start-” and the “Stop Frequency”. The “Step Width Calculation Parameters” and the “Step Width” specify how the frequency range is scanned.

The frequency range can be scanned upwards or downwards. The direction arises from the entered “Start-“ and “Stop Frequencies” and the “Step Width”. If the “Stop Frequency” is higher than the “Start Frequency” and the “Step Width” is greater than zero, the frequency range is scanned upwards. If the “Start Frequency” is higher than the “Stop Frequency” and the “Step Width” is smaller than zero, the frequency range is scanned downwards. At every start of a measurement a consistency check is performed. If the “Start frequency”, the “Stop Frequency” and the “Step Width” do not match one of the two described cases, an error message is displayed.

There are two scan modes, linear and non-linear. Linear scan means, that the frequency range is scanned in equal steps according to the value of “Step Width”. The “Max Factor” is ignored in this scan mode. The optimal step width is a compromise between measurement accuracy and measurement speed. A small step width leads to a high resolution, but slow measurement. A big step width shortens the measurement time at the expense of resolution. If too few points are measured near the series resonance frequency, the resonance will not be detected properly. In the non-linear mode the frequency steps are adjusted dynamically during the measurement. When the conductance changes rapidly with the frequency, the frequency steps are gradually decreased. In the non-linear mode the lower limit of the actual step width is given in “Step Width”. If the admittance is changing slowly with the frequency, the step width is gradually increased. The maximum allowed step width is given by the product of “Step Width” and “Max Factor”. The choice of the parameters “Step Width” and “Max Factor” has to be adjusted to the respective measurement setting. The parameter “Step Width” controls the number of measurement points near the series resonance frequency and hence the maximal achievable resolution. It should be chosen in a way that the number of measurement points in the resonance half width is sufficient to detect a resonance (see 2.3). A high “Max Factor” speeds up the measurement. But if it is too high, a narrow resonance peak could be missed. Therefore the product of the “Step

Width” and the “Max Factor” should not be greater than the half width of the searched resonance peak.

### 4.4.3 System parameters

The “System Parameters” determine which channel is used in the measurement. The System can be chosen as internal or external. Internal means that a PC or PXI computer system is used. External means that an external USB measurement box will be used for measurement. Each measurement system supports three measurement channels, numbered from 1 to 3. The channel can be selected in the “Channel” field.

### 4.4.4 Kernel electronics parameters

As the calculation of the admittance values depends on the type of kernel electronics used in the measurement, it is necessary to enter the parameters specifying the kernel electronics, the Kernel Electronics Method, the resistance  $R_C$  and the capacity  $C_C$ .

In the QxSens project two different versions of the kernel electronics have been developed. The two versions use different measurement principles, the voltage divider principle (VDP) and the compensated current principle (CCP). In this work only kernel electronics with VDP have been used. A detailed description of kernel electronics with CCP can be found in [14]. In the kernel electronics with VDP there are two voltages that can be used for measurement, the voltage across the resistance  $R_C$  (VDP- $V_C$  method) and the voltage across the sensor (VDP- $V_S$  method). As in most measurement applications investigated in the *QxSens* project the VDP- $V_C$  version of the kernel electronics is used, the field “Kernel Electronics Method” is set to VDP- $V_C$  by default.

VDP kernel electronics may be equipped with different resistors  $R_C$ . To get the best measurement results the resistor  $R_C$  of the kernel electronics should have approximately the same value as the motional resistance of the sensor. If the resistance of the sensor is not known, the measurement can be started with any resistor  $R_C$ . After the first measurement of the admittance of the sensor, its resistance can be calculated and a kernel electronics adapted to the sensor’s resistance can be used in further measurements. An additional capacitor  $C_C$  can be inserted in parallel to the resistor  $R_C$  to optimize signal-to-noise ratio.

## 4.4.5 Measurement quality parameters

As described in 4.2 the “Measurement Quality Parameters”, namely “Average”, “Wait” and “V\_RMS”, influence the precision of the measurement result. It is important to adapt these parameters to the particular measurement application.

The number of samples measured at each frequency for each signal ( $S_1..S_4$ ) is entered in the field “Average”. As shown in 4.2.5 a good choice for “Average” is 100. Decreasing the “Average” value speeds up the measurement, but the noise of the measured admittance curves increases. Setting “Average” to a value greater than 100 does not improve the signal-to-noise ratio significantly. It only increases the measurement time.

During the measurement the program waits the amount of ms given in “Wait” after each frequency step. The default value of “Wait” is 0 ms. Even if “Wait” is set to zero, the system waits at least 1 ms for the transient time of the kernel electronics. If the sensor connected to the kernel electronics shows transient phenomena, “Wait” should be set to  $3\tau$  (see 4.2.4), where  $\tau$  is the time constant of the transient phenomena.

The output voltage of the synthesizer is set in “V\_RMS”. Therefore “V\_RMS” is proportional to the voltage applied to the connected sensor. The smaller this value is, the smaller is the signal-to-noise ratio. When using the external USB *QxSens* system, the parameter “V\_RMS” must not be set to a value greater than 800 mV (see 4.2.5).

## 4.4.6 File parameters

After a measurement of an admittance spectrum, the measured data can be saved to the hard disk. The behaviour of the program is controlled with the “Save Options”. The “Save Options” can be set to three possible values, "Don't save", "Ask before saving" and "Save always". "Don't save" means that the measured data is only stored in the program memory and is not saved to the hard disk. When "Ask before saving" is selected, a dialog is displayed after each measurement, asking the user if the measured data should be saved. In this case, the user can choose where to save the measured data. "Save always" means that after each measurement the measured data is saved.

If the field “Path” is empty, a file dialog is displayed every time before the data is saved to the hard disk. If “Path” is set to a file on the hard disk, the measured data is saved into this file. If the chosen file already exists, the existing file will be overwritten.

In the output file the frequency and the corresponding conductance and susceptance are saved in the given order. The single values are separated by tab stops. Each frequency value is saved in a new line. A head line indicates which data are saved in which column.

Example of an output file: The frequency is saved in Hz and the conductance and susceptance values are saved in Siemens.

Frequency	Conductance	Susceptance
30000.000000000000	0.006693927571	-0.000004361800
40000.000000000000	0.006747640204	-0.000037239381
50000.000000000000	0.006703106686	-0.000033403365
60000.000000000000	0.006715324242	-0.000012240153
70000.000000000000	0.006724564359	-0.000030272109
80000.000000000000	0.006723374128	-0.000020521069
90000.000000000000	0.006723877043	-0.000059784634

#### 4.4.7 Baseline compensation parameters

As described in 4.2.3, a spurious baseline may affect the measurement result in some measurement applications. To overcome this problem, a compensation of the baseline can be done. This compensation is turned on when the “Type of Signal Transformation” is set to "Linear Underground Compensation".

The compensation subtracts a linear admittance curve from the measured data before the resonance evaluation is performed. This linear curve is defined by two admittance values that are measured during the initialization of the measurement. The two values are measured at two different frequencies that are calculated out of the “Start Frequency”, the “Stop Frequency” and the value entered in “Expand Frequency Range”. If the “Start Frequency” is smaller than the “Stop Frequency”, the lower admittance value is measured at the “Start Frequency” minus “Expand Frequency Range” and the second admittance value is measured at the “Stop Frequency” plus “Expand Frequency Range”. If the “Start Frequency” is greater than the “Stop Frequency”, “Start-“ and “Stop Frequency” are exchanged before calculating the frequencies of the admittance measurement.

#### 4.4.8 Results

If the measured admittance spectrum contains resonances, the resonance with the highest admittance peak is analysed and the “Resonance Values” are displayed. The “Resonance Values” are “Quality”, “Raw Quality”, “Series Resonance Frequency (SRFrequency)” and “Raw SRFrequency”. Also the “Equivalent Circuit Parameters” of the Van Dyke equivalent circuit of the sensor are calculated and displayed.

Three graphs display the measured admittance data, “Conductance vs. Frequency”, “Susceptance vs. Frequency” and “Susceptance vs. Conductance”. The measured data are displayed in the graphs as white lines. If a resonance peak is found, a simulated admittance spectrum calculated out of the equivalent circuit parameters is

additionally displayed in the respective graphs as red line. The scales of all graphs are automatically adjusted to the displayed data.

## 4.4.9 Error messages

The resonance measurement program displays error messages whenever an error occurs. Table 3 shows possible error messages and its reasons.

Error number	Error messages	Possible reasons	Actions to be taken
5000	No TE5100 board found.	There is no internal synthesizer TE5100 board installed in the computer system. The driver of the TE5100 board is not installed properly.	Install a TE5100 and the proper drivers in the computer system.
5001	An error occurred when trying to set a frequency on the TE5100 board.	The TE5100 board has an internal error.	Reboot the computer system and restart the measurement.
5002	An error occurred when trying to set an amplitude on the TE5100 board.	The TE5100 board has an internal error.	Reboot the computer system and restart the measurement.
5003	An error occurred in the calculation of the admittance values G and B. G and/or B are not a number.	The value Rc in the Kernel Electronics Parameters is set to 0. The Kernel Electronics is not connected to the port determined by the entered System Parameters.	Check the value of Rc in the Kernel Electronics Parameters. Connect the Kernel Electronics to the desired Channel.
5004	No resonance found in function FindFrequencies in CMAEval.dll.	There is no resonance peak in the measured admittance spectrum.	
5005	An error occurred in function CalcLSFQuality in CMAEval.dll.	The resolution of the measured data is not good enough for the evaluation of the resonance values.	Try to improve the resolution of the measurement.
5006	The Start and Stop Frequency and the Step Width are not consistent.	This error occurs when the Start Frequency is smaller than the Stop Frequency and the Step Width is negative or when the Start Frequency is greater than the Stop Frequency and the Step Width is positive.	Check the entered Scan Parameters.
5007	Step Width is zero.		Check the entered Step Width.
5010	An error occurred when sending command ... to the external synthesizer. Return value: ...	Maybe an error in the external synthesizer occurred.	Reboot the external measurement box by switching the box off and on again.
5012	No DAQmx device found.	There is no multifunctional IO card installed in the computer system.	Install a multifunctional IO card in the computer system.
5015	External synthesizer not found.	The external synthesizer in the external measurement box does not respond.	Check the connection of the external measurement box to the computer system. Reboot the external measurement box by switching the box off and on again.
5017	External synthesizer is not present or defective.	The external synthesizer in the external measurement box does not respond.	Check the connection of the external measurement box to the computer system. Reboot the external measurement box by switching the box off and on again.

Table 3: Error messages that can occur in the resonance measurement program.

## 4.5 Measurement results

The *QxSens* system is a multi purpose admittance measurement system. In principle, it can be used to measure admittance spectra of all kinds of passive two terminal electric devices. A main field of application is the measurement of RPC (resonant piezoelectric crystal) based sensors. The resonance measurement described in this chapter is the basis for all RPC based measurement applications developed in the *QxSens* project. In this chapter the measurement results of the *QxSens* resonance measurement system are compared to the measurement results obtained with an Agilent 4395A device operated in impedance analyzer mode. The 4395A is a network/spectrum/impedance analyzer from Agilent Technologies. For impedance

measurements an additional impedance test kit (the 43961A RF impedance test kit) is necessary. In contrast to the *QxSens* system the Agilent 4395A has to be calibrated before measuring. The comparison of both systems demonstrates that the *QxSens* resonance measurement system gives accurate measurement results in a wide frequency range from 50 kHz to 30 MHz. It also shows the high dynamic range of the admittance measurement reaching from 0.1  $\mu\text{S}$  to more than 100 mS.

To cover the wide frequency range different types of quartz sensors have been measured. In the lower frequency range from 50 kHz to 10 MHz viscosity sensors have been used. These QV sensors have been developed in the *QxSens* project and therefore are a good choice for testing the *QxSens* measurement system. QV sensors are very suitable for testing, because the quality factor  $Q$  and therefore the motional resistance  $R_1$ , that is inversely proportional to  $Q$ , can be adjusted by immersing the sensor into liquids of different viscosity, e.g. acetone or oil. The liquid layer on the surface of the QV sensor damps the oscillations of the quartz and as a consequence reduces the quality factor as well as the series resonance frequency. The decrease of the quality factor is in the range of three orders of magnitude or more. The ability of setting  $R_1$  to different values can be used to demonstrate the big admittance dynamic range of the measurement system, because the higher the motional resistance, the lower is the measured admittance. In the upper frequency range a temperature sensor (QT) with a series resonance frequency of about 29 MHz was used for testing the system. The QT sensor has a very low motional resistance and therefore a very narrow resonance peak. The small half width of the measured peak at a high series resonance frequency demonstrates the frequency resolution of the measurement system. In the frequency range between 10 and 30 MHz there are currently no *QxSens* sensors available. A standard quartz crystal with a series resonance frequency of 15 MHz was used instead of a sensor to show the accuracy of the *QxSens* measurement system in the middle frequency range.

All data graphs shown in this chapter have been created directly out of the raw measurement data. No additional data processing like smoothing or fitting was done. In most cases only the conductance spectrum is shown, as the susceptance spectrum does not show additional information. Only in some cases the susceptance spectrum is displayed in order to show the effects of the cable compensation. All measurements with the *QxSens* system have been done with kernel electronics in VDP- $V_C$  mode. The resistor  $R_C$  was adjusted to the motional resistance of the respective sensor, for low resistive sensors ( $R_1$  from 10  $\Omega$  to 15 k  $\Omega$ )  $R_C$  is 150  $\Omega$  and for high resistive sensors ( $R_1$  from 100 k $\Omega$  to 10 M  $\Omega$ )  $R_C$  is 82 k $\Omega$ . From the measurement results it can be seen that a very wide range of admittance values can be measured with just one type of kernel

electronics. To give comparable results the measurement configuration of the Agilent 4395A was set in a way, that the measurement time for both systems was the same.

### 4.5.1 QV sensor at 55 kHz

The measurement system comparison done here is started at the lower end of the frequency range. A QV-torsion sensor with a series resonance frequency of about 55 kHz is used. This sensor has a high motional resistance of about 100 k $\Omega$  in air. Hence, kernel electronics in VDP-V<sub>C</sub> mode with  $R_C = 82$  k $\Omega$  was used. The sensor was connected to the kernel electronics and the Agilent 4395A with a triaxial cable. It must be stated that the Agilent 4395A is not specified for such a low frequency, but it is still working and therefore can be used for comparison with the *QxSens* system.

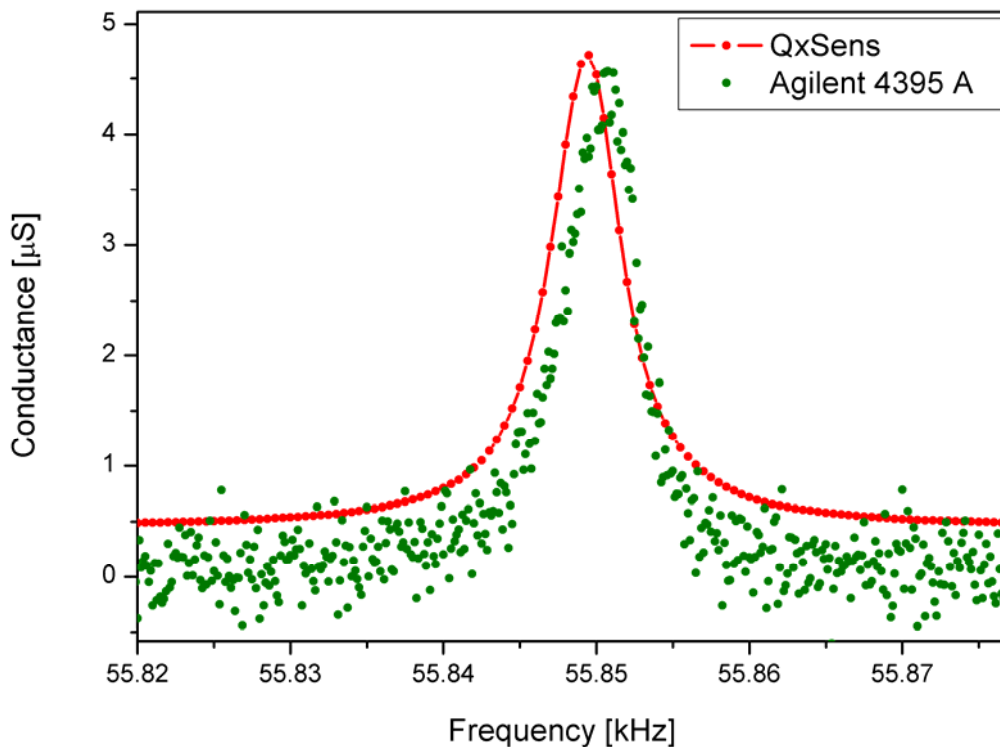


Figure 33: Comparison of the measurement systems with a QV-torsion sensor at 55 kHz. The conductance spectrum was measured of the dry sensor. The low conductance level causes spurious effects of the parallel capacitance. This is the reason for the noise in the Agilent 4395A measurement. The cable compensation of the *QxSens* system reduces the parallel capacitance and therefore the conductance spectrum measured with the *QxSens* system shows nearly no noise.

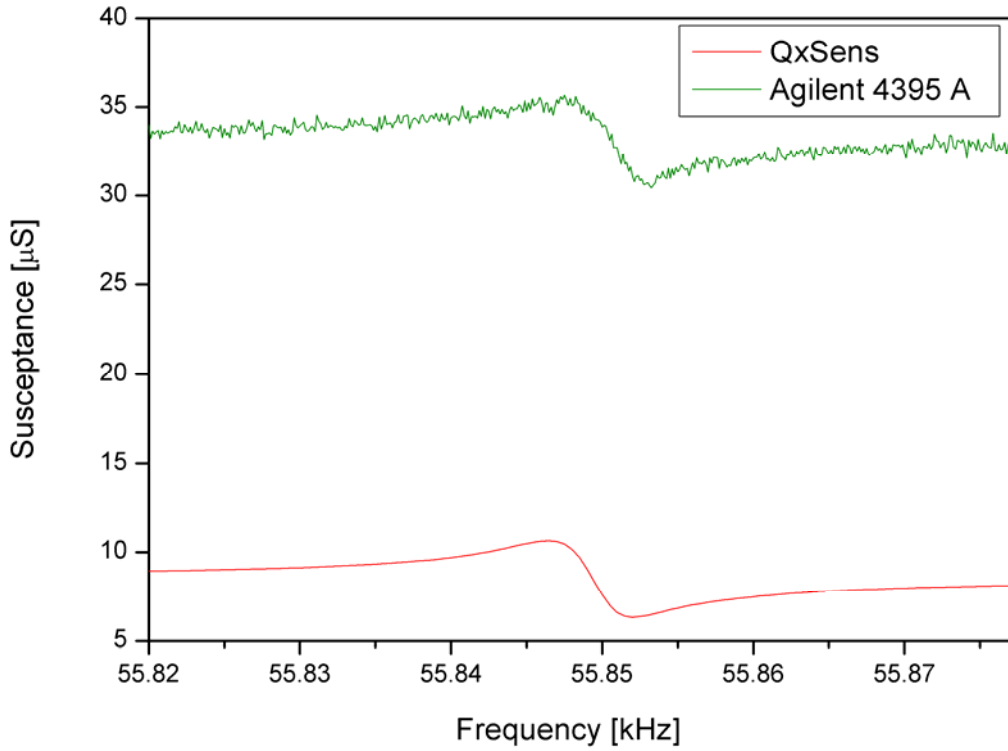


Figure 34 shows the susceptance spectra of the QV-torsion measurement in air ( $f_s=55$  kHz). The shape of the susceptance curves obtained with both measurement systems is the same, only the Agilent 4395A curve is shifted due to spurious effects coming from the parallel capacitance of the connection cable from the kernel electronics to the sensor. This shift leads to a higher noise of the admittance values. The cable compensation compensates this shift in the *QxSens* system. This improves the S/N ratio. The resonance evaluation, giving  $f_s$  and  $Q$ , is not disturbed by the susceptance shift.

	<i>QxSens</i>	Agilent 4395 A
$f_s$ [Hz]	55849.34	55850.48
$Q$	10154	9772

Table 4: Comparison of the measurement results of a QV-torsion sensor at 55 kHz measured with the *QxSens* measurement system and the Agilent 4395 A device.

The high motional resistance of the QV-torsion sensor leads to difficulties in the admittance measurement. As a consequence of the high  $R_1$  value the measured admittance values are very small. So the parallel capacitance  $C_0$  of the sensor shows a big influence on the measurement results. This influence becomes apparent in a low signal-to-noise ratio which can be seen in the admittance spectrum measured with the Agilent 4395A in Figure 33. The reason for the reduction of the S/N ratio is a shift of the susceptance spectrum by the parallel capacitance. In the *QxSens* system the cable compensation reduces the effective parallel capacitance and therefore the admittance spectrum measured with the *QxSens* system is much less noisy. Figure 34 shows the

susceptance shift of the Agilent 4395A without any compensation compared to the *QxSens* system with the cable compensation. It can be seen that the susceptance measured with the Agilent 4395A is four times higher. Yet the resonance evaluation, giving the quality factor and the series resonance frequency, is not influenced by this susceptance shift. The quality factor and the series resonance frequency calculate to nearly the same values with both measurement systems (see Table 4). The small difference of the series resonance frequency of about 1 Hz comes from the absolute error of the synthesizer used in the *QxSens* measurement system (see 3.1.1.1.2) as well as possible admittance measurement errors, that may shift the maximum of the conductance.

Immersing the sensor in acetone broadens the resonance peak and decreases the quality factor. The lower quality factor corresponds to a higher motional resistance and therefore the signal-to-noise ratio obtained with the Agilent 4395A is even worse in this measurement (Figure 35). It can be seen that the admittance spectrum taken with the *QxSens* system still shows still very low noise. The cable compensation and the measurement principle still work satisfactorily even though the kernel electronics are not adapted perfectly any more, as the motional resistance of the sensor is now much higher than the resistor  $R_C$  in the kernel electronics which was adapted for the sensor in air. Nevertheless the series resonance frequency and the quality factor of both measurement systems still match well.

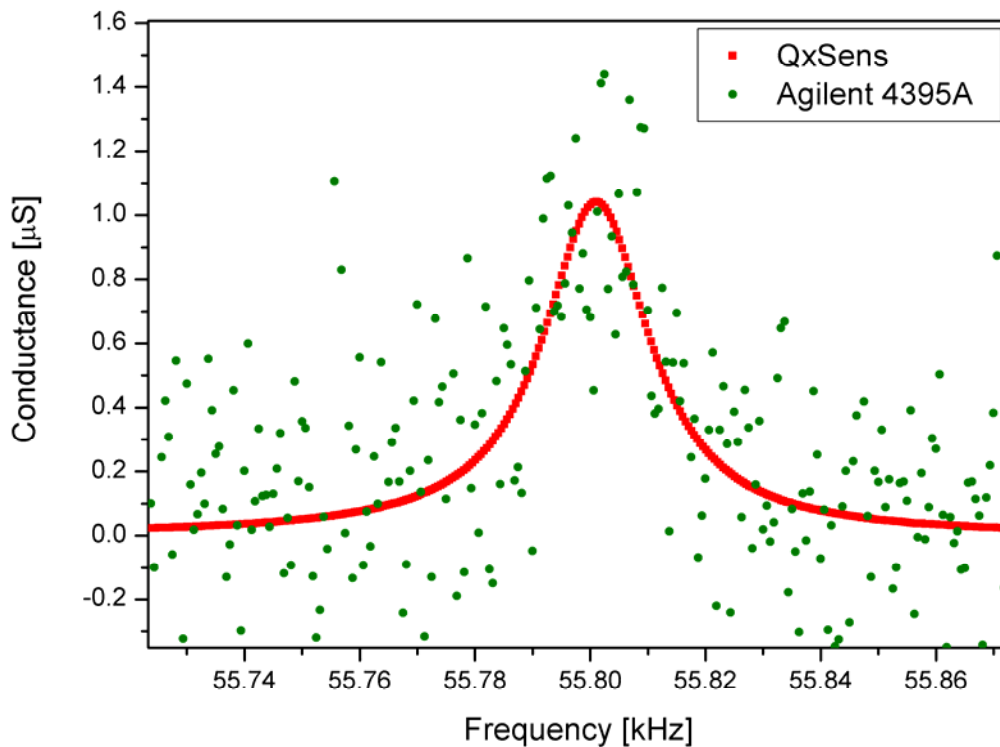


Figure 35: Measurement results of the QV-torsion sensor at 55 kHz immersed in acetone. The damping of the sensor as well as its motional resistance are increased. Therefore the conductance values are much lower than in air. The lower conductance level leads to very high noise in the Agilent 4395A measurement. The *QxSens* system with the cable compensation still gives precise measurement values. A higher averaging in the Agilent 4395A measurement would decrease the noise, but increase measurement time in comparison to the *QxSens* measurement time.

When the sensor is immersed in oil, the further decrease of the admittance signal to less than  $1 \mu\text{S}$  makes the S/N ratio obtained from the Agilent 4395A too low for a measurement. Therefore Figure 36 shows only the comparison of the conductance spectra in acetone and in oil, respectively, measured with the *QxSens* system. The displayed data in the graph are the raw measurement data. It can be seen that even in an admittance range of below  $1 \mu\text{S}$  the *QxSens* system gives reasonable measurement results. This shows the extremely wide admittance dynamic range of the system reaching down to  $0.1 \mu\text{S}$ .

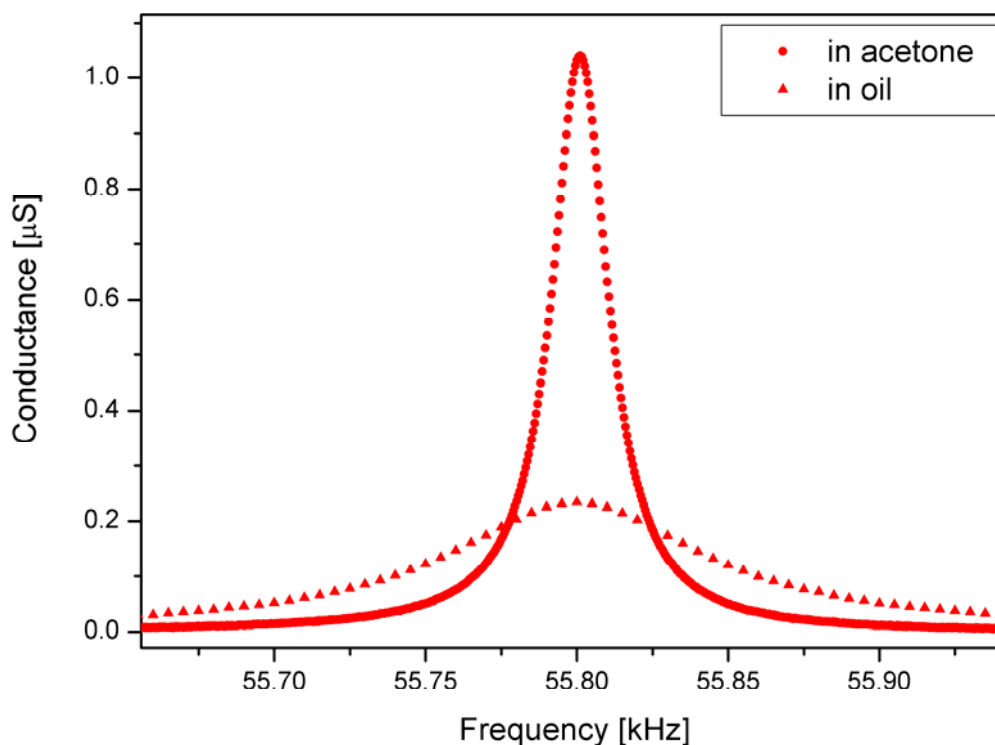


Figure 36: Comparison of the conductance of the QV-torsion sensor at 55 kHz immersed in acetone and oil, respectively. The much higher viscosity of the oil decreases the conductance maximum to 20% of the conductance maximum in acetone. Nevertheless, the *QxSens* system gives precise measurement results even at very low admittance values. The data displayed are the raw measurement data without any fitting or smoothing.

#### 4.5.2 QV sensor at 2.7 MHz

In the range of 3 MHz a QV-shear sensor with a series resonance frequency of about 2.7 MHz was used for testing. As the sensor is low resistance, a kernel electronics with an  $R_C$  of 150  $\Omega$  were used. The connection between the measurement systems and the sensor was done again with a triaxial cable.

Figure 37 shows the conductance spectra of the dry QV-shear sensor. It can be seen that in air the conductance peak is about 60 mS high and the frequency half width is about 10 Hz. This small half width is the reason, why the small difference between the series resonance frequencies obtained with the different measurement system of about 2 Hz is visible. This frequency difference comes from the absolute error of the synthesizer in the *QxSens* system at 2.7 MHz. However, both measurement systems show the same results with respect to conductance peak value and half width. Also the S/N ratio is high in both measurement results.

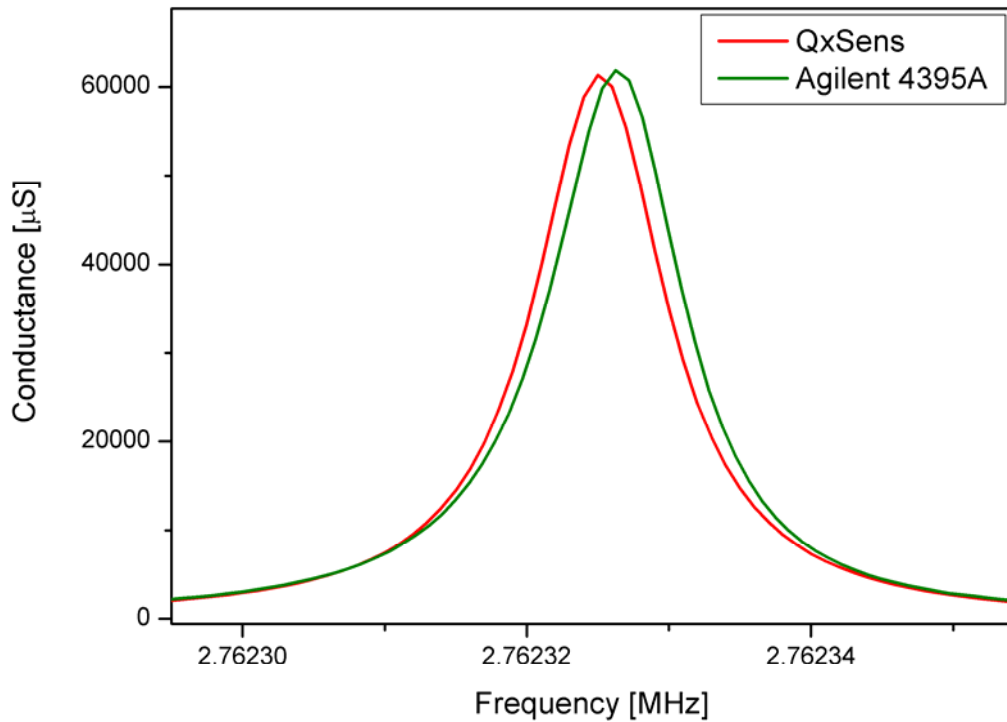


Figure 37: The conductance peaks obtained from the QV-shear sensor at 2.7 MHz show a very clear signal. Both peaks match in height and half width. The small difference in the series resonance frequency comes from the absolute frequency of the synthesizer in the *QxSens* system. It becomes visible because of the high frequency resolution of this measurement. The half width is only 10 Hz.

In the next two graphs (Figure 38 and Figure 39) the conductance and susceptance spectra of the sensor immersed in acetone are displayed. The lower quality factor of the resonance in acetone shows that the motional resistance of the sensor has increased and therefore the admittance signal has decreased. This becomes apparent in a reduction of the conductance maximum from 60000  $\mu\text{S}$  in air to 350  $\mu\text{S}$  in acetone. In this admittance range the effects of the parallel capacitance  $C_0$  can clearly be observed. The parallel capacitance shifts the susceptance curve measured by the Agilent 4395A to a baseline that is 1250  $\mu\text{S}$  higher than the baseline of the *QxSens* susceptance curve. This, in comparison to the conductance value of 350  $\mu\text{S}$ , high susceptance base reduces the signal-to-noise ratio of the Agilent 4395A admittance values. The shift of 1250  $\mu\text{S}$  calculates to a parallel capacitance of 73 pF at 2.7 MHz. This capacitance matches the theoretically predicted value of 71.25 pF, calculated from the capacitance of the cable per meter (according to the data sheet value of 95 pF/m) and the cable length used (0.75 m). This shows, that the susceptance shift does actually come from the parallel capacitance of the cable.

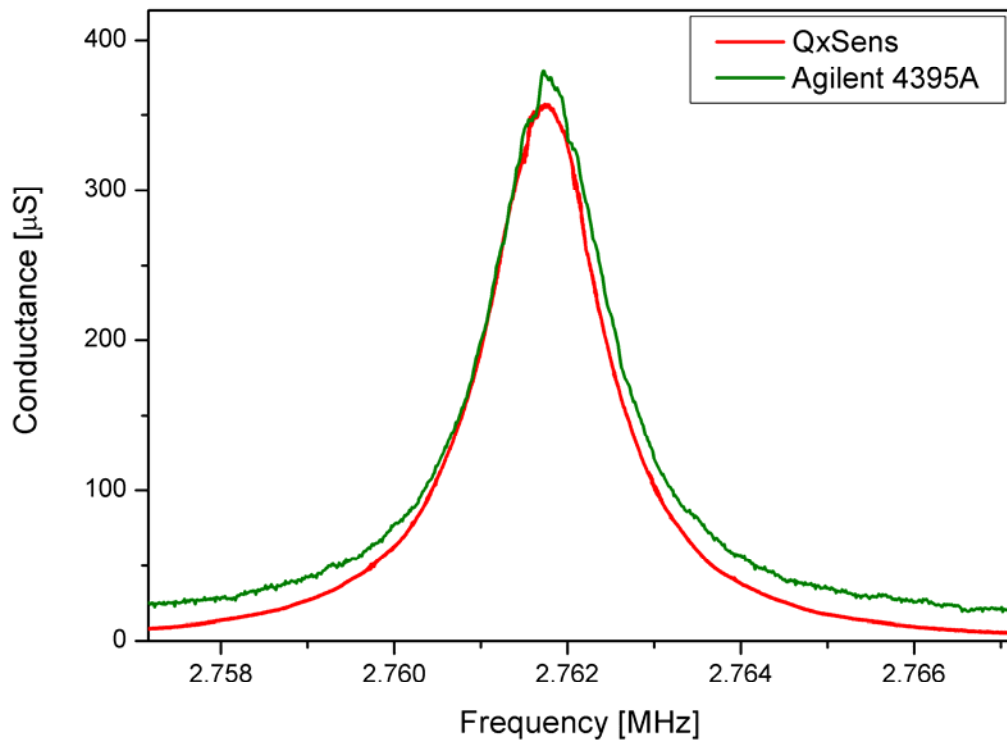


Figure 38 shows the conductance spectra of the QV-shear sensor in acetone. Both measurements give comparable results concerning series resonance frequency and quality factor. The small shift of the conductance baseline is caused by the different configurations of the measurement systems. But this shift does not influence the resonance evaluation.

In the *QxSens* system the cable compensation minimizes the influence of the parallel capacitance and hence of the susceptance shift. This is the reason why the admittance spectrum measured by the *QxSens* system shows hardly any noise. Moreover, the remaining susceptance shift caused by the cable does not influence the resonance evaluation, as the evaluation method used is independent from susceptance shifts (see 2.3). The small difference in the conductance baselines comes from the different system configurations and does not influence the resonance evaluation either. Considering these different conductance baselines, both systems show essentially equal values of conductance maximum and half width.

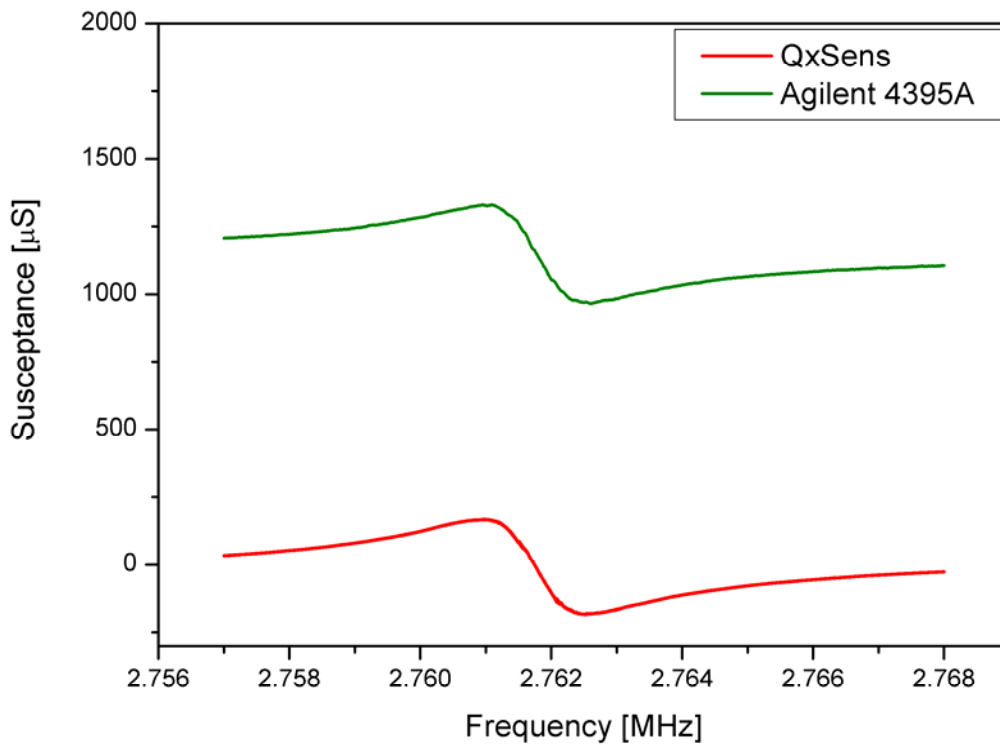


Figure 39 shows the susceptance curves of the QV-shear measurement in acetone. The shift of the Agilent 4395A curve is again caused by the parallel capacitance of the sensor cable. This shift has no effect on the evaluation of the locus of admittance but it decreases the signal-to-noise ratio. In the *QxSens* system the cable compensation compensates the effects of the cable and therefore improves the S/N ratio.

Figure 40 shows that immersing the sensor into oil further decreases the quality factor and the series resonance frequency while increasing the half width of the resonance peak. Again it can be seen that the cable compensation in the *QxSens* system reduces the noise in comparison to the uncompensated signal from the Agilent 4395A. The same conductance shift between the results of two measurement systems can be observed in this measurement, showing that the conductance shift only depends on the system configuration and not on the viscosity measured. Again the series resonance frequency and the quality factor calculate to essentially the same values for both measurement systems.

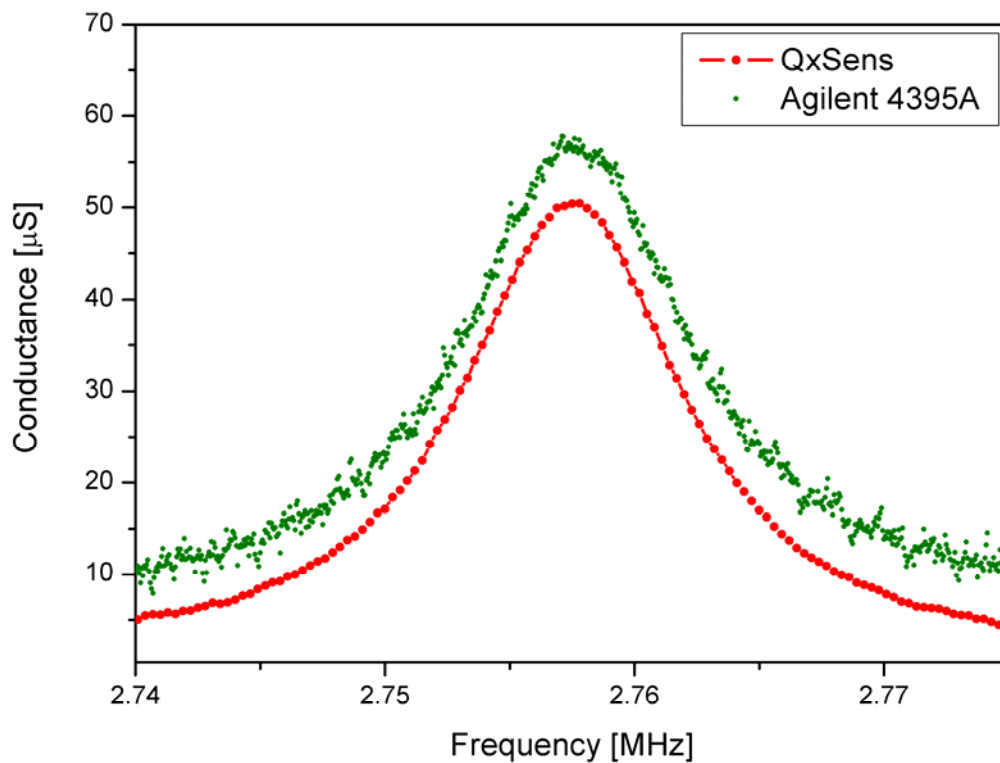


Figure 40: The conductance spectra of the QV-shear sensor, with a series resonance frequency of 2.7 MHz, immersed in oil. At this very small admittance level the spurious effects of the parallel capacitance can be observed clearly. The Agilent 4395A, which has no cable compensation, shows a very noisy signal. In contrast to this, the *QxSens* system with the cable compensation shows a much smoother conductance curve. Besides the noise, both systems give essentially the same results for the series resonance frequency and the quality factor. The small shift between the conductance spectra is caused by different system configurations and does not influence the resonance evaluation.

Comparing the *QxSens* measurement results from air and oil measurements shows the impressive capabilities of the *QxSens* system with respect to frequency resolution and admittance range. Both measurements have been done with the same hardware setup. Figure 41 shows the big dynamic admittance range that can be covered with only one hardware setup. The admittance values reach over three orders of magnitude, from 60000  $\mu\text{S}$  down to 60  $\mu\text{S}$ . The big change in the frequency resolution required for resonance detection can be seen by comparing the half widths of the two resonance curves. The half width of the dry sensor is only 10 Hz and increases to more than 10000 Hz when the sensor is immersed in oil.

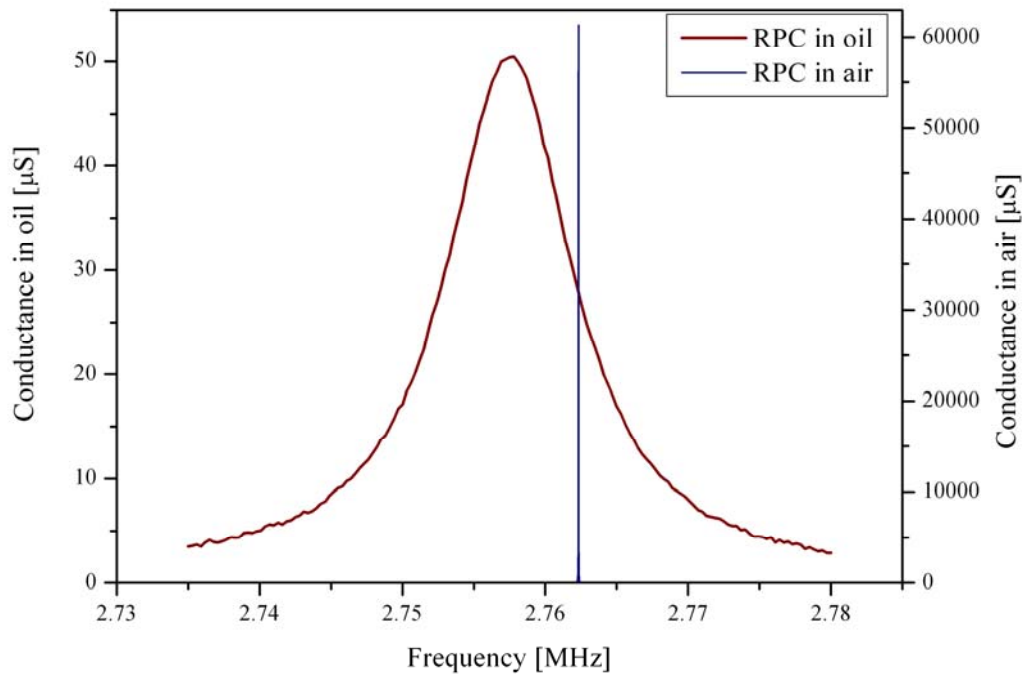


Figure 41: Comparison of the conductance spectra of a QV-shear sensor in air and in oil, respectively. Both measurements were done with the same hardware setup. The graph shows the big change of half width and conductance with increasing viscosity. It also shows the impressive ability of the *QxSens* system to measure a big dynamic range concerning frequency resolution and admittance with just one hardware setup.

### 4.5.3 QV sensor at 6 MHz

The QV-shear sensor used at 6 MHz is basically the same as the QV-shear sensor for 2.7 MHz except that the quartz crystal used has a different series resonance frequency of approximately 6 MHz. From Figure 42 it can be seen, that the noise of the conductance spectra is very low, even though the conductance peak in air here is much lower than the conductance peak of the 2.7 MHz sensor in air. The reason is, that both measurement systems (*QxSens* and the Agilent 4395A) are optimal to use in the range around 6 MHz. The zoom of the conductance maximum in Figure 42 shows the well corresponding measurement results of the *QxSens* system and the Agilent 4395A. The difference in the measured series resonance frequencies due to the absolute error of the *QxSens* synthesizer (about 5 Hz) is very small compared to the half width of the peak (about 1200 Hz) and therefore invisible.

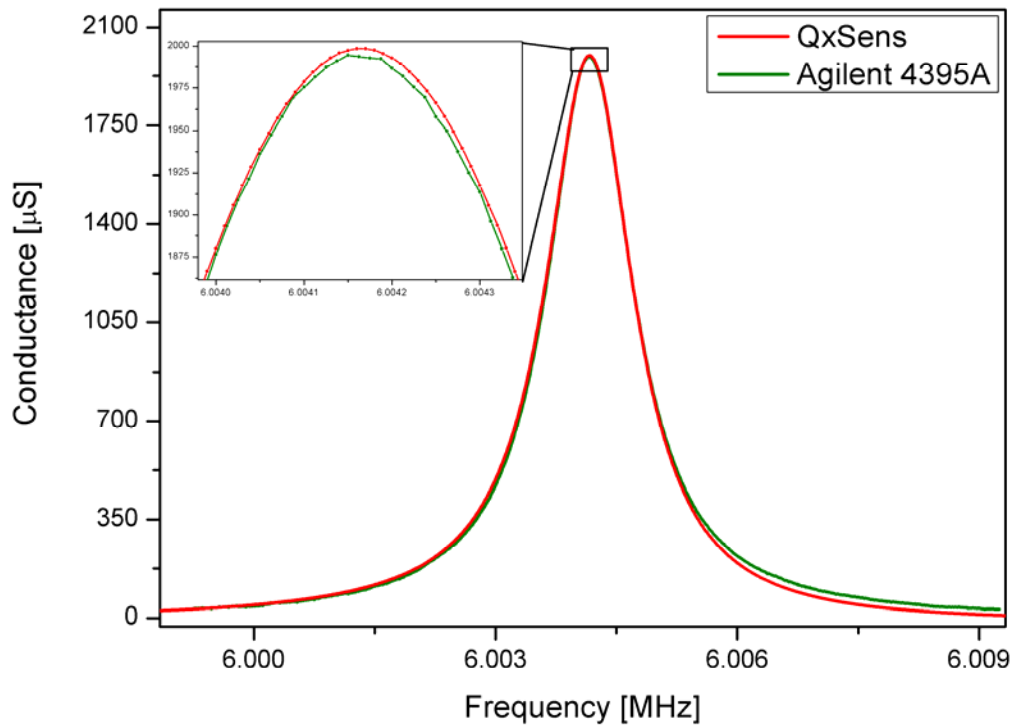


Figure 42 shows an excellent overlap of the conductance curves obtained with the Agilent 4395A and the *QxSens* system, respectively. The range of 6 MHz is an optimal frequency range for both measurement systems. This is also the reason for the almost noise-free measurement results. The zoom shows the exact matching of both measurement systems near the series resonance frequency.

With the sensor immersed in oil the Agilent 4395A shows a noisier signal that again comes from spurious cable effects but the conductance curves taken by both measurement systems still match excellent (Figure 43). The cable compensation of the *QxSens* system reduces the cable effects and therefore the S/N ratio of the *QxSens* measurement result is much higher. The resonance evaluation of both curves gives essentially the same series resonance frequency and quality factor.

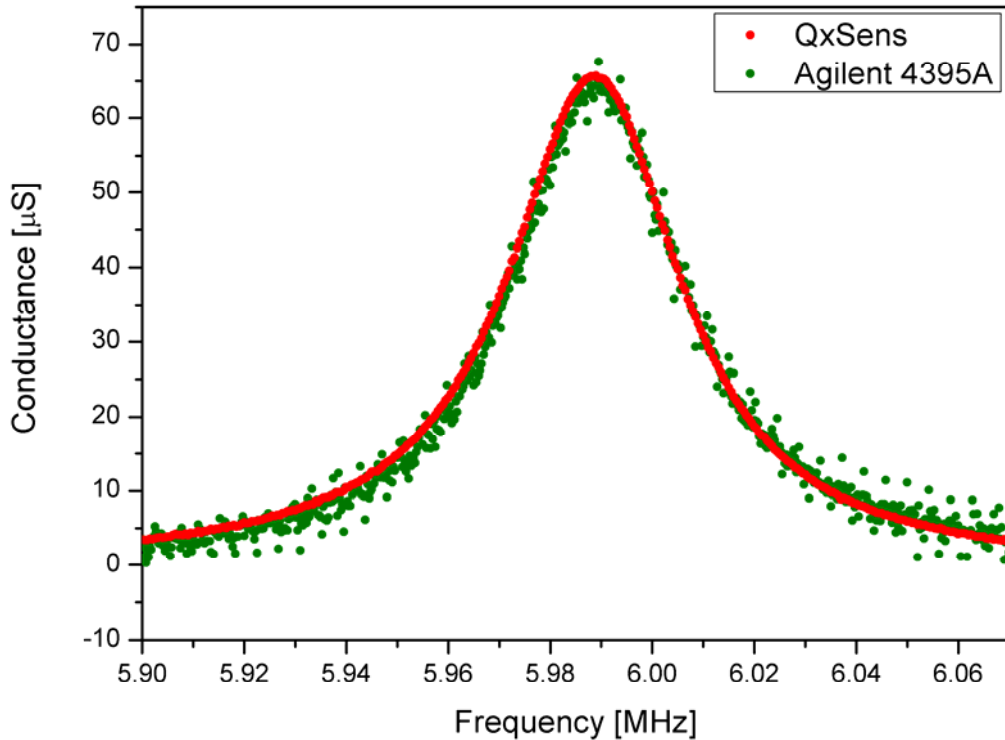


Figure 43: The conductance spectrum of a QV-shear sensor at 6 MHz immersed in oil. The Agilent 4395A curve shows a worse S/N ratio than the *QxSens* curve. This is due to the cable compensation that is only available for the *QxSens* system. The high damping of the oil decreases the admittance level so much that the spurious effects of the cable capacitance become noticeable.

#### 4.5.4 Standard quartz at 15 MHz

In this work viscosity sensors have been available only up to 10 MHz. The temperature sensors developed in the *QxSens* project have a series resonance frequency of about 29 MHz. To demonstrate the accuracy of the *QxSens* system in the range between 10 and 29 MHz a standard oscillating quartz crystal with a nominal series resonance frequency of 15 MHz packaged into standardized quartz housing with a nominal series resonance frequency of 15 MHz was used. These crystals are typically used as frequency normal in oscillator circuits. For the measurement kernel electronics with an  $R_C$  of 150  $\Omega$  were used. The crystal was connected to the kernel electronics using the *QxSens* triaxial cable. In contrast to the measurements described before, here the sensor was directly (without a cable) connected to the Agilent 4395A. Figure 44 shows the measured conductance spectra. It can be seen that both curves show a very high signal-to-noise ratio. Also the half width is the same for both curves. The small difference between the series resonance frequencies comes from the absolute error of the *QxSens* synthesizer and the influence of the cable between the sensor and the kernel

electronics. The missing cable in the Agilent 4395A measurement is also the reason for the small difference in the conductance peak height.

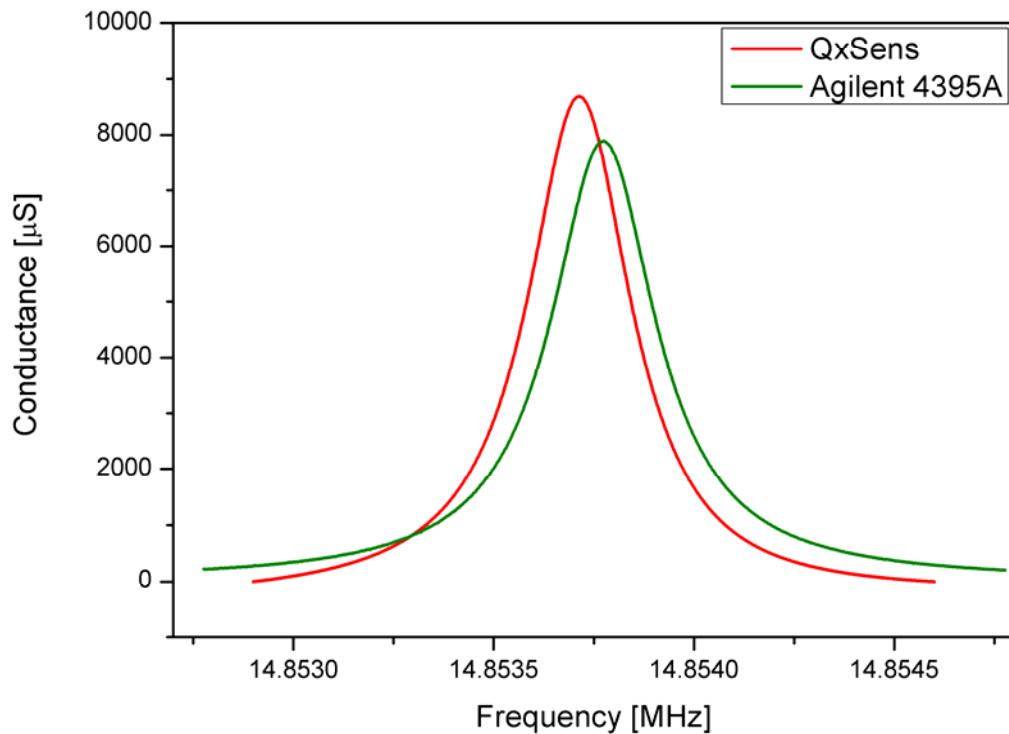


Figure 44: Comparison of the conductance spectra of a standard oscillating quartz crystal with a nominal series resonance frequency of 15 MHz. Both measurement systems give clear measurement results. The difference in the series resonance frequency and the height of the conductance peak comes from the absolute error of the *QxSens* synthesizer and from the fact, that the sensor was connected directly to the Agilent 4395A, but with a cable to the *QxSens* system.

#### 4.5.5 QT sensor at 29 MHz

Temperature sensitive sensors usually have a very low motional resistance. As a consequence they show a very narrow resonance peak. The kernel electronics used in this case have an  $R_C$  of  $150 \Omega$ . Due to the high measurement signal, the effects of the parallel capacitance  $C_0$  are negligible. This is also the reason for the excellent S/N ratio of both measurement results (Figure 45). As the half width of the peak is small, the difference between the measured series resonance frequencies due to the absolute error of the synthesizer and the influence of the cable between the kernel electronics and the sensor, becomes apparent. This measurement result demonstrates the high frequency resolution of the *QxSens* system. It can resolve a few Hz even in the high frequency range of about 30 MHz.

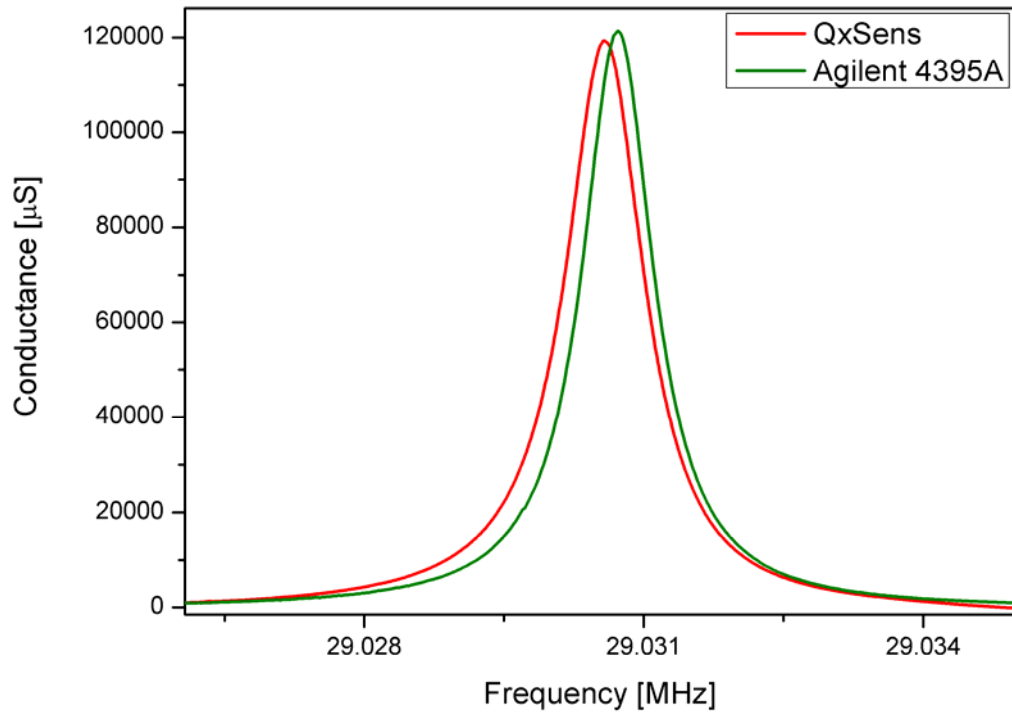


Figure 45: Comparison of the Agilent 4395A with the *QxSens* system measuring a QT sensor at 29 MHz. Both measurement systems show a very high signal-to-noise ratio and a good match of the measured half width. The absolute error of the synthesizer and the influence of the cable, that is only used with the *QxSens* system, are the reasons for the small frequency difference and the different heights of the conductance peaks.

# 5 Measurement applications

Measuring physical quantities with RPC sensors is based on resonance measurement and evaluation of one or more resonance values, e.g.  $f_s$ ,  $Q$  or  $R_1$ . A measurement consists of the recording of an admittance spectrum, the resonance evaluation and the calculation of the measurement result with the sensor response function. The resonance measurement can be done with a LabVIEW module, that was developed according to the resonance measurement process described in the previous chapter. The module is controlled by input parameters, as described in 4.4. The output of the resonance measurement module are the resonance values, the equivalent circuit values and information about the timing of the measurement. In this chapter the two main measurement applications, that the *QxSens* project dealt with, are described, the temperature measurement with QT sensors and the viscosity measurement with QV sensors.

Physical measurands change the behaviour of RPCs in different ways. In viscosity measurement, the series resonance frequency and the quality factor of the QV sensor depend on the viscosity of the measured fluid. The change of the series resonance frequency is small compared to the maximum frequency range, that is given by the measurement range of the sensor. The frequency range for the resonance measurement can be kept small and a linear frequency scan is the optimal resonance measurement method. The QT sensor changes its series resonance frequency with temperature. The half width and height of the resonance peak are nearly unchanged. The narrow resonance peak moves along the frequency axis in a comparably large frequency range. Therefore a possibility had to be developed to track and measure the peak fast enough while maintaining high measurement speed. The Peak Tracking Measurement is such an optimized peak tracking and measuring algorithm.

The *QxSens* system is a multi-purpose measuring system, that can be used in laboratories as well as in industrial processes. It has to be configured depending on the current measurement task. To make the configuration fast and simple an automatic system configuration was developed. Each sensor has its own configuration file that contains all the necessary information. It is like a “driver” for the sensor. The future goal of this solutions is, that when buying a new sensor, the “installation” of the sensor in the measurement system is done by simply copying the configuration file to a specific path on the computer. The rest of the configuration is then done automatically. Then the user must only choose the sensor out of a pop down menu in the software interface.

## 5.1 Peak Tracking Measurement(PTM)

The temperature measurement with QT sensors is based on the change with respect to temperature of the series resonance frequency of a narrow series resonance peak in a wide frequency range with respect to temperature. The height and the half width of the series resonance peak keep nearly unchanged. Scanning the whole frequency range, that corresponds to the measurement range of the sensor, in every measurement would lead to a very long measurement time. A better way is to search for the peak once and keep track of it in further measurements. The scanned frequency range can then be reduce to a small range around the peak, speeding up the measurement. The Peak Tracking Measurement (PTM) described in this chapter is such a tracking algorithm. This tracking algorithm was developed in the *QxSens* project especially for temperature measurement with QT sensors. Furthermore, the algorithm can be used for any measurement with RPC based sensors, where the physical measurand is correlated to the series resonance frequency of a narrow peak, with the half width and height remaining nearly constant. The tracking does not improve measurement speed, if the peak does almost fill the whole frequency range. In this case a nonlinear resonance scan of the whole frequency range is faster. A limitation for the PTM is the maximum slope of the measurand, respectively the series resonance frequency, with respect to time ( $T_S$ ). The speed of the measurement must be significantly greater than the maximum slope of the series resonance frequency. If the measurement value changes too fast or jumps, the algorithm cannot track the peak anymore.

The Nassi-Shneiderman diagram in Figure 46 shows the functionality of the PTM. The parameter  $t_m$ , that indicates the time when the last series resonance peak was found, controls the two types of frequency scans performed in the PTM, a whole frequency scan and a small peak tracking scan. When the PTM is called the first time, or no resonance peak was found in the preceding run of the PTM, indicated by  $t_m$  being zero, a frequency scan covering the whole frequency range is performed in order to find the peak that should be kept track of. The whole frequency range is given by the lower frequency  $f_{\min}$  and the higher frequency  $f_{\max}$  and corresponds to the measurement range of the sensor.

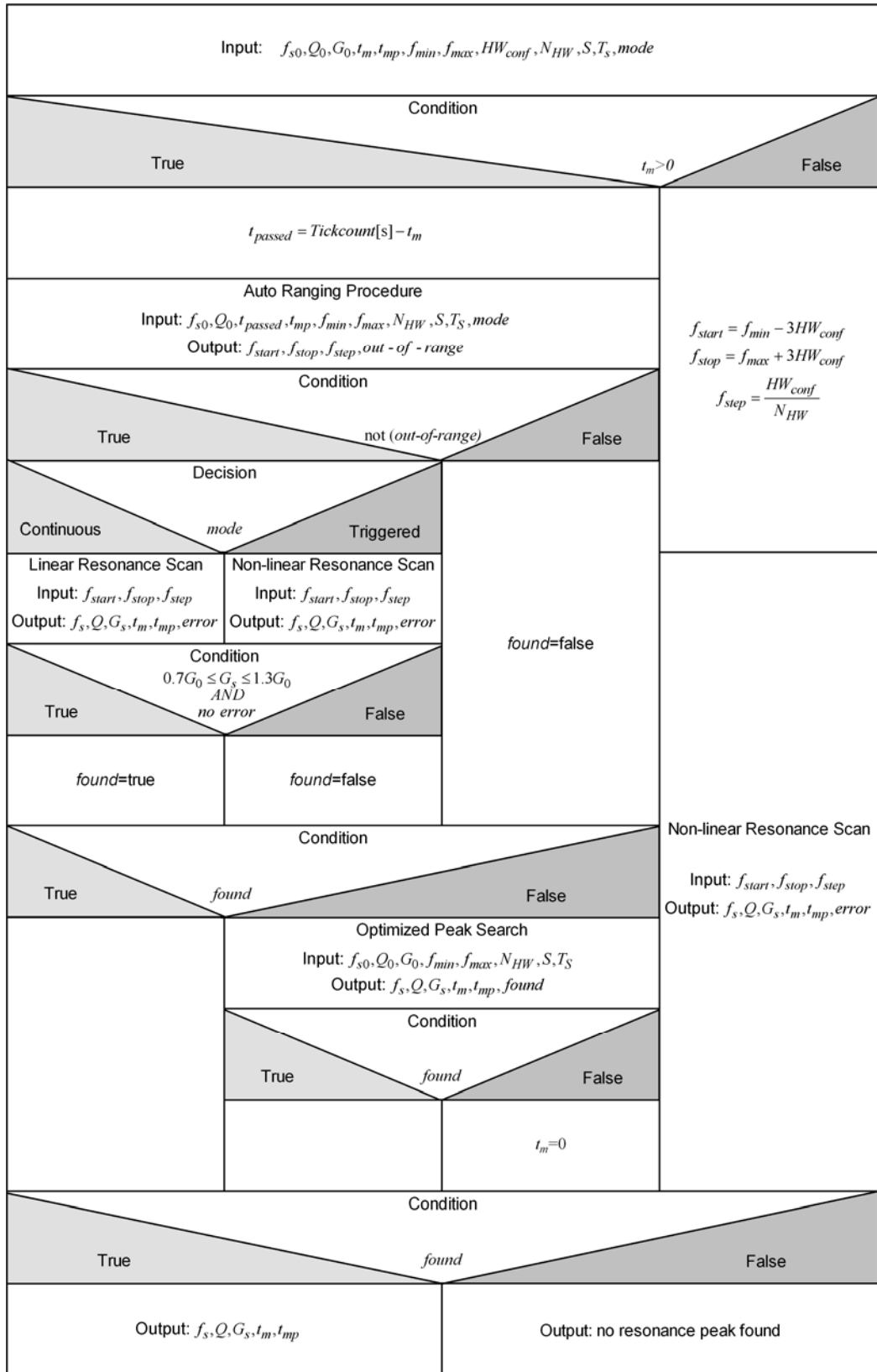


Figure 46: Nassi-Shneiderman diagram of the Peak Tracking Measurement. The PTM first searches a peak in the whole frequency range. Once the peak was found, the system tracks the peak.

If the series resonance frequency  $f_s$  is near one of the limits, the resonance peak can exceed the given frequency range and is likely to be missed. In order to ensure the detection of a resonance peak near the frequency limits, the measured frequency range

is extended by 3 half widths of the resonance peak. In the first run of the PTM, or when the preceding run of the PTM failed, the half width of the searched resonance peak must be given as configuration parameter  $HW_{conf}$ . As mentioned above, one condition for using the PTM is that the half width of the series resonance peak is nearly constant.  $HW_{conf}$  is therefore a sensor specific parameter that is independent from the measurement. The start frequency  $f_{start}$ , the stop frequency  $f_{stop}$  and the step width  $f_{step}$  used in the resonance scan are then calculated using

$$\begin{aligned} f_{start} &= f_{min} - 3HW_{conf} \\ f_{stop} &= f_{max} + 3HW_{conf} \\ f_{step} &= \frac{HW_{conf}}{N_{HW}} \end{aligned} \quad (34)$$

where  $N_{HW}$  is the number of measurement points within the half width. It determines the precision of the measurement result. As shown in 4.1.2  $N_{HW}$  should be set to 15.

The resonance scan is done using the resonance measurement according to chapter 4. The non-linear mode of the resonance measurement is the best choice for finding a small peak within a wide frequency range. It optimizes measurement speed by giving precise measurement results at the same time. A resonance peak is only found, if there is exactly one peak with a conductance of at least 70% of the maximum conductance value in the whole spectrum (see 4.3.5.1). If there is no peak or more than one peak complying to this condition, tracking is not possible. The results of the resonance measurement, which are also the output parameters of the PTM, are the series resonance frequency  $f_s$ , the quality factor  $Q$ , the conductance at the series resonance frequency  $G_s$ , the time it takes to measure one measurement point  $t_{mp}$  and the time of the measurement  $t_m$ . The time of the measurement  $t_m$  is given in seconds and set to the computer system's tick counter in the resonance measurement module.

When the PTM is called the next time, the results from the preceding resonance measurement are used to track the peak. First the time difference  $t_{passed}$  between the last measurement and the current measurement is calculated to

$$t_{passed} = Tickcount[s] - t_m \quad (35)$$

where  $Tickcount[s]$  is the computer systems tick counter in seconds. Then the Auto ranging procedure (ARP) calculates the minimum frequency range, that must be scanned in the resonance measurement in order to track the peak. It uses the series resonance frequency  $f_{s0}$  and the quality factor  $Q_0$  from the preceding PTM as starting point for the calculation of the frequency range. The calculation is based on the measurement speed, the maximum time slope of the measurand and the time difference

between the last measurement and the current measurement. The ARP returns the scan parameters for the resonance measurement,  $f_{start}$ ,  $f_{stop}$  and  $f_{step}$ . If the calculated frequency range exceeds the maximum frequency range of the sensor or the measurand changes too fast compared to the measurement speed, the ARP fails and the *out-of-range* flag of the ARP is set to true. A detailed description of the ARP and its calculations is given in 5.1.1.

If the ARP returns a valid frequency range, a resonance scan is done in this frequency range. If the ARP fails, that means the *out-of-range* flag of the ARP is true, the resonance scan is skipped and a peak search is started directly after the ARP. The kind of resonance scan done depends on the current mode of the PTM. The PTM can be run in two modes, determined by the *mode* input parameter. The continuous mode is optimized for consecutive measurements, e.g. temperature monitoring, whereas the triggered mode enables peak tracking even if the PTM measurements are not done consecutively. The viscosity measurement with QV/QT sensor combinations is an example for the usage of the PTM in triggered mode. The QT temperature measurement, using the PTM, and the QV viscosity measurement, using a standard resonance measurement, are done alternately. The resonance scan can also be done in two modes. The linear scan mode gives precise measurement results in any measurement setting. The main disadvantage of this mode is, that the measurement time depends linearly on the width of the scanned frequency range. This means, when scanning wide frequency ranges, the linear scan mode is very slow. In the non-linear scan mode the frequency steps are adapted dynamically. On the one hand, this leads to an acceleration of the resonance scan in frequency ranges where the admittance changes only slightly. On the other hand, additional measurement points have to be measured when reducing the step width in the range of the resonance peak. That means, the non-linear resonance scan is optimized for measuring a small peak in a wide frequency range. The linear resonance scan is used instead, when the scanned frequency range is small compared to the half width of the peak, as the non-linear scan mode cannot accelerate the measurement in this case. Therefore in triggered mode the PTM does a non-linear resonance scan, whereas in continuous mode a linear resonance scan is done. If a peak is found in the resonance scan, it has to be checked, if it is the tracked peak. This check is done by comparing the conductance height of the peak  $G_s$  to the conductance height of the tracked peak  $G_0$ . The conductance at the series resonance

frequency may vary up to 30% from one measurement to another. Therefore the peak is identified as being the tracked peak, if condition (36) is fulfilled.

$$0.7G_0 \leq G_s \leq 1.3G_0 \quad (36)$$

The variation of 30% has been determined empirically for the QT sensors used in the *QxSens* project. It has to be adapted, if other sensor types are used with the PTM. If the detected resonance is the tracked peak, the PTM is finished. If no resonance is detected or condition (36) is not fulfilled, a peak search is started.

The peak search could be done by scanning the whole frequency range, which would lead to a very long measurement time. As the last position of the peak  $f_{s0}$  is known, another possibility to search the peak is, to start a pendulum search at  $f_{s0}$ . The Optimized Peak Search (OPS) developed in the *QxSens* project does such a pendulum scan. It starts the search at the last measured series resonance frequency  $f_{s0}$  and scans small frequency ranges alternately up- and downwards. An overlap of the frequency ranges ensures that the peak is not missed. The pendulum scan is done until either the peak is found or the whole frequency range has been scanned. A detailed description of the OPS is given in 5.1.2. If the peak is found, the PTM is finished and the ARP starts to track the peak again in the next run of PTM. The OPS fails, if the peak jumps or moves to fast along the frequency axis during the search. In this case, the whole frequency range has to be scanned for the peak in the next run of the PTM. Therefore the time indicating the last measurement of the peak  $t_m$  is set to zero.

In summary, it can be said that the main advantage of the PTM is its ability to track a resonance peak at a high measurement speed. This is achieved by keeping the number of time-consuming resonance measurements as low as possible. In general there is just one initial total frequency scan. All following scans are limited to a very small frequency range. Only if the resonance peak moves unexpectedly, the ARP “looses” the peak and the OPS is started. The pendulum scan in the OPS also scans only the smallest necessary frequency range in order to find the peak again.

### 5.1.1 Auto Ranging Procedure (ARP)

The Auto Ranging Procedure calculates the optimized frequency range for tracking a resonance peak, whose series resonance frequency changes with time. The calculation starts at the last known peak position  $f_{s0}$ . This frequency is used as centre for the calculated frequency range. The width of the frequency range is then calculated depending on the maximum change of the series resonance frequency since the last measurement. The calculation is done in a way, that the measurement speed is optimized. The results of the ARP,  $f_{start}$ ,  $f_{stop}$  and  $f_{step}$ , determine the frequency range and the step width for the resonance measurement. If the possible change of the series

resonance frequency exceeds the maximum frequency range of the sensor or the measurement speed is too low compared to the maximum time change of the measurand, the ARP indicates this by setting the flag *out-of-range* to true.

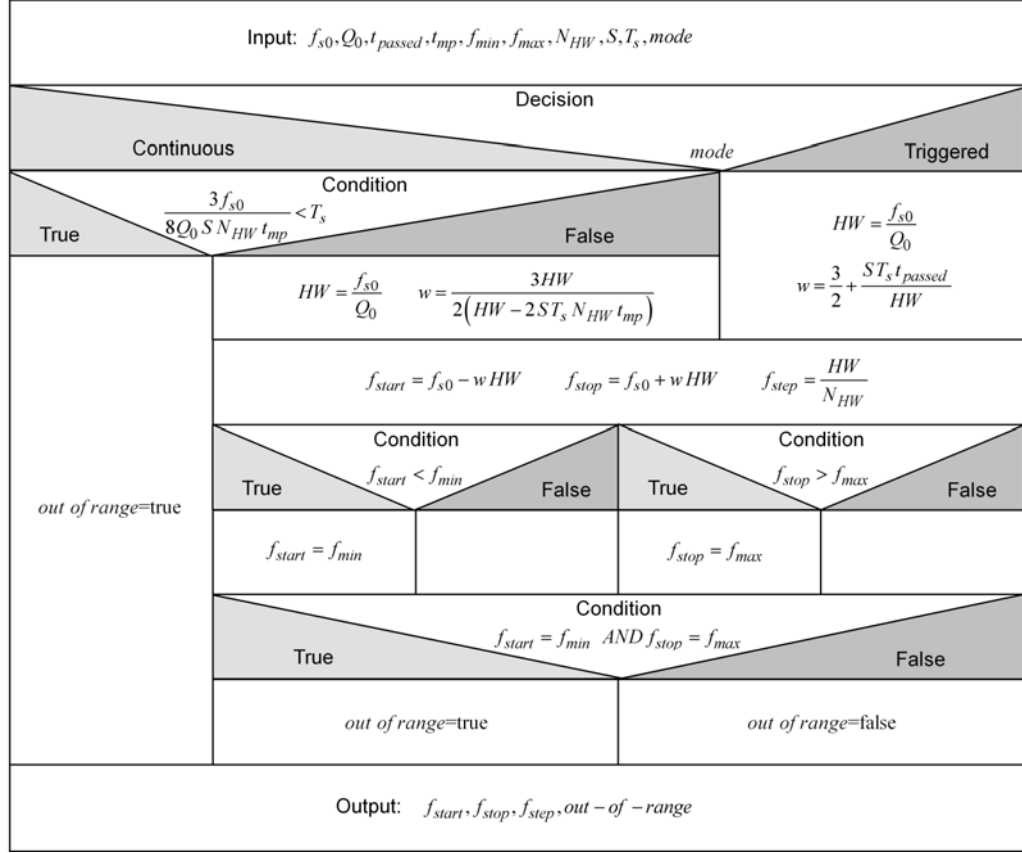


Figure 47: Nassi-Shneiderman diagram of the Auto Ranging Procedure. The ARP calculates the frequency interval that must be measured in order to keep track of a moving resonance peak.

The Nassi-Shneiderman diagram in Figure 47 shows how the ARP works. Depending on the *mode*, different formulas are used to calculate the frequency range. The derivation of the formulas used in the ARP was described in [21]. The frequency range is calculated by taking  $f_{s0}$  as centre, then adding and subtracting respectively the half width  $HW$  of the resonance multiplied by a weight factor  $w$  (37). The step width  $f_{step}$  is calculated by dividing the half width  $HW$  by the number of points per half width  $N_{HW}$ . The half width is calculated according to (6).

$$\begin{aligned}
 HW &= \frac{f_{s0}}{Q_0} \\
 f_{start} &= f_{s0} - wHW \\
 f_{stop} &= f_{s0} + wHW \\
 f_{step} &= \frac{HW}{N_{HW}}
 \end{aligned} \tag{37}$$

The frequency range, that must at least be measured to enable a detection of a resonance, is  $f_{s0} \pm 3/2HW$ . So  $w$  must be greater or equal to 3/2. In triggered mode, the

calculation of  $w$  is based on the time passed since the last measurement was started  $t_{passed}$ . The maximum frequency change since the last measurement is given by multiplying the sensitivity  $S$  of the sensor by the maximum slope of the measurand  $T_s$  and the time passed since the last measurement  $t_{passed}$ .  $w$  therefore calculates to

$$w = \frac{3}{2} + \frac{S T_s t_{passed}}{HW} \quad (38)$$

In continuous mode, where consecutive measurements are done, the measurement speed is used instead of the time since the last measurement as basis for the calculation of the frequency range. The measurement speed is given by the time per measurement point  $t_{mp}$ . The number of measured points in the last measurement  $N$  depends on  $w$  and can be calculated from (37) by dividing the frequency range by the step width. Multiplying  $t_{mp}$  by  $N$  gives  $t_{passed}$ . Inserting  $t_{passed}$  into (38) and solving the recursion leads to (39).

$$w = \frac{3HW}{2(HW - 2ST_s N_{HW} t_{mp})} \quad (39)$$

Formula (39) is only valid, as long as the maximum slope of the measurand  $T_s$  is smaller than  $3/8$  of the measurement speed in measurand-units per second. If  $T_s$  is greater than this value, the ARP is not able to calculate an appropriate frequency range and therefore sets the *out-of-range* flag to true.

The calculated frequency range is checked on both ends against the limits  $f_{min}$  and  $f_{max}$ . If a limit is exceeded, the respective value is set to the limit. If the calculated frequency range is the whole frequency range, the *out-of-range* flag is set to true, indicating that an optimized frequency range could not be calculated.

## 5.1.2 Optimized Peak Search (OPS)

The Optimized Peak Search is a search algorithm that finds a narrow resonance peak in a given frequency range. It is designed especially for searching a peak, which last series resonance frequency is known. A requirement for the OPS is, that the half width and height of the searched peak keep nearly unchanged during the search. Starting at the last known series resonance frequency, a pendulum scan scans small frequency ranges alternately up- and downwards. This is a method, how to speed up finding a way out of a one dimensional labyrinth [22]. The search stops, if either the peak has been found or the whole frequency range has been scanned. The peak is identified by its maximum conductance value. Assuming that the peak has not moved too far away from its original position, only a few scans are needed to find the peak. Therefore the pendulum scan is much faster than a full linear scan of the whole

frequency range. However, there are some conditions, described later in this chapter, where a scan of the whole frequency range is faster and the OPS does a whole frequency scan instead of the pendulum scan.

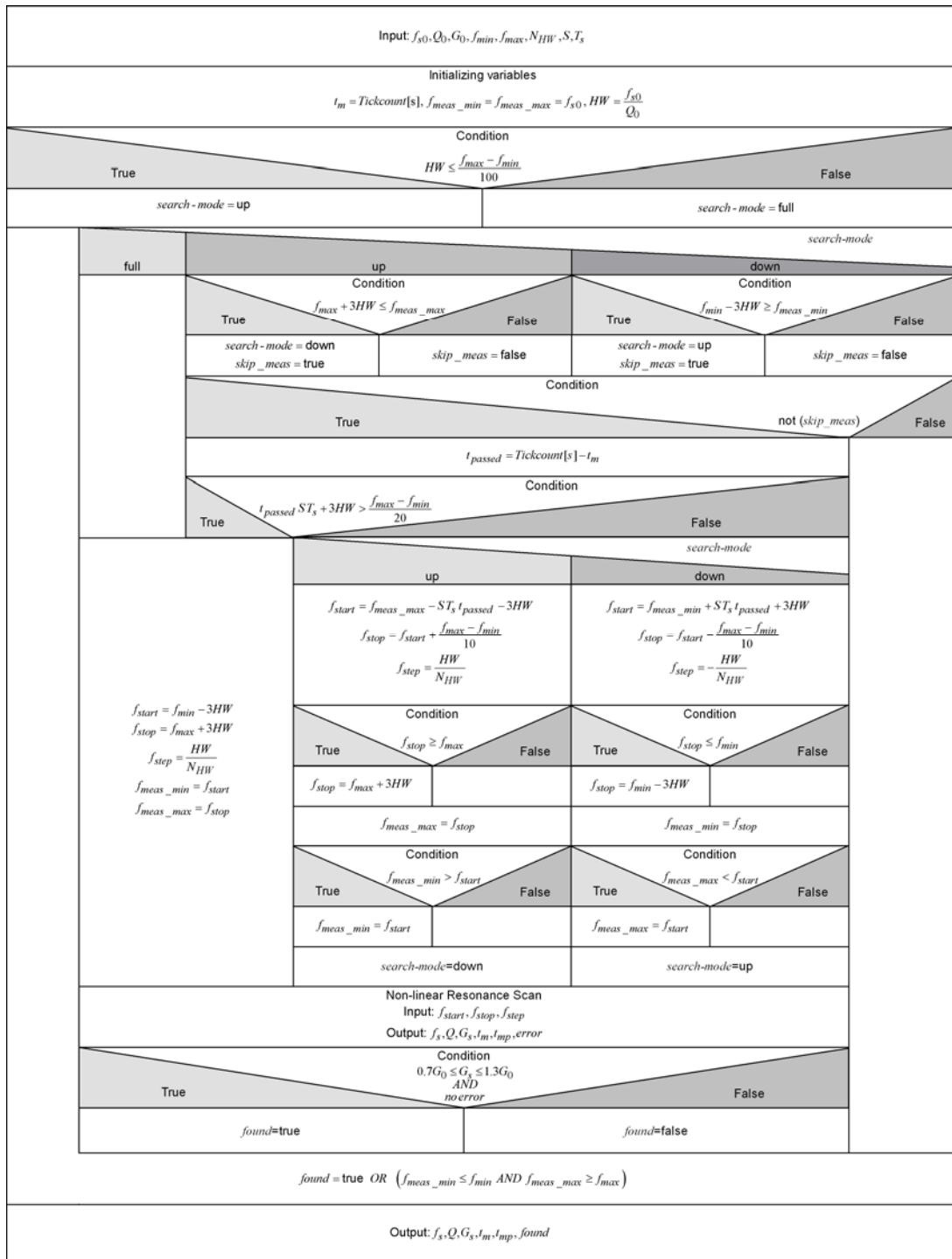


Figure 48: Nassi-Shneiderman diagram of the Optimized Peak Search. The OPS finds a resonance peak by means of a pendulum search starting at the last known series resonance frequency.

The Nassi-Shneiderman diagram in Figure 48 shows the functionality of the OPS. In the first step of the OPS an initialization of variables is done. The variable  $t_m$  indicates the time of the last resonance measurement and is set to the computer system's

tick counter in seconds (shown in Figure 48 as  $Tickcount[s]$ ). The frequency range, that has already been scanned, is determined by  $f_{meas\_min}$  and  $f_{meas\_max}$ . At the beginning of the search,  $f_{meas\_min}$  and  $f_{meas\_max}$  are initialized to the series resonance frequency of the searched peak  $f_{s0}$ , as the search starts at this frequency. The *search-mode* may have three values, “up” and “down”, indicating the direction of the pendulum search and “full” indicating a full scan over the whole frequency range. The width of the searched peak is defined by its half width  $HW$  and is calculated by dividing  $f_{s0}$  by  $Q_0$ , the quality factor of the searched peak. Condition (40) gives the upper empiric limit of the peak width that is searched with a pendulum scan.

$$HW \leq \frac{f_{max} - f_{min}}{100} \quad (40)$$

If the half width of the peak is greater than a hundredth of the whole measurement range, the full scan of the whole frequency range is used and the *search-mode* is set to “full”. The reason for this is, that the non-linear full scan is very fast, when measuring wide resonance peaks, and so the pendulum scan does not accelerate searching of wide peaks. Moreover, a wide peak could even be missed in a pendulum scan due to the small scan ranges used in the pendulum scan. If a pendulum scan is done, the *search-mode* is initially set to “up”.

The actual search is done in a loop, which runs until either the peak was found or the whole frequency range has been searched. In the “full” search mode, the loop is only passed once. The frequency range for the resonance measurement is calculated to

$$\begin{aligned} f_{start} &= f_{min} - 3HW \\ f_{stop} &= f_{max} + 3HW \\ f_{step} &= \frac{HW}{N_{HW}} \end{aligned} \quad (41)$$

The extension of the frequency range by  $3 HW$  is done, in order to be able to find a peak that is close to a limit of the frequency range. If a peak is close to the lower or upper limit of the given frequency range, the resonance peak may exceed this limit and therefore would not be detected if the resonance measurement ends exactly at the given limit. As described in 5.1.1, the extension of the measurement range has to be at least  $3/2 HW$ , to be able to detect a resonance peak with a stable series resonance frequency. But generally in sensor applications the peak is moving along the frequency axis and therefore the extension of the frequency range must be enlarged. Using two times  $3/2 HW$  has proven to be sufficient for any peak search. A division of the half width  $HW$  by the number of points per half width  $N_{HW}$  gives the minimum step width for the non-linear resonance measurement. The full scan searches for the peak in the whole frequency range in just one measurement. Therefore the two variables determining the already scanned frequency range  $f_{meas\_min}$  and  $f_{meas\_max}$  are set to the start and the stop

frequency, respectively. If a peak has been detected in the non-linear resonance scan, the peak is checked against the searched peak by comparing the maximum conductance of the detected peak  $G_s$  with the maximum conductance of the searched peak  $G_0$ , as already described in 5.1. For *QxSens* QT sensors, a difference of up to 30% has been determined empirically (42).

$$0.7G_0 \leq G_s \leq 1.3G_0 \quad (42)$$

In order to identify the searched peak uniquely, there must be not more than one peak in the whole frequency range searched, that fulfils condition (42). If there are two or more peaks of approximately the same height, the OPS is not able to find the peak. If condition (42) is fulfilled, the peak is identified as the searched peak and *found* is set to true. Otherwise *found* is false. As the whole frequency range was already scanned, the loop terminates and the OPS is finished.

In “up” or “down” search mode, the pendulum search is started. In every pass of the loop the frequency parameters  $f_{start}$ ,  $f_{stop}$  and  $f_{step}$  for the resonance measurement are calculated based on the already measured frequency range, given by  $f_{meas\_min}$  and  $f_{meas\_max}$ . First the OPS checks if the already measured frequency range has already exceeded the appropriate limit of the whole frequency range. If a limit has been reached, no further search needs to be done in this scan direction. If the scan direction is up, condition (43) is checked. If it is down, condition (44) is used. These conditions take also the 3 *HW* extension described before into account.

$$f_{meas\_max} \geq f_{max} + 3HW \quad (43)$$

$$f_{meas\_min} \leq f_{min} - 3HW \quad (44)$$

If one of these two condition ((43),(44)) is true, the scan direction is reversed and the rest of the loop is passed. A pendulum search scan always starts at a border of the already measured frequency range. An overlap of the scan ranges ensures that the peak can be found, even if it has moved into the frequency range already measured during the last scan. This overlap depends on the sensitivity of the sensors  $S$ , the maximum change of the measurand with time  $T_s$  and the time passed since the last measurement  $t_{passed}$ .  $S \cdot T_s \cdot t_{passed}$  is the maximum change of the series resonance frequency of the searched peak since the last measurement. Including also the 3 half widths, that are used for the resonance detection of a peak near the border of a scan range, the overlap calculates to

$$\begin{aligned} t_{passed} &= Tickcount[s] - t_m \\ overlap &= S T_s t_{passed} + 3HW \end{aligned} \quad (45)$$

The width of one scan range in the pendulum search is always set to a tenth of the whole frequency range. This calculation of the scan range has been determined

empirically for the *QxSens* QT sensors. If the overlap is greater than half of a scan range, the pendulum search will scan constantly approximately the same frequency range (46). As this does highly increase search time, the pendulum search is interrupted in this case and the OPS switches to the full scan mode.

$$ST_s t_{passed} + 3HW > \frac{f_{max} - f_{min}}{20} \quad (46)$$

In the next step the parameters for the resonance scan are calculated. (47) gives the calculation of the parameters for the up-scan. The start frequency is calculated based on the higher limit of the already measured range  $f_{meas\_max}$ . The overlap given in (45) is then subtracted from  $f_{meas\_max}$ . The stop frequency is calculated by adding the width of a scan range to the start frequency. The absolute value of the step width is the same as in the full scan, only the scan direction must also be regarded in the sign of the step width. Scanning up, the step width has a positive sign, whereas scanning down a negative sign is used.

$$\begin{aligned} f_{start} &= f_{meas\_max} - ST_s t_{passed} - 3HW \\ f_{stop} &= f_{start} + \frac{f_{max} - f_{min}}{10} \\ f_{step} &= \frac{HW}{N_{HW}} \end{aligned} \quad (47)$$

In the up-scan the upper limit of the whole frequency range may be reached. If the stop frequency  $f_{stop}$  exceeds the upper limit  $f_{max}$ , it is set to  $f_{max} + 3 HW$ . In the down-scan the calculations are done in the same way, only with the opposite direction.

$$\begin{aligned} f_{start} &= f_{meas\_min} + ST_s t_{passed} + 3HW \\ f_{stop} &= f_{start} - \frac{f_{max} - f_{min}}{10} \\ f_{step} &= -\frac{HW}{N_{HW}} \end{aligned} \quad (48)$$

The start frequency may be smaller than the lower limit of the whole frequency range  $f_{min}$ . If this is the case  $f_{start}$  is set to  $f_{min} - 3 HW$ . As the already scanned frequency range will be wider after the resonance scan, the variables determining the already scanned range,  $f_{meas\_min}$  and  $f_{meas\_max}$ , are adapted to the new values. Finally the search direction is reversed, indicating that the next pendulum scan goes in the other direction.

If the non-linear resonance scan does not detect any resonance, it raises an error. If a resonance is detected, the resulting output parameters are used to identify the searched peak using (42). If a peak is identified, *found* is set to true and the loop is terminated. Otherwise *found* is false and unless the whole frequency range was scanned, the loop continues with the next pass. The output parameters of the OPS are the output

parameters of the last resonance measurement and in addition the flag *found* indicating, if the searched peak was found.

Figure 49 shows an example of the Optimized Peak Search. This example should make the algorithm more clear. The series resonance frequency of a peak was measured to  $f_{s\_meas}$ . The time, that had passed since this measurement is given in  $t_{passed}$ . The peak's series resonance frequency is currently at  $f_{s\_curr}$ . The 1<sup>st</sup> scan is done upwards and starts at the last measured frequency, including the 3 *HW* extension. If the peak is not in the frequency range covered by the 1<sup>st</sup> scan, a 2<sup>nd</sup> scan has to be done downwards starting at the lower end of the measured range  $f_{meas\_min}$  plus the necessary overlap. The second 2<sup>nd</sup> scan does not find the peak, either. So the OPS jumps to the higher end of the already scanned range  $f_{meas\_max}$  minus the overlap and scans upwards again. In this 3<sup>rd</sup> scan a resonance is detected. The conductance at the series resonance frequency is compared with the searched peak's conductance and if it is within the range of  $\pm 30\%$  of the previous peak height, the peak was found and the search is terminated. It can be seen that after only three scans of small frequency ranges the peak could be found. A full scan over the whole frequency range would take more than 3 times longer.

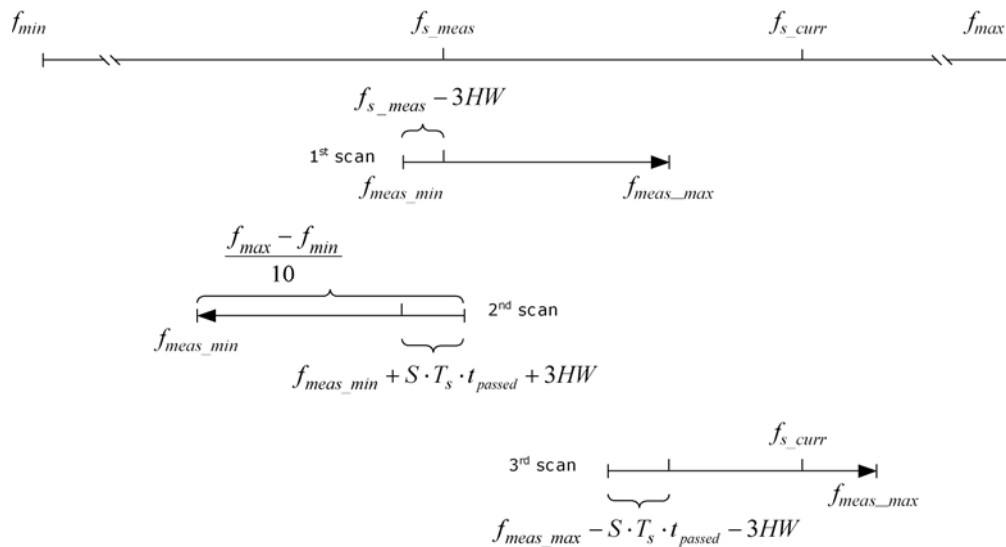


Figure 49: Example, showing how the Peak Search works. On top of the picture the whole frequency range is shown, limited by  $f_{min}$  and  $f_{max}$ . The last measured series resonance frequency  $f_{s\_meas}$  and the current series resonance frequency  $f_{s\_curr}$  are marked. The Peak Search starts the search at  $f_{s\_meas} - 3HW$ , where  $HW$  is the half width of the peak. The 3  $HW$  are needed for the peak to be detected when it is exactly at  $f_{s\_meas}$ . The Peak Search scans the tenth part of the whole measurement range in one scan. After the first scan the search jumps back to the minimum of the already searched frequency range  $f_{meas\_min}$ . In addition to the 3  $HW$  the maximum change of the measurand during the 1<sup>st</sup> scan is also factored in the start frequency of the 2<sup>nd</sup> scan  $f_{meas\_min} + S \cdot T_s \cdot t_{passed} + 3HW$ , where  $S$  is the sensitivity in [Hz/unit],  $T_s$  is the maximum time slope of the measurand in [unit/s] and  $t_{passed}$  is the time that one scan takes. The scan is done in the other direction and as no resonance is found, the search jumps to the maximum of the already measured frequency range regarding the same factors as in the 2<sup>nd</sup> scan, now  $f_{meas\_max} - S \cdot T_s \cdot t_{passed} - 3HW$ . In this example the resonance is found in the 3<sup>rd</sup> scan. The Peak Search was successful and is terminated.

## 5.2 Automatic system configuration

Like any other measurement system the *QxSens* measurement system allows to be configured with regard to the respective measurement purpose. Many parameters concerning the measurement range, the measurement quality and the sensor response have to be set correctly. The *QxSens* system was developed as a multi-purpose measurement system, that can be used in laboratories as well as in industrial processes. Generally it can be assumed, that a standard user of the measurement system is not familiar with all the types of parameters. The automatic system configuration simplifies the operation of the *QxSens* measurement system. The user only has to select the channel where the sensor is connected and to choose the name (type) of the connected sensor from a list.

This easy automatic system configuration is based on the so called qxd-files, the *QxSens* data files. These are configuration files containing all necessary configuration data that determine the parameters for a specific sensor. A qxd-file is like a “driver” for the sensor. The producer of a *QxSens* sensor has to provide the qxd-file. It has to be installed in the computer of the *QxSens* system. This is done by simply copying the qxd-file to the configuration file path. The configuration file path can be set in every measurement application and should be the same for all measurement applications in a computer system.

A qxd-file has the same structure as an ini-file, that means the file contains sections written in square brackets and in these sections the entries are written as “name=value” pairs. Each section in a qxd-file corresponds to one sensor configuration. The name of the sensor configuration is the name of the section. The first parameter is always the *SensorType*. It determines the type of the sensor, e.g. QT or QV, and hence the following parameters are depending on the sensor type. The second parameter that is also used for all sensors is the *ElectronicsName*. The used measurement electronics are sensor-specific. The parameter *ElectronicsName* determines the electronics used for the measurement. The configuration of the electronics can be found in a separate section in the qxd-file. This section is named according to the *ElectronicsName*. In this section the first parameter *ElectronicsType* determines the type of measurement electronics used. In the *QxSens* system the kernel electronics are used and therefore *ElectronicsType* is set to “KE”, standing for kernel electronics. The other parameters of the kernel electronics are then  $R_C$ ,  $C_c$  and the method  $V_c$  or  $V_s$ . The sensor-specific parameters for the QT and QV sensors developed in the *QxSens* project, are described in the particular sections later in this chapter.

Example body of a qxd-file:

```
[QT_2.7Mhz]
SensorType=QT
...Sensor specific data...
ElectronicsName=KE150

[KE150]
ElectronicsType=KE
Rc=150
Cc=0
Kernel-Electronics-Method=Vc
```

When the measurement application is started, all qxd-files in the configuration file path are read. The application filters only those sensors that can be used with this application, e.g. a temperature measurement application reads only sensors with SensorType=QT. All sensors found are displayed in a listbox. The only “configuration” that has to be done by the user is to chose the appropriate sensor in the listbox and to select the channel on which the sensor is connected. When a sensor is selected, the application automatically reads all configuration data into memory. No further configuration is necessary.

## 5.3 Temperature measurement with QT sensors

In 3.1.3.1 it is described how temperature measurement with QT sensors works. A very small series resonance peak moves in a wide frequency range. Therefore temperature measurement is based on the PTM algorithm. In order to reduce the user interaction to a minimum, the automatic system configuration is extended with QT sensor specific information. The software design and the user interface of the QT measurement software are described in this chapter.

### 5.3.1 Configuration data

In 5.2 the general part of the qxd-files used by the automatic system configuration was described. Every sensor configuration is encapsulated in a section. The parameter SectionType determines the kind of sensor used. In this case it is “QT”. Depending on the sensor type different sensor specific configuration parameters are needed. The QT measurement application uses the Peak Tracking Measurement as basis for the measurement. The measured series resonance frequency is then translated to a temperature value using the sensor response function. The first QT specific parameters in the qxd-file are  $K_1$ ,  $K_2$ ,  $K_3$ ,  $f_0$  and  $T_0$ , the coefficients of the QT sensor response function (8). The frequency range, that corresponds to the measurement range of the

sensor, is determined by  $f_{\min}$  and  $f_{\max}$ . HW is the configuration half width  $HW_{conf}$ , that is used to determine the step width of the first resonance measurement (see 5.1). As in the PTM linear and non-linear resonance scans are performed, the maxfactor for the non-linear scan is given in the configuration file as NonLinearScanMaxFactor. This factor specifies the maximum acceleration in a non-linear scan. It should be as high as possible to decrease measurement time, but it is limited by the width of the peak, as if the system accelerates too much, the peak can be missed. The value 100 was determined experimentally and has proven to be a good choice for all *QxSens* QT sensors. The number of points per half width  $N_{HW}$  is set to 15 for all sensors as this value is recommended. The values Average, V\_RMS and Wait are used to control the measurement quality. The ElectronicsName parameter was already described in 5.2.

Example of a QT sensor qxd-file:

```
[QT_2.7Mhz]
SensorType=QT
K1=22.861787E+3
K2=5.030781E+6
K3=-7.996686E+9
f0=6.3441230000E+6
T0=295.149994
fMin=6300000
fMax=6400000
HW=650
NonLinearScanMaxFactor=100
NHW=15
Average=5
V_RMS=1000
Wait=0
ElectronicsName=KE150

[KE150]
ElectronicsType=KE
Rc=150
Cc=0
Kernel-Electronics-Method=Vc
```

## 5.3.2 Measurement process

The QT temperature measurement starts with the automatic system configuration. When the configuration is finished, an infinite measurement loop is started. A Peak Tracking Measurement is used to track and measure the series resonance peak. The temperature is calculated out of the series resonance frequency. Then the measured temperature values are displayed and can be saved to disk. This very simple measurement process enables high measurement speed and provides up to 90 temperature measurements per minute.

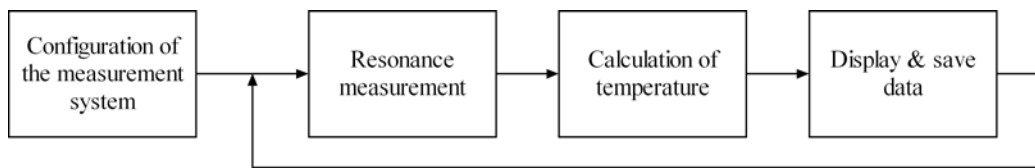


Figure 50: Schematic drawing of the temperature measurement process.

### 5.3.2.1 Configuration of the measurement system

The configuration of the QT measurement system is based on the automatic system configuration described in 5.2. All qxd-files in the configuration file path are searched for sections with `SensorType=QT`. The user then selects the sensor and the configuration data from the selected sensor is read. Additional to the sensor the user selects the channel to which the sensor is connected and the type of *QxSens* measurement system, that is used – internal or external. The DAQ device and the synthesizer of the measurement system are then found automatically by the same procedure as in the self organizing module described in 4.3.1.

### 5.3.2.2 Resonance measurement

QT sensors have a small and high series resonance peak that changes its series resonance frequency with temperature. The frequency range, where the resonance peak moves, is large compared to the width of the resonance peak. Therefore the Peak Tracking Measurement is used for resonance measurement of QT sensors. The PTM is called once per pass of the infinite measurement loop.

The input parameters for the first call of the PTM are the maximum frequency range, given by  $f_{min}$  and  $f_{max}$ , the number of points per half width  $N_{HW}$  and the configuration half width  $HW_{conf}$ , determining the approximate half width of the series resonance peak, the sensitivity of the sensor  $S$ , the maximum change of the measurand with time  $T_s$  and the *mode*.  $f_{min}$ ,  $f_{max}$ ,  $N_{HW}$  and  $HW_{conf}$  are set to the values of the selected sensor configuration in the automatic system configuration. The other three values,  $S$ ,

$T_s$ , and *mode*, have to be set by the user. The sensitivity of the sensor  $S$  is a function of frequency. It is the inverse of the first derivative of the sensor response function (50),  $1/T'(f)$ , and calculates to (49). In the ARP and the OPS the sensitivity  $S$  is calculated at the last measured series resonance frequency ( $S(f_s)$ ).

$$S(f) = \frac{1}{T'(f)} = \frac{1}{\frac{k_1}{f_0} + 2\frac{k_2}{f_0}\frac{f-f_0}{f_0} + 3\frac{k_3}{f_0}\left(\frac{f-f_0}{f_0}\right)^2} \quad (49)$$

$T_s$  is set to the maximum temperature slope. The PTM has two different modes. A continuous mode for consecutive measurements and a triggered mode for periodical measurements, where the time between two measurements is large compared to one measurement time. This means, that there are also the same two modes in the QT measurement application. The continuous mode can be used for monitoring temperature, and the triggered mode is used particularly in viscosity measurements where a QT sensor is mounted right next to a QV sensor. In the viscosity measurement a temperature value and a viscosity value are measured alternately. This means that between two QT measurements another measurement takes place and therefore the triggered mode of the QT measurement system is the appropriate mode.

In all further calls of the PTM the series resonance values and the timing information from the last resonance measurement are provided as additional input parameters.

### 5.3.2.3 Calculation of temperature

If the temperature sensitive series resonance peak was found, the sensor response function (50) is used for calculating the temperature  $T$  [9]. The parameters of the sensor response function have already been set in the configuration of the measurement system. The temperature is calculated in Kelvin and can be converted to °C by just adding 273.15 to the Kelvin value.

$$T(f_s) = T_0 + k_1 \frac{(f_s - f_0)}{f_0} + k_2 \left( \frac{(f_s - f_0)}{f_0} \right)^2 + k_3 \left( \frac{(f_s - f_0)}{f_0} \right)^3 \quad (50)$$

### 5.3.2.4 Display & save data

The calculated temperature value is displayed as numeric value and in a thermometer control. A graph displays the temporal development of the temperature values. In a parameter it can be controlled how far back in time the temperature values are displayed.

Optionally the measured data can be saved to a file. The file saves the time since the measurement start and the temperature values measured. There is a parameter that

controls how often the data is saved. Saving the data after every measurement strongly increases measurement time, because the actually saving to the hard disk takes a while. The output file is a text file with a header and TAB separated values: The time is saved in seconds and the temperature is saved in Kelvin.

Time	Temp
0	283.23
0.7	283.32
1.4	283.55

### 5.3.3 Software user interface

The QT measurement software (Figure 51) is controlled by using the buttons “Start” and “Stop”. After pressing the “Start” button the configuration data is read and the measurement is started. The LED “Run” indicates that the measurement is running. Pressing the “Stop” button saves all unsaved data, if the “Save” switch is on, and stops the measurement.

When the application is started, all QT sensor configurations found in the qxd-files in the “Configuration File Path” are displayed in the listbox “Sensor”. The connected sensor has to be chosen from this list. The “System” indicates whether an internal *QxSens* measurement system or the external USB version is used. The application uses this value to automatically detect the measurement hardware. The “Sensor Number” determines the channel to which the sensor is connected. The maximum temperature slope is entered in “TSlope”. This value is needed for the tracking of the resonance peak during the measurement. In the “Version” selector the mode of the Peak Tracking Measurement, continuous or triggered, can be set. In this software normally the continuous mode would be used. The “Version” selection was implemented only for testing the different modes. The number of seconds back in time that are displayed in the “Temperature” diagram, is set in the “Display last ... seconds” control.

The current temperature is displayed as number and in the thermometer. The “UNIT” can be switched from Kelvin to Celsius. The “Temperature” graph displays the chronological temperature data back to the value given in “Display last ... seconds”. If the unit is switched, the graph is also adapted to the new unit.

The measured temperatures can be saved to a text file. To save the data the “Save” switch must be turned on. Then the measured data are saved periodically to the file given in “Path” periodically. The period is controlled by the “Save every ... seconds” control.

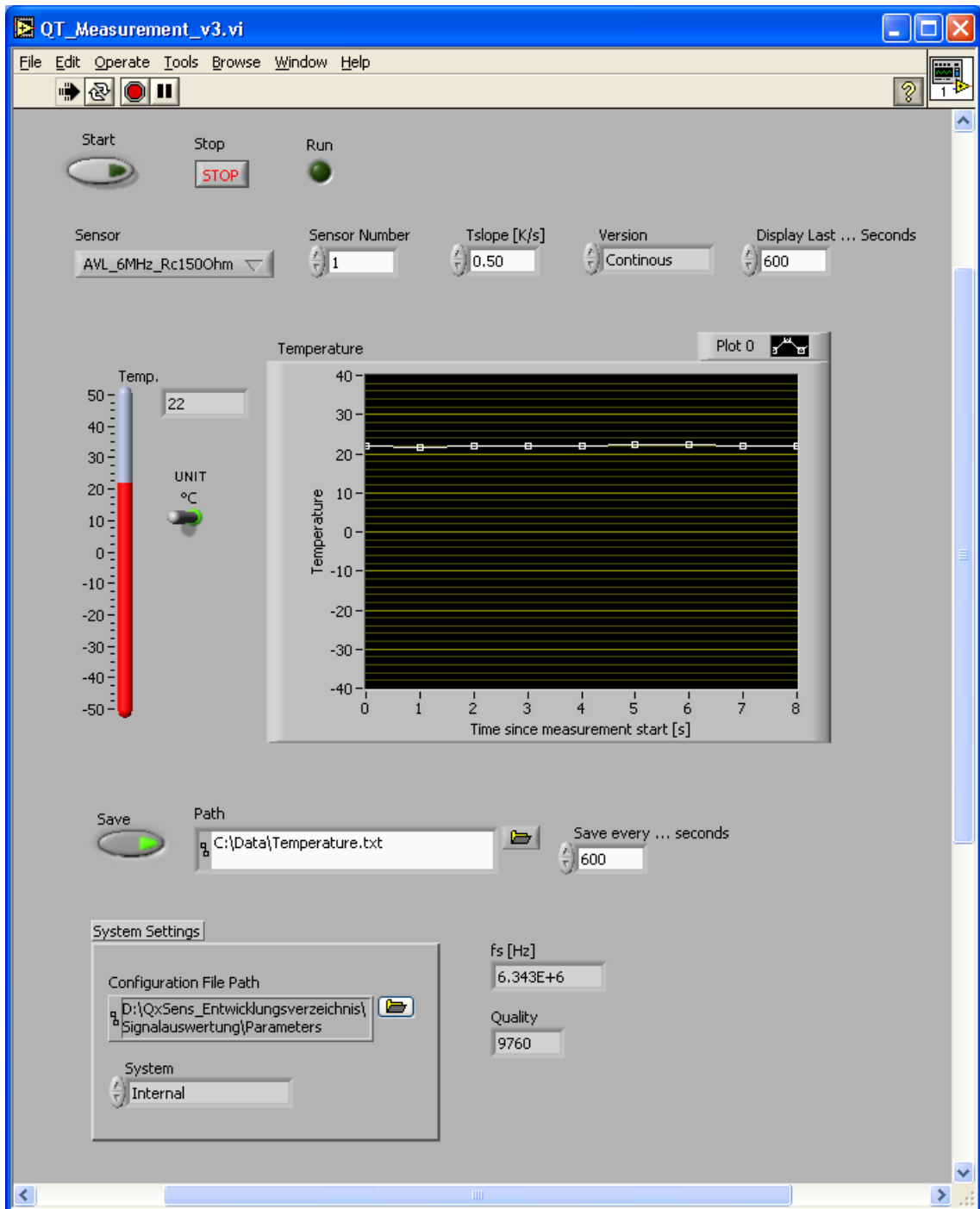


Figure 51: User interface of the QT Measurement program.

### 5.3.4 Measurement results

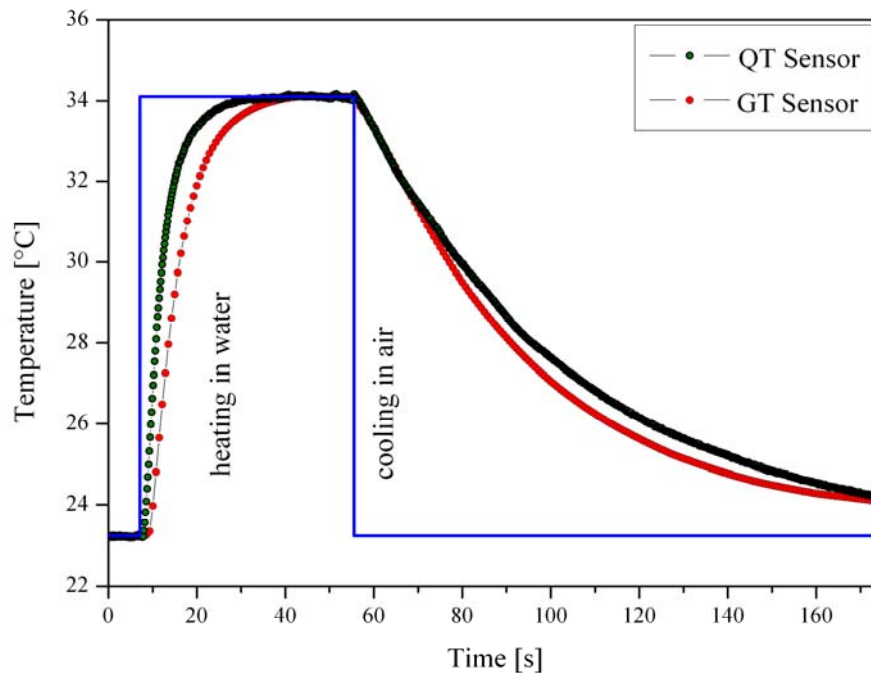


Figure 52: Exemplary temperature measurement result obtained with a 29 MHz quartz crystal sensor (QT) and a 6 MHz gallium-orthophosphate crystal sensor (GT). The blue line shows the temperature step function that was applied to the sensors. The responses of the sensors show different time-constants, that are due to the different sensor constructions.

Exemplary temperature measurements were done with a QT- and a GT-sensor. The results are shown in Figure 52. The sensors were heated in a water bath from 23 to 34 °C and then cooled in air. To enable a high measurement speed the averaging was set to only 10. This results in a measurement time for one measurement value of less than 0.5 s, but causes very noisy measurement results. To decrease the measurement noise the displayed data was calculated by always averaging over the last 5 temperature results. The slightly different time constants of the sensors are due to different sensor constructions.

## 5.4 Viscosity measurement with QV sensors

In 3.1.3.2 it is described how viscosity measurement with QV sensors works. It is stated, that a calibration is needed to get precise measurement results. A detailed description of how to calibrate a QV sensor is given in this chapter. The automatic system configuration is extended with QV sensor specific information to reduce the user

interaction in the QV measurement application. Also the software design and the user interface of the QV measurement application are described.

## 5.4.1 Calibration

As described in 3.1.3.2 a calibration is essential to get precise viscosity measurement results with QV sensors. In the first part of this chapter, the theoretical considerations about the QV sensor calibration are explained. In the other two parts, a description of the implementation of the theory, including a detailed description of how to calibrate a sensor with the developed *QxSens* QV calibration software, is given.

### 5.4.1.1 Theory of QV calibration

The viscosity describes the physical property of a liquid to resist shear induced flow. Isaac Newton was the first to describe the viscosity of an ideal fluid. He defined the basic law:

$$\tau = \eta \cdot \dot{\gamma} \quad (51)$$

where the viscosity  $\eta$  is the proportionality coefficient between the shear stress  $\tau$  and the shear rate  $\dot{\gamma}$ .

In Figure 53 a physical system consisting of two parallel plates and a liquid between the two plates is shown. A force  $F$  applied tangentially to an area  $A$ , being the interface between the upper plate and the liquid's underneath, leads to a flow in the liquid layer.

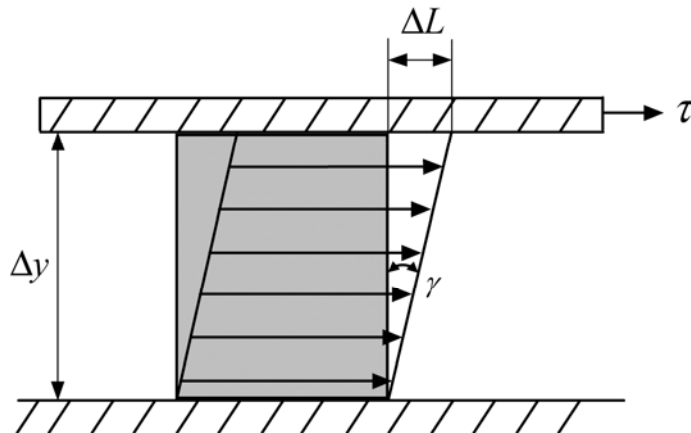


Figure 53: Flow between two parallel plates. The plate on top is moving parallel relative to the bottom plate. Between the two plates there is the liquid, whose viscosity should be measured.

The shear stress is defined as the ratio between the force  $F$  and the area  $A$ . Its SI unit is Pascal.

$$\tau = \frac{F}{A} \quad [\tau] = \text{Pa} \quad (52)$$

The flow speed  $v$  of the liquid drops from the maximum flow speed  $v_{max}$  at the upper plate to  $v_{min}=0$  at the lower, stationary plate. Assuming laminar flow, that means infinitesimally thin liquid layers slide on top of each other, the speed drop, named shear rate, is defined as

$$\dot{\gamma} = \frac{d\gamma}{dt} = \frac{dL}{dy} = \frac{dv}{dy} \quad [\dot{\gamma}] = \text{s}^{-1} \quad (53)$$

Its SI unit is  $\text{s}^{-1}$ . In case of the two parallel plates with a linear speed drop across the gap the differential in (53) is reduced to

$$\dot{\gamma} = \frac{v_{max}}{\Delta y} \quad (54)$$

The dynamic viscosity  $\eta$  is obtained by solving equation (51) [23]. Its SI unit is  $\text{Pa}\cdot\text{s}$ .

$$\eta = \frac{\tau}{\dot{\gamma}} \quad [\eta] = \text{Pa}\cdot\text{s} \quad (55)$$

The viscosity depends on different, independent physical quantities. One of them is the temperature of the liquid. All experiences show that the viscosity is heavily influenced by changes of the temperature  $T$  of the liquid. Although there does not exist a full theory of the temperature/viscosity behaviour, different mathematical models based on empirical studies have been developed. One possibility to assume the temperature variation of viscosity is described by Vogel's equation.

$$\eta = \kappa \cdot e^{\left(\frac{\theta_1}{\theta_2 + T}\right)} \quad (56)$$

where  $\eta$  is the viscosity in  $\text{mPa}\cdot\text{s}$ ,  $T$  is the temperature of the liquid in  $^{\circ}\text{C}$  and  $\kappa$  in  $\text{mPa}\cdot\text{s}$ ,  $\theta_1$  and  $\theta_2$  in  $^{\circ}\text{C}$  are the fit constants for a given liquid.

The temperature dependence of viscosity of well known fluids can be used to calibrate viscosity sensors. For the *QxSens* system specific calibration oils, with a temperature/viscosity behaviour well described by Vogel's equation, have been used for the calibration of the QV sensors.

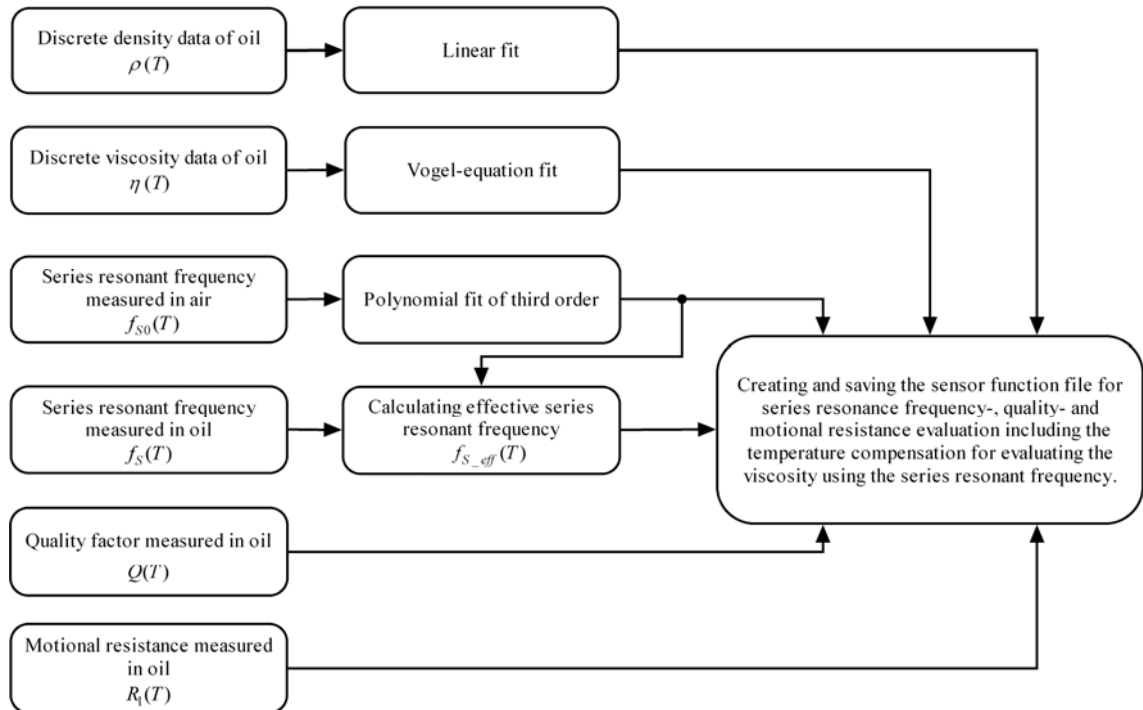


Figure 54: Schematic overview of the QV sensor calibration.

The principle of the QV sensor calibration is shown in Figure 54. The sensor response function of a QV sensor (9) shows, that the resonance is not only influenced by viscosity, but by the product of viscosity and density  $\eta \cdot \rho$ . To be able to calculate this product for the whole temperature range, where the calibration should be done, the continuous functions of viscosity and density with respect to temperature must be known. The viscosity and density values of the calibration oils used in the *QxSens* project (S20, S200 and N1000 from Cannon Instrument, USA) are given at discrete temperature values between 20 and 100°C. Fit algorithms are used to get continuous functions for viscosity and density over temperature (see Figure 55). The density changes linearly with temperature between 20 and 100°C. Therefore a linear function is fit into the density data points. The viscosity function is calculated in a fit using Vogel's equation (56). With these two functions, the viscosity/density product can be calculated at any temperature between 20 and 100°C. An extrapolation of the functions is possible, but outside the given temperature range, chemical and physical effects can cause significant deviations from the used fit models for viscosity as well as density.

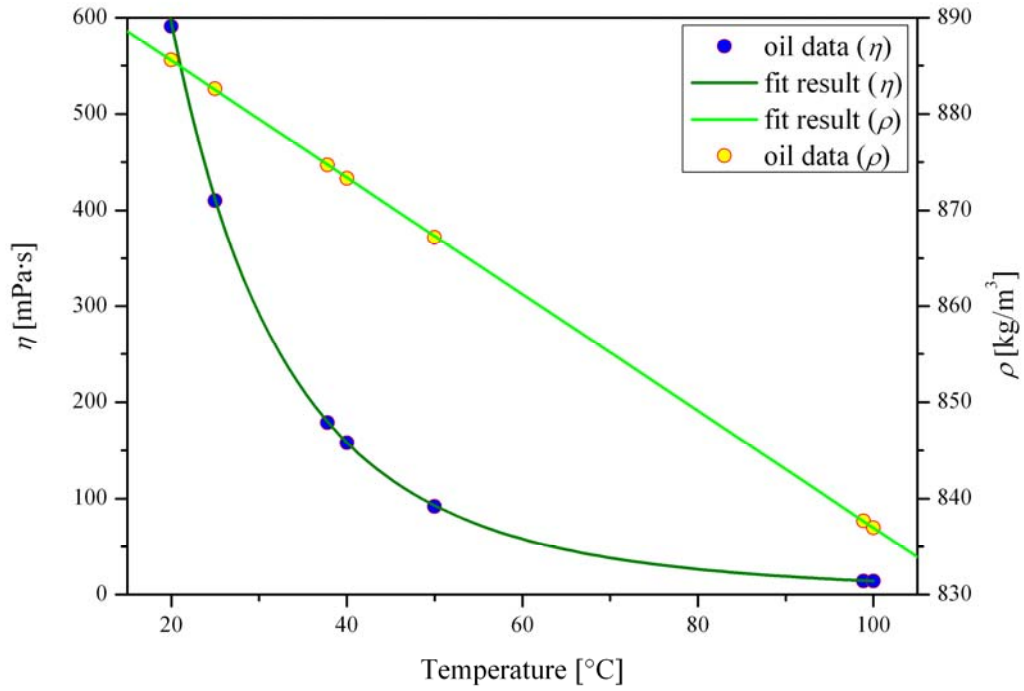


Figure 55: Continuous functions for the density and viscosity are calculated out of the discrete density and viscosity data of the calibration oils. A linear function is fit into the density data and a fit in Vogel's equation is used for viscosity. The fit results for the calibration oil S200 are displayed in this graph.

The calibration measurement is done by measuring the series resonance of a QV sensor immersed in a calibration oil. The measured series resonance frequency  $f_s$ , the quality factor  $Q$  and the motional resistance  $R_l$  are saved for different oil temperature. The series resonance frequency of a QV sensor shows a temperature drift, that is independent from the load of the sensor and that disturbs the viscosity measurement results, unless it is compensated. The compensation of this temperature effect is done by first measuring the series resonance frequency of the QV sensor in air  $f_{s0}$  in the temperature range between 20 and 100°C. The measured frequency/temperature behaviour can best be described by a polynomial function of third order. For the calculation of the calibration data, an effective series resonance frequency  $f_{s\_eff}$  is used instead of the measured value  $f_s$ .  $f_{s\_eff}$  at a given temperature  $T$  is calculated out of the measured series resonance frequency  $f_s(T)$  and the polynomial from the temperature compensation  $f_{s0}(T)$  (57). It is the temperature corrected series resonance frequency at 20°C. This correction makes the calibration function of the viscosity/density product temperature independent.

$$f_{s\_eff}(T) = f_s(T) - (f_{s0}(T) - f_{s0}(20)) \quad (57)$$

In contrast to the series resonance frequency, the quality factor and the motional resistance are not concerned by this temperature drift and therefore a compensation is

not necessary. The calibration function is finally created by assigning the values  $f_{s\_eff}(T)$ ,  $Q(T)$  and  $R_l(T)$  to the product of viscosity and density at the given temperature.

In the viscosity measurement these calibration functions are used to calculate  $\eta \cdot \rho$  out of one of the measured values  $f_s$ ,  $Q$  or  $R_l$ . In this calculation the same frequency correction as described above has to be done before evaluating the viscosity/density product out of the measured series resonance frequency. Therefore, in the calibration, the four polynomial coefficients of the temperature compensation function  $f_{s0}(T)$  have to be saved together with the data points of the calibration curves. The measured frequency  $f_s$  is first transformed in  $f_{s\_eff}$  using (57), and then the viscosity/density product  $\eta \cdot \rho$  is calculated out of  $f_{s\_eff}$ .

The calibration function of one calibration oil enables the viscosity measurement within the given viscosity range of this calibration oil from 20 to 100°C. In order to extend the viscosity measurement range, different calibration oils have to be used. In the *QxSens* project the calibration oils S20, S200 and N1000 from Cannon Instrument have been used. The single calibration functions of these oils are combined to an overall calibration function covering a wide viscosity range from 3000 Pa·s down to 0.8 Pa·s.

Two single calibration functions are combined to a joint calibration function by calculating intermediate values in the frequency range, where the two functions overlap. If  $c_1$  and  $c_2$  are two calibration functions, depending on the series resonance frequency  $f_s$ , where  $c_1$  is the calibration function of the lower viscosity range, (58) shows how the combined calibration function  $c_{12}$  is calculated.

$$c_0(f_s) = c_1(f_s) + (c_2(f_s) - c_1(f_s)) \frac{f_s - c_{1\_fs\_min}}{c_{2\_fs\_max} - c_{1\_fs\_min}}$$

$$c_{12}(f_s) = \begin{cases} c_2(f_s) & f_s \leq c_{1\_fs\_min} \\ c_0(f_s) & c_{1\_fs\_min} \leq f_s \leq c_{1\_fs\_max} \\ c_1(f_s) & c_{1\_fs\_max} \leq f_s \end{cases} \quad (58)$$

where  $c_{1\_fs\_min}$  is the minimum measured frequency of the calibration function  $c_1$ , and  $c_{2\_fs\_max}$  is the maximum measured frequency of the calibration function  $c_2$ . Figure 56 shows the combination of two calibration functions. The measurements have been done with a QV-torsion sensor KN334 from Flucon and the calibration oils S20 and S200.

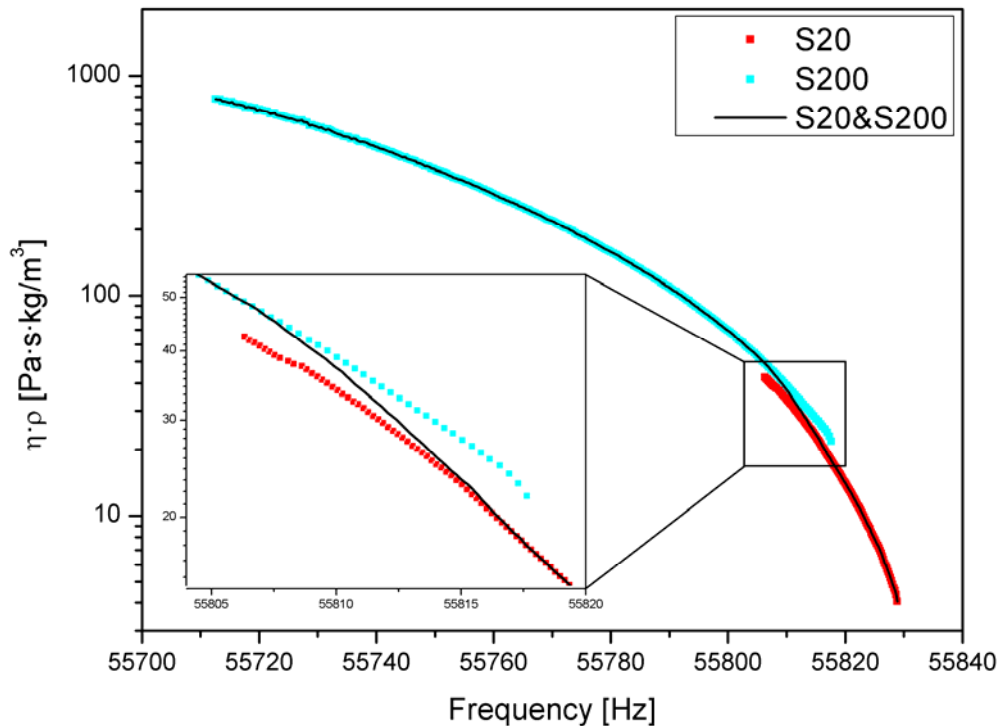


Figure 56: The measurement results of two calibration measurements with the KN334 QV sensor from Flucon in an S20 (red) and an S200 (cyan) calibration oil. The overall calibration function (blue) was calculated using (58). In the zoomed window the transfer from one calibration function to the other can be seen in more detail.

#### 5.4.1.2 Calibration measurement

The calibration of a QV sensor is based on measurements of the series resonance of the sensor in different calibration oils with respect to temperature (see 5.4.1.1). For each calibration oil, a temperature scan from 20 to 100°C has to be performed. It is therefore necessary to be able to control the temperature of the calibration oil within this temperature range. Therefore the *QxSens* measurement system is used in combination with a controllable water bath CB 13-25 from Heto Lab Equipment. The temperature of this water bath can be controlled by an output channel of the NI DAQ device in the *QxSens* computer system. A special metal housing, that contains the calibration oil, enables the evaluation of up to 3 sensors in parallel in one temperature scan. Figure 57 shows the metal housing with 3 different sensors in the water bath. In addition to the oil measurements, a measurement in air is needed for the compensation of the temperature drift concerning the series resonance frequency. For this air measurement, the sensor is put into an oven. The oven is heated up to 100°C, turned off and then cools down to 20°C in 6 hours giving a temperature slope of 0.2°C/min. This slow temperature slope guarantees thermal equilibrium for each measured data point.



Figure 57: Three sensors mounted in a specially developed metal housing, that is put in a water bath. This measurement system is used for calibration of QV sensors.

The user interface of the QV calibration software is divided into four sections (Figure 58). The first section contains the system control and the temperature control. The other three sections are used to control the three sensors, that can be connected to the *QxSens* system.

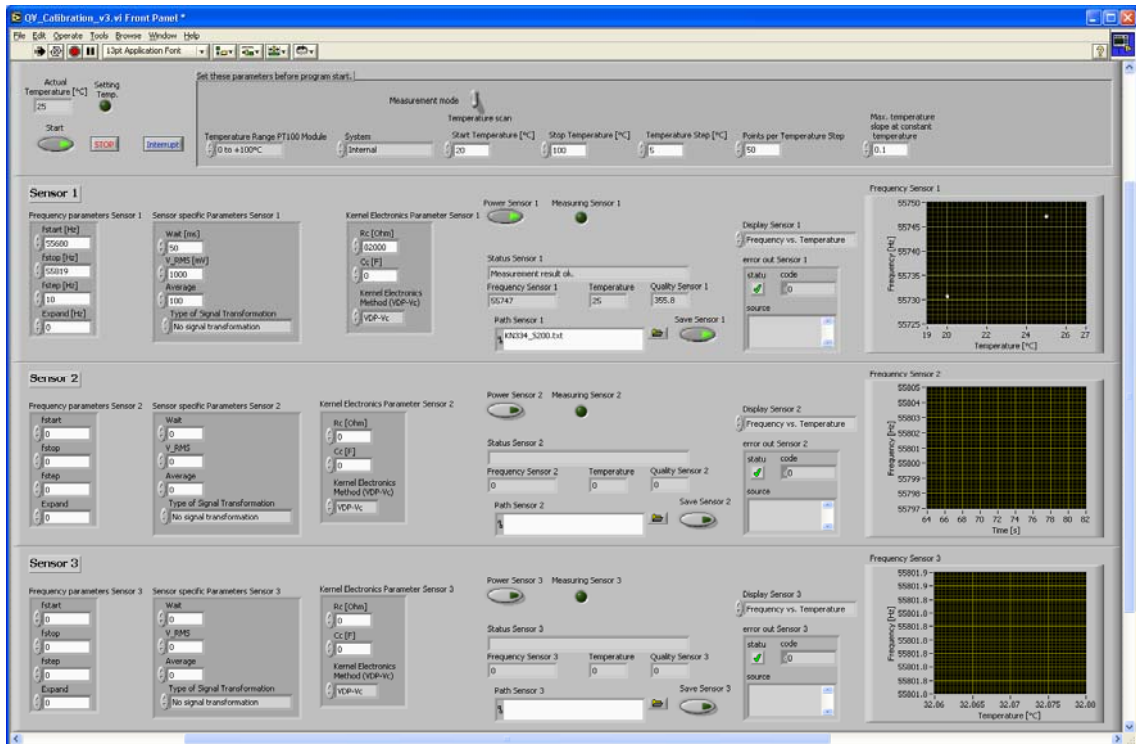


Figure 58: User interface of the QV Calibration software.

The settings in the first section have to be set, before the application is started. The parameter “Temperature Range PT100 Module” has to be set, depending on the

PT100 measurement module mounted in the *QxSens* computer system (see 3.1.1.1.3). The parameter “System” determines if the internal or the external version of the *QxSens* system is used. The calibration measurement can be done in two modes, controlled by the “Measurement mode” parameter. In continuous mode, measurements with all connected sensors are done continuously. In temperature scan mode, the temperature range given by “Start Temperature” and “Stop Temperature” is scanned stepwise. The temperature step width is given in the parameter “Temperature Step”. All temperature values have to be entered in degrees Celsius. At each temperature step, a certain number of data points, given in “Points per Temperature Step”, are measured with all connected sensors. Then the water bath is set to the next temperature step. While the temperature of the water, and thus the calibration oil in the metal housing, changes slowly to the new value, the temperature of the oil is monitored continuously. The “Setting Temp.” LED is turned on as long as the temperature changes. A desired temperature is reached per definition, if the measured temperature slope is smaller than the value given in “Max. temperature slope at constant temperature”. Only if this condition is true, the resonance measurements at this temperature are started. This ensures, that all data points are measured in thermal equilibrium. Figure 59 shows the temperature progress in a temperature scan from 20 to 100°C in steps of 5°C. In the zoomed graph, it can be seen, that the temperature fluctuation at a temperature step is smaller than 0.05°C. After setting all necessary parameters, the measurement can be started by clicking on the “Start” button. An interruption of the measurement is possible any time by clicking on “Interrupt”. A message box is displayed and the measurement is interrupted until the message box is confirmed by clicking on “OK”. Clicking the “Stop” button, stops the measurement after having finished the current resonance measurement.

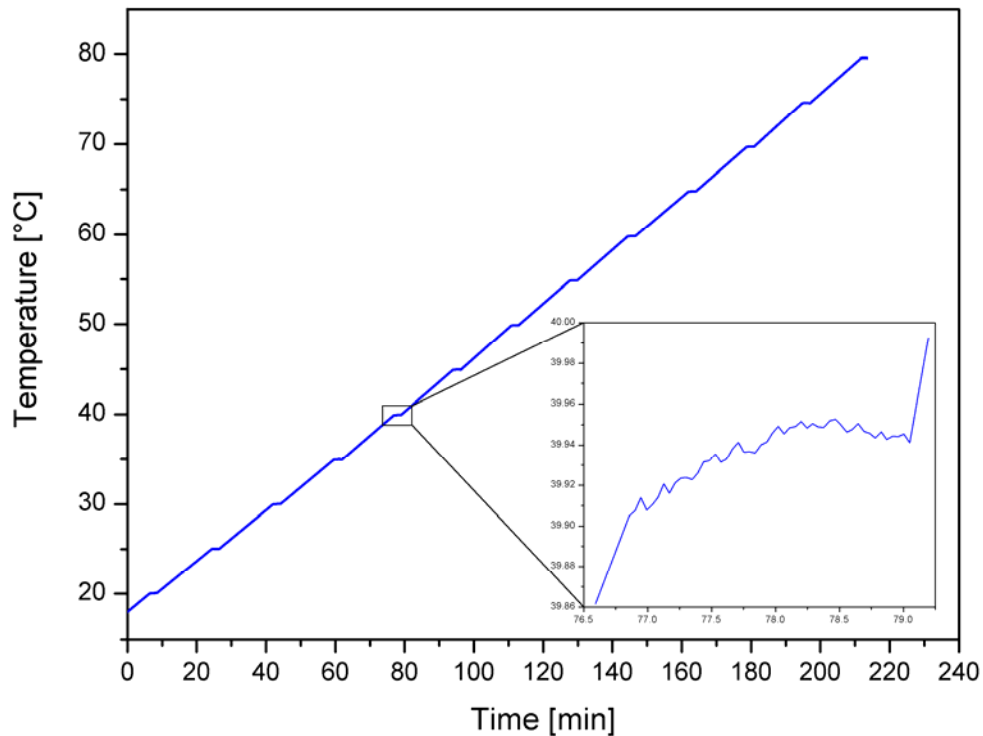


Figure 59: Time behaviour of the oil temperature in a calibration measurement in temperature scan mode. The temperature scan goes from 20 to 80°C in steps of 10°C. At each temperature step, calibration measurements are done. The detailed view at 40°C shows the stability of the oil temperature during the calibration measurement.

Up to three sensors can be connected to the *QxSens* system at the same time. The QV calibration software is able to measure all these sensors in parallel. In the measurement, all sensors are addressed in a cycle: Sensor 1 → Sensor 2 → Sensor 3 → Sensor 1. A sensor is skipped, if its “Power” button is turned off. Whenever a resonance measurement is done with a sensor, the sensor’s “Measuring” LED lights up. The sensor number in the QV calibration software corresponds to the channel number of the *QxSens* system. The parameters of each sensor have to be set, according to the description in 4.4, where the start frequency, the stop frequency and the step width are entered in “fstart”, “fstop” and “fstep”, respectively. The baseline compensation parameters are entered in “Expand” and “Type of signal transformation”. After each resonance scan, the measured temperature, series resonance frequency and the quality factor are displayed. Depending on the setting of the parameter “Display”, a graph shows the measured series resonance frequency with respect to temperature or time. Information about the status of the last measurement is shown in the “Status” indicator. A description of all possible states is given in Table 5.

Status	Description	What to do
Measurement result ok.	The measurement was successful.	
Peak too small for measurement value.	If the step-width is greater than (half width/3) of the measured peak, the correct evaluation of the admittance circle is not guaranteed anymore. In this case, a correct measurement result cannot not be obtained.	Reduce the step-width.
No resonance found. Initial scan started.	No resonance was found. A possible reason is, that the viscosity changed dramatically and the system couldn't follow the peak so fast. Therefore an initial scan of the whole frequency range of the sensor will be done in the next measurement.	
No resonance found -> power off.	If no resonance was found, a whole frequency scan is done three times. If there is still no resonance found, after the third try, the sensor is turned off.	Check the entered start and stop frequency. The resonance might be out of the entered range.
Error -> Initial scan started	If an error occurs, the system starts again with a whole frequency scan.	
Error -> Power off.	If the error still occurs after the third whole frequency scan, the sensor is turned off.	Check the error indicator for the detailed error message.

Table 5: Possible status messages of the QV Calibration software.

If the sensor's "Save" button is on, the measured calibration data are stored in the file given in "Path". The file is a text file with a header and TAB separated values. The values are given in the following units: Temp [K], Frequency [Hz], Quality [1], Time [s], R1 [Ohm], C1 [F], L1 [H], C0 [F].

Example of a calibration file:

```
Temp      Frequency  Quality  Time  R1      C1      L1      C0
84.184    55831.48   2428    8.2   97462   1.2E-15 6746.16 2.5E-11
```

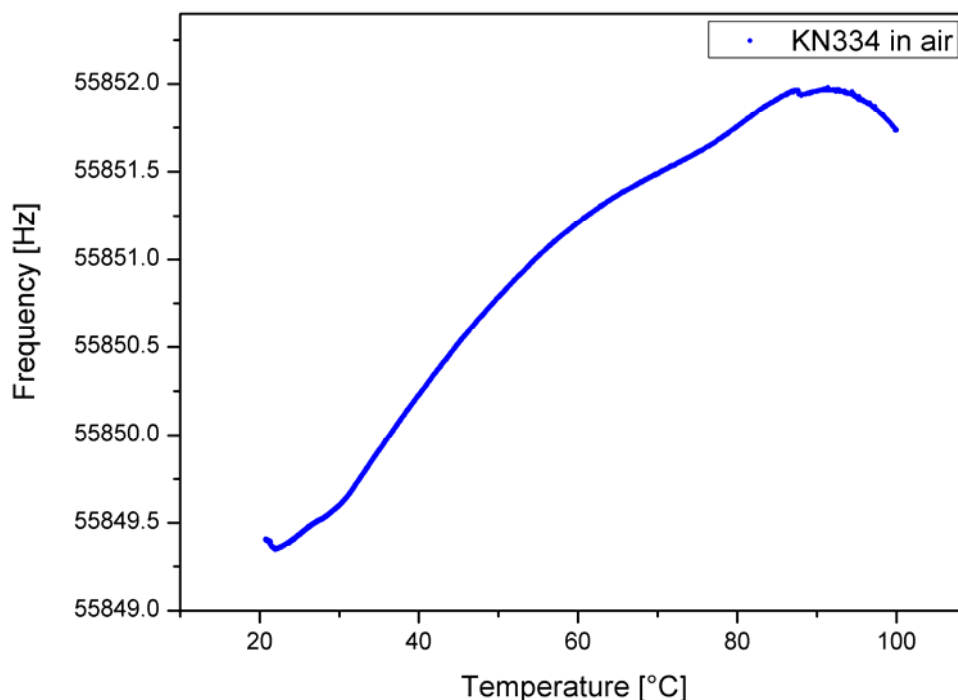


Figure 60: Measurement result of a temperature compensation measurement in air. The QV sensor KN334 was put in an oven at 100°C. The series resonance frequency was measured during the cooling phase using the QV calibration software in continuous mode.

Figure 60 shows the measurement result of the KN334 QV sensor from Flucon in air. The sensor was put in an oven and heated up to about 100°C. Then the oven was turned off. The door of the oven kept closed and so the oven slowly cooled down to about 20°C room temperature. The calibration software was used in continuous mode.

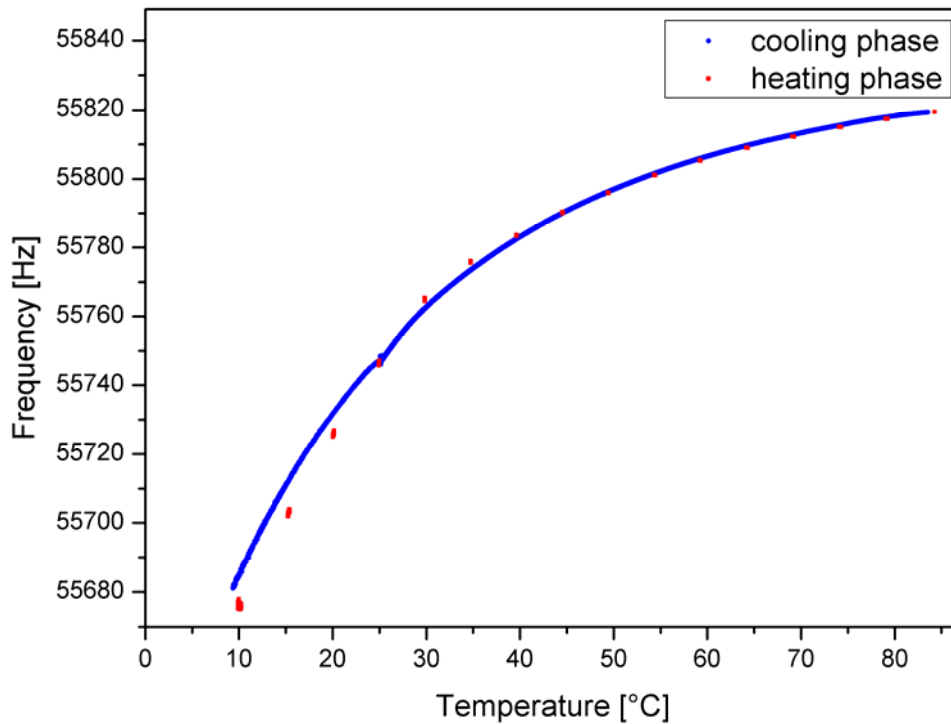


Figure 61: Measurement results of calibration measurements with a KN334 QV sensor in S200 calibration oil. First the oil was heated up in a temperature scan. Calibration measurement have been done every 10°C from 10 to 90°C. Then the heating was turned off and the calibration software was used in continuous mode during the cooling.

In Figure 61 the measurement results of the KN334 QV sensor in S200 calibration oil are displayed. First the calibration software was used in temperature scan mode, heating up the calibration oil from 10 to 90°C in steps of 10°C (red dots). At 90°C the calibration software was switched to continuous mode and the heating of the water bath was switched off. The system cooled down to room temperature, which was about 25°C. Then the temperature of the water bath was set to 10°C to further cool down the water.

### 5.4.1.3 Calculation of the calibration function

In this chapter the software, that implements the calculations described in 5.4.1.1, is explained. The VogelGleichung&SensCalib application calculates the calibration function out of the density and viscosity data of the calibration oil, the results of the temperature compensation measurement in air and the resonance

measurement in the calibration oil. The FunctionStep application combines two calibration functions measured in different calibration oils with the same sensor.

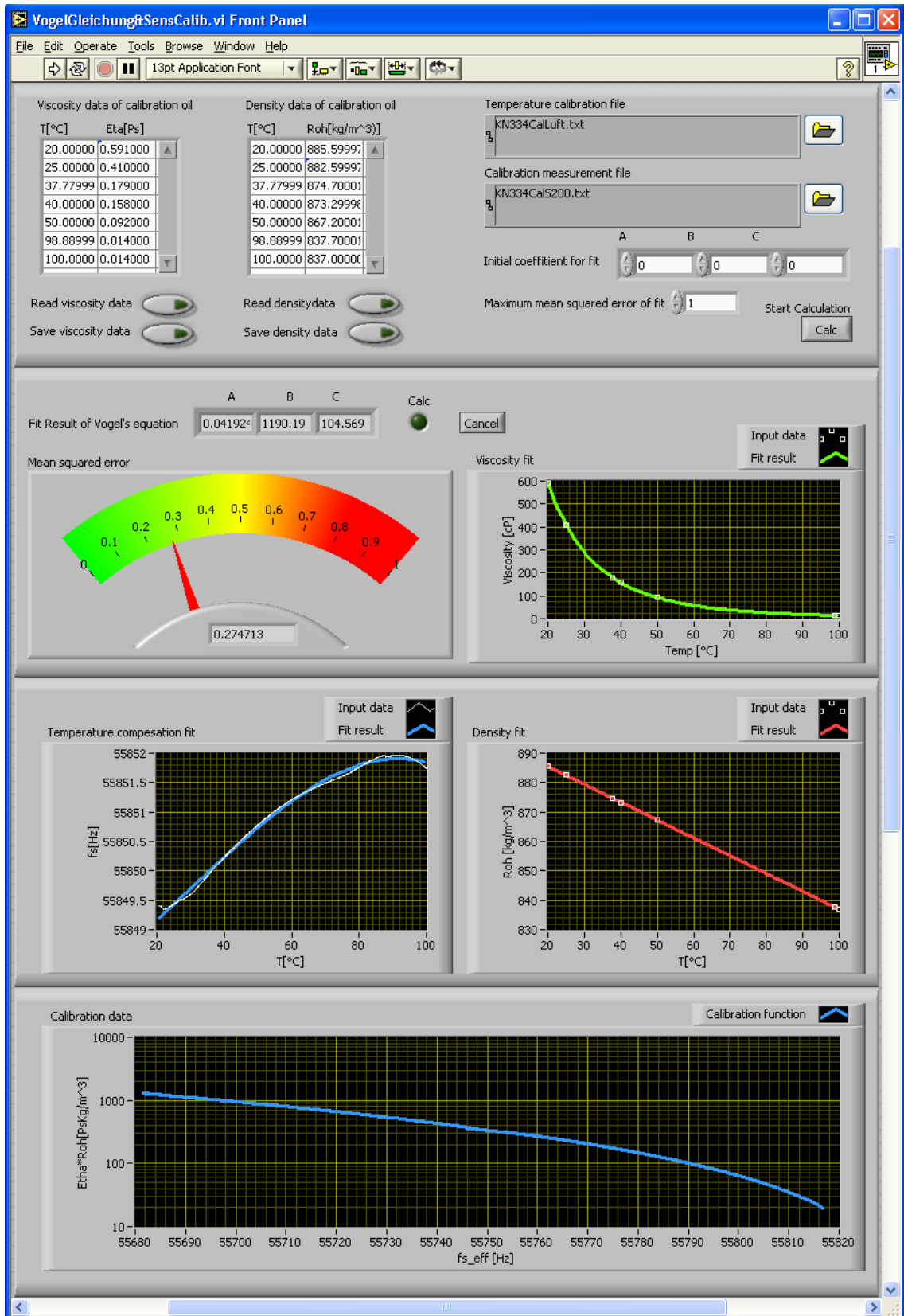


Figure 62: User interface of the VogelGleichung&SensCalib application.

Figure 62 shows the user interface of the VogelGleichung&SensCalib program. The discrete viscosity data of the calibration oil can either be entered manually in a table or read from a text file, which contains TAB separated values, in the form “temperature<TAB>viscosity”. If the data shall be read from file, the button “Read viscosity data” must be turned on. When the calculation is started, a file dialog appears, where the data file can be chosen. To save manually entered viscosity data after calculation, the button “Save viscosity data” has to be turned on. The same applies to the input of the density data. The field “Temperature calibration file” contains the path to the data file of the temperature compensation measurement in air. The field “Calibration measurement file” contains the path to the data file of the calibration measurement in the calibration oil.

A click on “Calc” starts the calculation and the “Calc” LED lights up. First, the entered viscosity data is fit into Vogel’s equation using the Levenberg-Marquardt algorithm. The algorithm uses a set of start-coefficients for the fit. They can be entered in the fields “A”, “B” and “C” in “Initial coefficients for fit”, where “A” is  $\kappa$ , “B” is  $\theta_1$  and “C” is  $\theta_2$ . After the calculation of the fit parameters, the mean squared error, indicating the difference between the calculated fit-function and the entered data, is calculated. Unless the mean squared error is smaller than the value entered in “Maximum mean squared error of fit”, the algorithm is called again, now with the last calculated fit-parameters as start-coefficients. When the mean squared error is small enough, the calculation is stopped and the calculated coefficients of Vogel’s equation (56) are displayed. A comparison of the entered data and the final fit-function is displayed in the “Viscosity fit” graph. Also the final mean squared error is displayed. The entered density data are fit in a linear function, which is displayed in the “Density fit” graph. The measurement results from the temperature compensation measurement have to be thinned out before the polynomial of third order can be fit into the data. The reason for this is, that the data points have been measured continuously while the oven cooled down slowly from 100 to 20°C. The temperature slope during this cooling is not constant. In fact it is about 5 times higher at the start of the cooling, when the air in the oven is hot, than at the end of the cooling. That means, that the data points are not distributed uniformly over the measured temperature range. This non-uniform distribution will disturb the fit results, unless it is compensated. Hence, before the polynomial fit is done, the number of data points is reduced in a way, that the data distribution becomes uniform. After this reduction, the polynomial fit is calculated and the result is displayed in the graph “Temperature compensation fit”.

In the last step, the temperature compensation of the series resonance frequency is done using (57). Then the measured calibration values,  $f_s(T)$ ,  $Q(T)$  and  $R_I(T)$ , from the “Calibration measurement file” are assigned to the viscosity/density product at the

temperature  $T$ . Finally, a file dialog is displayed, where the filename and path of the calibration file can be entered.

The calibration file is a text-file. It is split into two parts. In the first two lines the polynomial coefficients of the temperature compensation fit are saved. A header line is followed by the four TAB separated coefficients  $A_0$  to  $A_3$  of the polynomial

$$f_{s_0}(T) = A_0 + A_1T + A_2T^2 + A_3T^3 \quad (59)$$

Then a second header line indicates the start of the calibration data rows. The data are TAB separated. Here is an extract of a calibration file:

```
Polynomial Fit Data
5.584819E+4  4.157688E-2  4.167278E-4  -4.674177E-6
Frequency    Eta*Rho      Quality      R1
5.582878E+4  3.781854E+0  2.404606E+3  9.857377E+5
5.582876E+4  3.794427E+0  2.403186E+3  9.861000E+5
5.582876E+4  3.799786E+0  2.402580E+3  9.862542E+5
```

In the Functionstep program (Figure 63) two calibration functions can be combined. The condition for the combination of two calibration functions is, that the calibration functions, measured with the same sensor in different calibration oils and calculated with the VogelGleichung&SensCalib application, must overlap.

The input parameters in the “Input parameters” section are the paths to the calibration files, entered in “Function 1” and “Function 2”, respectively, and the parameters for a possible previous data reduction. If “Previous data reduction” is on, the number of data points in the calibration files are thinned out, before stitching the functions. The data reduction is done by deleting data points, which frequency difference to the adjacent data point is smaller than “Reduction of Function (No.)” times the “maximum frequency difference between two adjacent data points”. This reduction shortens calculation time and also leads to a uniform distribution of the data points. The input parameters have to be set, before the program is started. When the program is started and “Previous data reduction” is on, the data points are reduced as described. Then the two functions are combined to one calibration function according to (58). The original functions and the resulting function are displayed in the graphs in the “Results” section. If “Save”, in the “Output parameters” section, is on, the resulting calibration function is saved in “Save path”. The file format is the same as the format of the input files. Figure 56 in 5.4.1.1 shows the combined functions of two calibration files from the KN334 QV sensor in S200 and S20 calibration oils, respectively.

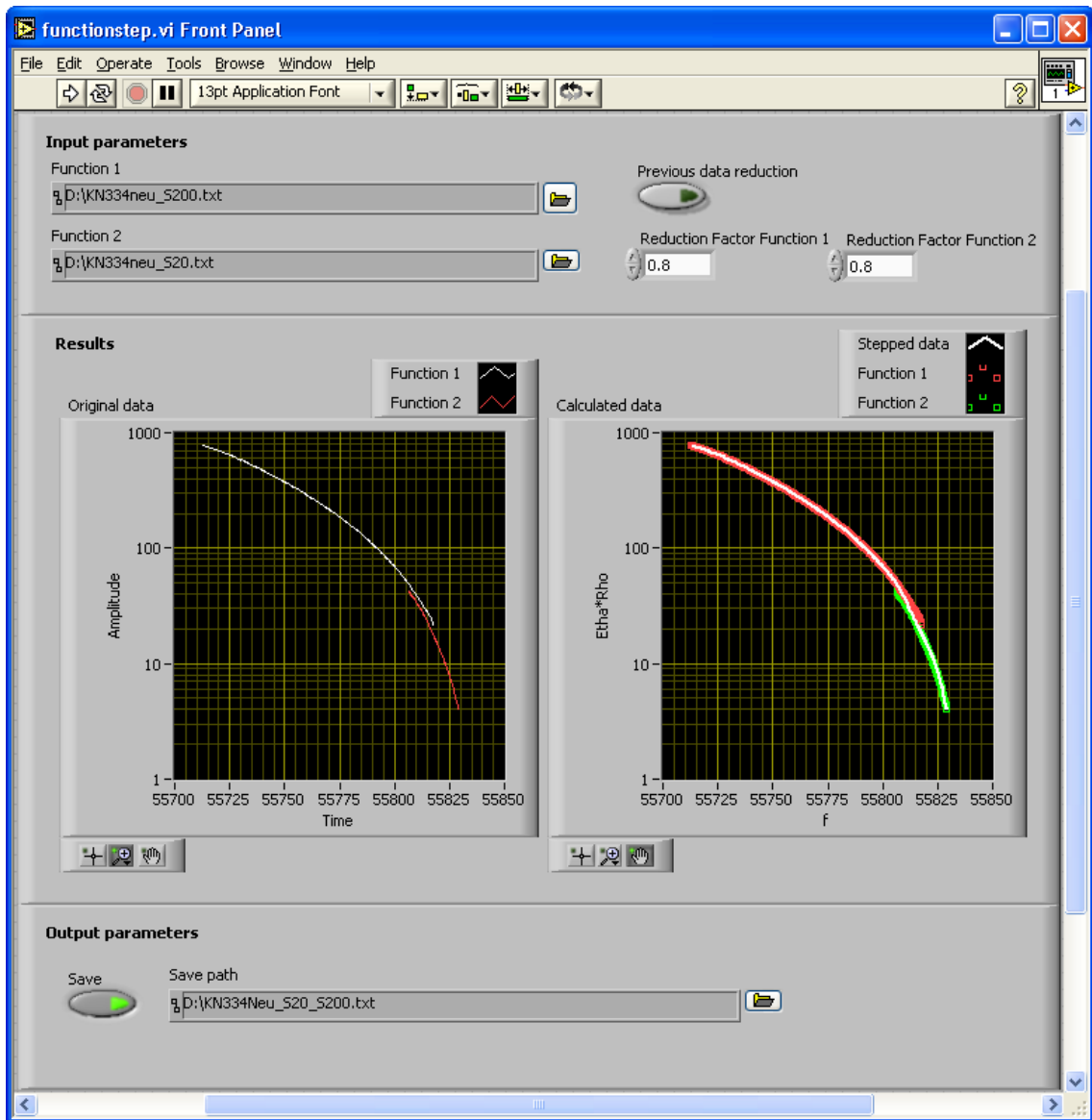


Figure 63: User interface of the Functionstep program.

## 5.4.2 Configuration data

In section 5.2 the general part of the qxd-files used by the automatic system configuration was described. Every sensor configuration is encapsulated in a section. The parameter SectionType determines the kind of sensor used. For viscosity measurements it is “QV”. Depending on the sensor type different sensor-specific configuration parameters are needed. The most important sensor-specific parameter is the Calib-Filename. This parameter contains the path to the calibration file, that is used for the calculation of the viscosity-density product out of the measured resonance values. This calculation can be based on different values. The parameter Calib-Column controls, which value is used. “1” represents the series resonance frequency  $f_s$ , “3” the quality factor  $Q$  and “4” the motional resistance  $R_l$ . A spline interpolation with the data points is calculated, giving the sensor response function  $\eta\rho(x)$ , where  $x$  stands for the

physical value, which the evaluation is based on. As described in 5.4.1.1, a temperature compensation is not only necessary in the calibration process based on the series resonance frequency, but also in the evaluation. Therefore a temperature measurement has to be done parallel to the resonance measurement. The sensor-type used for this temperature measurement is determined by the parameter Temp-Sensorname. Possible values are all QT-sensor names from the qxd-files in the configuration file path and PT100. A sensor with a built in PT100 can only be used on channel 1 of the *QxSens* system (see 3.1.1.1.3). In some cases, described in 4.2.3, a baseline compensation improves the measurement results. If this baseline compensation should be used, the parameter Signal-Transformation has to be set to the value “Subtract linear underground”. The values Average, V\_RMS and Wait are used to control the measurement quality. The ElectronicsName parameter was already described in 5.2.

Example of a QV sensor qxd-file:

```
[QV_KN334]
SensorType=QV
Calib-Filename=KN334_S200_S20.txt
Calib-Column=1
Temp-Sensorname=PT100
Signal-Transformation=
Average=200
V_RMS=1000
Wait=10
ElectronicsName=KE82000
[KE82000]
ElectronicsType=KE
Rc=82000
Cc=0
Kernel-Electronics-Method=Vc
```

### 5.4.3 Measurement process

The QV viscosity measurement starts with the automatic system configuration. When the configuration is finished, an infinite loop is started. In this loop a measurement subroutine for each sensor is called. This subroutine measures the temperature and resonance, calculates the viscosity-density product and displays the measurement results. If a sensor is powered off, the viscosity measurement of this sensor is skipped.

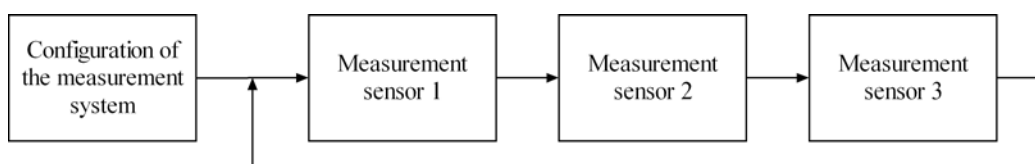


Figure 64: Schematic overview of the viscosity measurement process

### 5.4.3.1 Configuration of the measurement system

The configuration of the QV measurement system is based on the automatic system configuration described in 5.2. All qxd-files in the configuration file path are searched for sections with SensorType=QV. For each channel, the user selects the connected sensor from a list of all found QV sensors. Then the configuration data of the selected sensors are read. The frequency parameters  $f_{start}$ ,  $f_{stop}$  and  $f_{step}$  used in the initial resonance measurement are calculated out of the calibration data using

$$\begin{aligned}
 HW_{max} &= \frac{f_{max}}{Q_{min}} & HW_{min} &= \frac{f_{min}}{Q_{max}} \\
 f_{start} &= f_{min} - \frac{3}{2} HW_{max} \\
 f_{stop} &= f_{max} + \frac{3}{2} HW_{max} \\
 f_{step} &= \frac{HW_{min}}{5} \\
 expand &= \frac{f_{stop} - f_{start}}{2}
 \end{aligned} \tag{60}$$

where  $f_{max}$  and  $f_{min}$  are the maximum and minimum frequency and  $Q_{max}$  and  $Q_{min}$  are the maximum and minimum quality factor in the calibration data of the sensor. The measured frequency range is extended by three maximum half widths to ensure, that the whole calibrated range can be measured. The parameter “expand” is used in the baseline compensation, when the Signal-Transformation parameter of the sensor is set to “Subtract linear underground”. Additional to the sensor, the user selects the type of QxSens system, that is used – internal or external – and the type of PT100 temperature module mounted on the interface electronics – 0 to +100°C or -100 to +200°C. The DAQ device and the synthesizer of the measurement system are then found automatically by the same procedure as in the self organizing module described in 4.3.1.

### 5.4.3.2 Viscosity measurement with one sensor

The QV measurement system addresses all three sensors in an infinite loop. The actual measurement process is the same for all three sensors. The temperature is measured before and after the resonance measurement. The temperature mean value is then used in the temperature compensation and in the calculation of the viscosity-density product. The measurement results are then displayed and can be saved to disk.

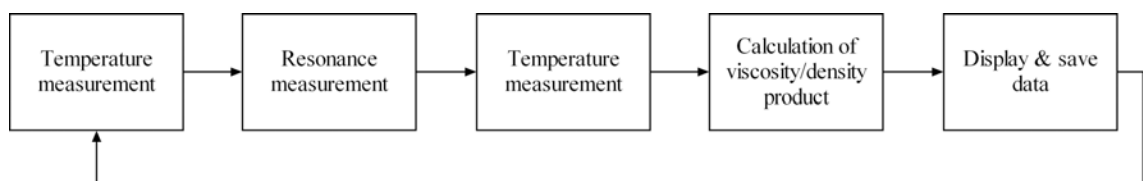


Figure 65: Schematic drawing of the viscosity measurement process with one QV sensor

### 5.4.3.2.1 Temperature measurement

Prior to the resonance measurement, a temperature measurement is done. The temperature value is needed for the compensation of the temperature drift of the series resonance frequency. There are two types of temperature sensors used in QV sensors, QT and PT100. A special LabVIEW program implements the temperature measurement with QT sensors described in 5.3. This module is used for sensors with a built in QT sensor. When a sensor with a PT100 is used, which is only possible on channel 1, the temperature is calculated out of the measured voltage  $U$  on the PT100. Depending on the selected PT100 measurement module, different formulas are used, (61) for the “0 to +100°C” module, and (62) for the “-100 to +200°C” module.

$$T = 20 \cdot U \quad (61)$$

$$T = 60 \cdot U - 100 \quad (62)$$

After the resonance measurement, a second temperature measurement is done. The final temperature value is calculated as mean value of the two measurement results. This allows precise viscosity measurements even in liquids with rapidly changing temperature.

### 5.4.3.2.2 Resonance measurement

The resonance scan is done using the resonance measurement according to chapter 4. The measured frequency range is generally not much wider than the total width of the series resonance peak. Therefore the resonance measurement is done in linear mode. The initial frequency settings, calculated in the configuration, are used in the first resonance measurement. In all further resonance measurements, the frequency settings are calculated out of the respective last measurement results. The viscosity and density of the measured liquid effects affects all characteristic values of the series resonance peak of a QV sensor, especially the series resonance frequency, the quality factor and the motional resistance. All QV sensors used in this work have a broad resonance peak, compared to the whole calibrated frequency range. This means, that peak tracking is much easier than in the temperature measurement. The frequency settings for the next resonance measurement are simply calculated out of the measured series resonance frequency  $f_s$  and the quality factor  $Q$  using

$$\begin{aligned} HW &= \frac{f_s}{Q} \\ f_{start} &= f_s - 2 \cdot HW \\ f_{stop} &= f_s + 2 \cdot HW \\ f_{step} &= \frac{f_{stop} - f_{start}}{40} \\ expand &= 2 \cdot HW \end{aligned} \quad (63)$$

If the step width, used in the current resonance measurement, is greater than  $HW/3$ , too few data points are measured within the admittance circle. In this case, the result of the resonance measurement has to be discarded, because the results of the evaluation of the admittance circle would show too much errors. The next resonance measurement will then be done with the initial frequency settings, calculated in the configuration.

#### 5.4.3.2.3 Calculation of viscosity

If the viscosity evaluation is based on the series resonance frequency, the temperature compensation must be calculated first. Therefore the effective series resonance frequency  $f_{s\_eff}$  is calculated out of the measured series resonance frequency  $f_s$  and the temperature compensation polynomial  $f_{s0}(T)$  using (57). The coefficients  $A_0$  to  $A_3$  for the temperature compensation polynomial (59) are read from the second line of the calibration file (see 5.4.1.3). Depending on the configuration parameter Calib-Column, the viscosity/density product is calculated by evaluating the sensor response function  $\eta\rho(f_{s\_eff})$ ,  $\eta\rho(Q)$  or  $\eta\rho(R_l)$ .

#### 5.4.3.2.4 Display & save data

The measured values  $f_s$ ,  $Q$  and  $T$  and the calculated viscosity-density product are displayed in numeric controls. In addition to the numeric controls, a graph displays the temporal development of the viscosity-density product either with respect to temperature or time.

Optionally the measured data can be save to a file. The file saves the temperature, the viscosity-density product, the time since the measurement start, the measured resonance values and the equivalent circuit parameters. After each viscosity measurement, a row with the data is appended to the file. The file is a text file with a header and TAB separated values. Here is an example of such a file. The units of the columns are as follows: Temp [K], Eta\*Rho [Pa\*s\*kg/m<sup>3</sup>], fs [Hz], Q [1], R1 [Ohm], C1 [F], L1 [H], C0 [F].

Temp	Eta*Rho	Time	fs	Q	R1	C1	L1	C0
47.9	29.12	4.0	55814.4	886	2.675E+6	1.2E-15	6757	2.4E-11
47.9	29.52	7.3	55814.0	874	2.663E+6	1.2E-15	6783	2.4E-11

#### 5.4.3.2.5 Error handling

An error handling has been implemented, to ensure, that the viscosity measurement system does not stop all measurements because of an error, that concerns only one sensor. When an error occurs during viscosity measurement with a specific sensor, this error is displayed and the system tries to start the respective measurement again in the next pass of the global loop. If no resonance could be found in the resonance measurement or the measurement result has been discarded, because the step width was too small, the system starts the next resonance measurement with the initial

frequency settings. If, after three trials, there is still no viscosity measurement result, the system automatically powers off the corresponding sensor.

### 5.4.4 Software user interface

The software user interface of the QV measurement software is divided into four sections (Figure 66). The first section contains the measurement system control. The other three sections are used to control the three sensors, that can be connected to the *QxSens* system.

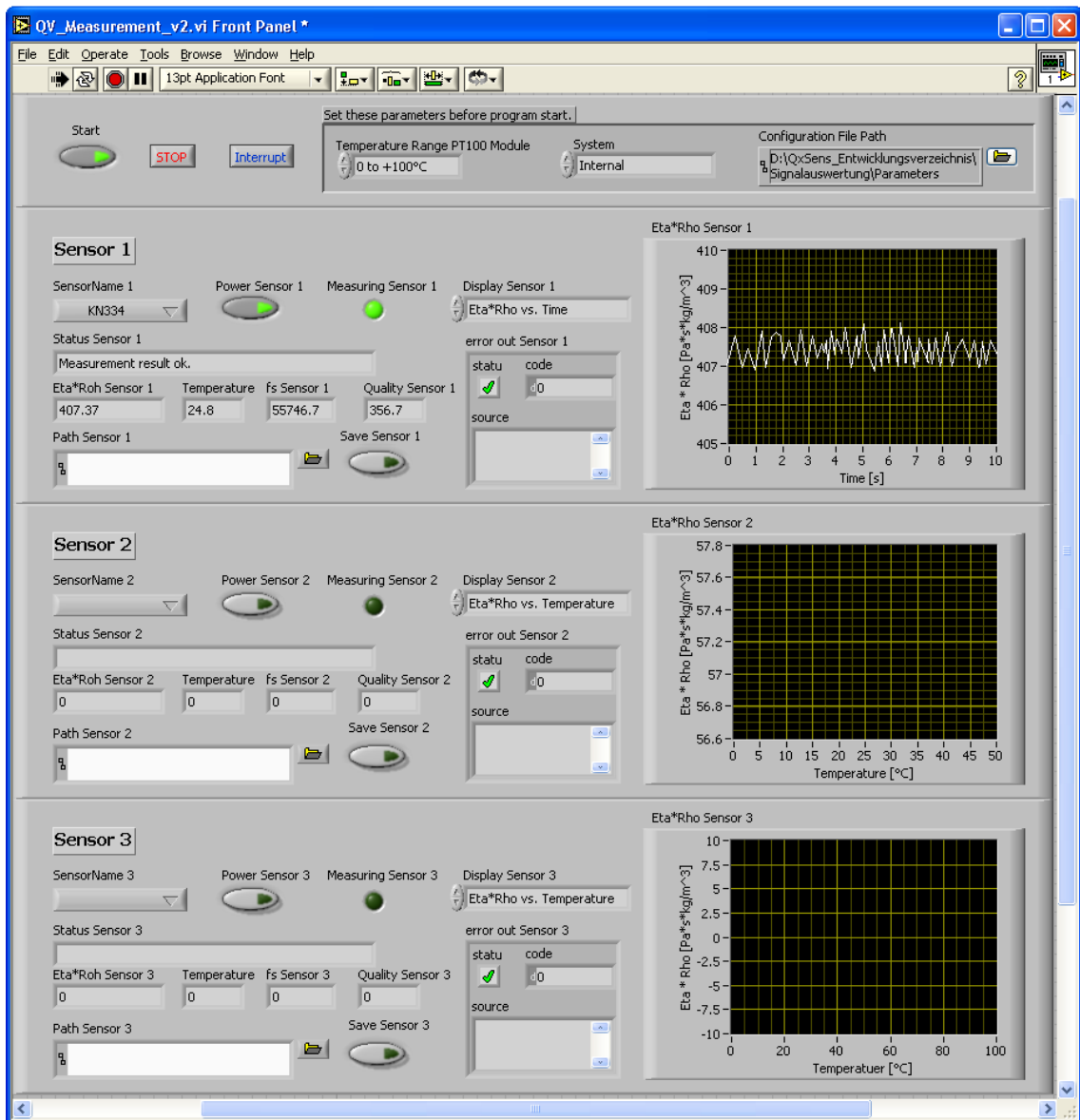


Figure 66: User interface of the QV measurement program.

The settings in the first section have to be set, before the application is started. The parameter “Temperature Range PT100 Module” has to be set, depending on the PT100 measurement module mounted in the *QxSens* computer system (see 3.1.1.1.3).

The parameter “System” determines if the internal or the external version of the *QxSens* system is used. All QV-sensors found in the qxd-files in the “Configuration File Path” are displayed in the “SensorName” lists.

After setting all necessary parameters, the measurement can be started by clicking on the “Start” button. An interruption of the measurement is possible all the time by clicking on “Interrupt”. A message box is displayed and the measurement is interrupted until the message box is confirmed by clicking on “OK”. Clicking the “Stop” button, stops the measurement procedure after having finished the current measurement.

Up to three sensors can be connected to the *QxSens* system at the same time. The QV measurement software is able to evaluate all these sensors in parallel. In the measurement all sensors are addressed in a cycle: Sensor 1 → Sensor 2 → Sensor 3 → Sensor 1. A sensor is skipped, if it’s “Power” button is turned off. Whenever a viscosity measurement is done with a sensor, the sensor’s “Measuring” LED lights up. The sensor number in the QV measurement software corresponds to the channel number of the *QxSens* system. The connected sensor can be chosen in the list “SensorName”. The parameters for this sensor are then read automatically from the configuration file. After each viscosity measurement, the measured viscosity-density product, temperature, series resonance frequency and quality factor are displayed. Depending on the setting in the parameter “Display”, a graph shows the measured viscosity-density product with respect to temperature or time. Information about the status of the last measurement is shown in the “Status” indicator. A description of all possible states is given in Table 6. If the sensor’s “Save” button is on, the measured data are saved in the file given in “Path”.

Status	Description	What to do
Measurement result ok.	The measurement was successful.	
Peak too small for measurement value.	If the step-width is greater than (half width/3) of the measured peak, the correct evaluation of the admittance circle is not guaranteed anymore. In this case, a correct measurement result cannot not be obtained.	Reduce the step-width.
No resonance found. Initial scan started.	No resonance was found. A possible reason is, that the viscosity changed dramatically and the system couldn't follow the peak so fast. Therefore an initial scan of the whole frequency range of the sensor will be done in the next measurement.	
No resonance found -> power off.	If no resonance was found, a whole frequency scan is done three times. If there is still no resonance found, after the third try, the sensor is turned off.	Check the entered start and stop frequency. The resonance might be out of the entered range.
Error -> Initial scan started	If an error occurs, the system starts again with a whole frequency scan.	
Error -> Power off.	If the error still occurs after the third whole frequency scan, the sensor is turned off.	Check the error indicator for the detailed error message.

Table 6: Possible status messages of the QV measurement software.

## 5.4.5 Measurement results

Two exemplary viscosity measurement results are presented here. In both measurements, the temperature dependence of the viscosity-density product was

measured. The sample was heated up and the QV measurement application was used for measurement during the cooling of the sample. The measurement results for SAE 15W40 motor oil from Castrol are displayed in Figure 67. The measurement results for viscose from Lenzing AG, Austria, are displayed in Figure 68.

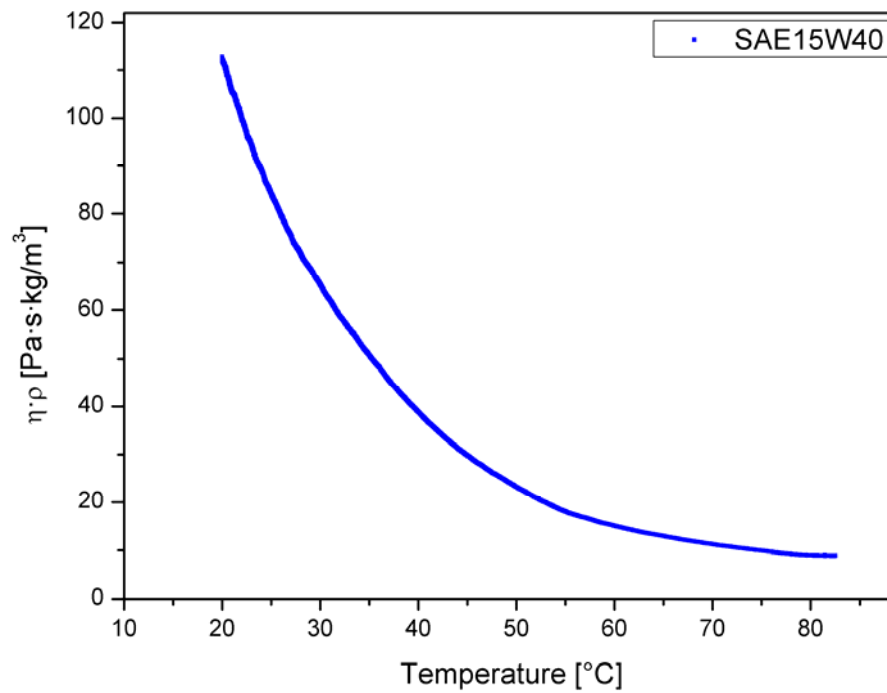


Figure 67: Viscosity measurement result for Castrol SAE 15W40 motor oil measured with a KN334 QV-torsion sensor from Flucon. The oil was heated up to 83°C. During the cooling phase, down to 20°C, the viscosity-density product was measured continuously.

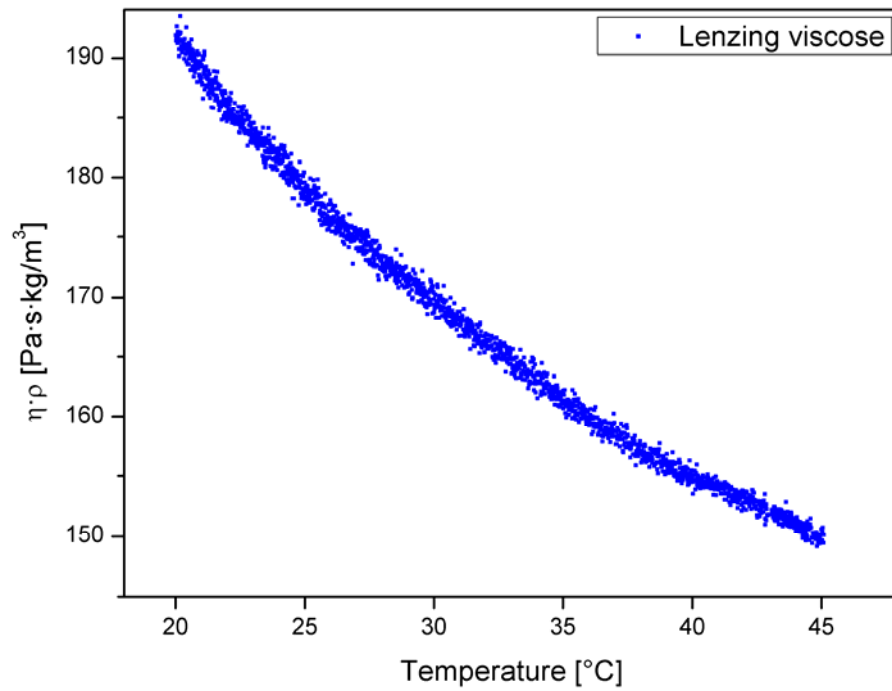


Figure 68: Viscosity measurement result for viscose from Lenzing AG, Austria, measured with a KN370 QV-torsion sensor from Flucon. The viscose was heated up to 45°C. During the cooling phase, down to 20°C, the viscosity-density product was measured continuously.

# List of figures

Figure 1: The graphical representation of a complex admittance value. The value can be expressed in Cartesian coordinates with the real axis as x-axis and the imaginary axis as y-axis, $\underline{Y}=G+iB$ or in polar coordinates with the magnitude $ \underline{Y} $ and the phase angle $\varphi$ , $\underline{Y}= \underline{Y} e^{i\varphi}$ .....	7
Figure 2: Van Dyke equivalent circuit of a piezoelectric crystal sensor.....	8
Figure 3: Locus of admittance of a resonance of a piezoelectric resonator with the characteristic frequencies marked.....	8
Figure 4: Schematic description of the <i>QxSens</i> system. The different parts and the signal-flow between them is displayed.....	10
Figure 5: Absolute error of the output frequency of the synthesizer used in the <i>QxSens</i> system. The absolute frequency error depends on the output frequency. The output frequency of the synthesizer was measured with a HP 5372A high performance frequency and time analyzer.....	12
Figure 6: Block diagram of the signal processing in the interface electronics.....	13
Figure 7: Picture of the PC version of the <i>QxSens</i> system. The important parts for the <i>QxSens</i> system are marked.....	14
Figure 8: Picture of the PXI version of the <i>QxSens</i> system. The interface electronics are mounted on the right side of the chassis.....	15
Figure 9: Picture of the open housing of the external USB version of the <i>QxSens</i> system.....	16
Figure 10: The voltage divider principle used in the VDP kernel electronics. The generator voltage $V_G$ is applied to the voltage divider consisting of the sensor $Z_S$ and the resistor $R_C$ shunted by a capacitor $C_C$ . $V_S$ is the sensor signal, that is used as measurement signal in the VDP- $V_S$ version. $V_C$ is used as measurement signal in the VDP- $V_C$ version.....	17
Figure 11: Picture of the kernel electronics.....	18
Figure 12: Picture of the QV-shear sensor.....	21
Figure 13: Picture of the QV-torsion sensor.....	21
Figure 14: Diagram of the working principle of the cable compensation. The sensor signal is decoupled and applied to the inner shielding over a resistor $R_f$ .....	22
Figure 15: Block diagram of the signal processing in the VDP- $V_C$ kernel electronics. The voltage divider is shown without the capacitance $C_C$ . The voltage across $R_C$ is converted by the differential receiver amplifier ( $\Delta$ ). The signal $S_1$ to $S_4$ are the DC signals used in the computer system to calculate the measured admittance value. To change the block diagram to VDP- $V_S$ only the differential receiver amplifier has to be removed and the sensor is then directly connected to the multipliers.....	23
Figure 16: Comparison of a resonance voltage signal digitized with a 12-bit AD converter with and without dithering. Without dithering (red line) the voltage curve cannot be resolved, which results in steps in the digitized signal. With dithering (green line) the 12-bit AD converter has an increased resolution.....	25
Figure 17: Simulation of different point densities measured as points within a resonance half width. The standard deviation of the series resonance frequency depends on the number of points measured in a half width and the signal noise. The graph shows simulated data for noise levels of 2 to 10%. In many measurement applications, the noise is less than 4%. This means, that about 15 points per half width are enough for precise measurements. Increasing the number does not improve measurement results.....	29
Figure 18: Comparison between the linear and the non-linear scan mode. This figure shows measurements using the linear scan mode with low resolution (100 Hz step width) and high resolution (1 Hz step width) and the non-linear scan with dynamically adapted step width. It can be seen that the low resolution linear scan skips the peak. The high resolution linear scan measures the peak with a very high resolution but also measures many points besides the peak, that do not give more information. The non-linear scan adjusts the step width dynamically and therefore scans only the peak with high resolution, which leads to an increase in measurement speed.....	32

Figure 19: Locus of admittance of the comparison between the linear and the non-linear scan mode (see Figure 18). .....	33
Figure 20: shows the effect of the DC offset compensation. A resistor with a nominal value of 390 $\Omega$ was measured with the DC offset compensation turned on and off. The non-compensated measurement shows a strong drive level dependency, which is associated with a signal distortion during the admittance scans of RPC sensors. ....	34
Figure 21: shows the functionality of the baseline compensation. The red line shows the raw measurement data without any compensation. The baseline (blue line) is calculated out of the conductance values at the start and the stop frequency of the measurement. The green line shows the compensated conductance curve. ....	36
Figure 22 shows the disturbing effect of the transient phenomena. The transient phenomena influence the measurement results of the series resonance frequency and the quality factor. Only after a time delay at least $3 \tau$ the measurement results of the series resonance frequency and the quality factor are quite correct. ....	37
Figure 23: The noise of the admittance measurement results depends on the level of the measurement signal and the averaging value. To get different signal levels, four different resistors have been measured with the same kernel electronics. Each resistor has been measured with an increasing averaging value. At each averaging value the mean value ( $\mu$ ) and the standard deviation ( $\sigma$ ) of the admittance have been calculated out of 1000 measurements. $3\sigma/\mu$ is then the uncertainty of the admittance measurement results. Firstly, it can be seen that matching kernel electronics (match here for 150 Ohm) produce much less noise in the measurement results than mismatched kernel electronics. Secondly, the measurement results show that an averaging value greater than 100 does not further improve measurement accuracy. ....	39
Figure 24: Schematic overview of the resonance measurement process. ....	40
Figure 25: Schematic overview of the initialization of the resonance measurement. ....	42
Figure 26: Schematic drawing of the non-referenced single-ended mode of the DAQ device [20]. The input channels are signals referenced to AISENSE. ....	44
Figure 27: Schematic overview of the frequency scan loop in the resonance measurement process. ....	48
Figure 28: Nassi-Shneiderman diagram of the stop condition for the dynamic step width calculation algorithm. The stop condition is true if the frequency scan has reached the stop frequency. The scan direction is also taken into account. The output is either a true stop condition or the next frequency value. ....	52
Figure 29: Nassi-Shneiderman diagram of the dynamic step width calculation algorithm. In the first 15 runs of the frequency scan loop the step width calculation is done linearly. If more than 15 previous measurement values are available, the conductance noise is calculated as mean value of the last 15 conductance changes. The conductance difference from the last to the current measurement is then compared to this noise level. If the conductance difference exceeds four times the noise level, the step width is reduced to improve measurement precision. Otherwise, if the conductance is still within the noise level, the step width is increased to speed up the measurement. After checking if the stop condition is already fulfilled, the output values are the parameters for the next admittance data acquisition. ....	54
Figure 30: Schematic overview of the resonance evaluation in the resonance measurement process. ....	55
Figure 31: Nassi-Shneiderman diagram of the Calculate Aspect Ratio function. This function calculates the scaling for the graph, that displays the locus of admittance. For the locus of admittance being displayed as a circle, the graph must be quadratic and both axes must have the same scaling. The <i>Border</i> parameter determines the border around the locus-circle (in percent of the calculated scaling range). ....	58
Figure 32: Screenshot of the user interface of the QxSens resonance measurement program. ....	59
Figure 33: Comparison of the measurement systems with a QV-torsion sensor at 55 kHz. The conductance spectrum was measured of the dry sensor. The low conductance level causes spurious effects of the parallel capacitance. This is the reason for the noise in the Agilent 4395A measurement. The cable compensation of the <i>QxSens</i> system reduces the parallel capacitance and therefore the conductance spectrum measured with the <i>QxSens</i> system shows nearly no noise. ....	66
Figure 34 shows the susceptance spectra of the QV-torsion measurement in air ( $f_s=55$ kHz). The shape of the susceptance curves obtained with both measurement systems is the same, only the Agilent 4395A curve is shifted due to spurious effects coming from the parallel capacitance of the connection cable from the kernel electronics to the sensor. This shift leads to a higher noise of the admittance values. The cable	

compensation compensates this shift in the <i>QxSens</i> system. This improves the S/N ratio. The resonance evaluation, giving $f_s$ and $Q$ , is not disturbed by the susceptance shift.....	67
Figure 35: Measurement results of the QV-torsion sensor at 55 kHz immersed in acetone. The damping of the sensor as well as its motional resistance are increased. Therefore the conductance values are much lower than in air. The lower conductance level leads to very high noise in the Agilent 4395A measurement. The <i>QxSens</i> system with the cable compensation still gives precise measurement values. A higher averaging in the Agilent 4395A measurement would decrease the noise, but increase measurement time in comparison to the <i>QxSens</i> measurement time. ....	69
Figure 36: Comparison of the conductance of the QV-torsion sensor at 55 kHz immersed in acetone and oil, respectively. The much higher viscosity of the oil decreases the conductance maximum to 20% of the conductance maximum in acetone. Nevertheless, the <i>QxSens</i> system gives precise measurement results even at very low admittance values. The data displayed are the raw measurement data without any fitting or smoothing. ....	70
Figure 37: The conductance peaks obtained from the QV-shear sensor at 2.7 MHz show a very clear signal. Both peaks match in height and half width. The small difference in the series resonance frequency comes from the absolute frequency of the synthesizer in the <i>QxSens</i> system. It becomes visible because of the high frequency resolution of this measurement. The half width is only 10 Hz.....	71
Figure 38 shows the conductance spectra of the QV-shear sensor in acetone. Both measurements give comparable results concerning series resonance frequency and quality factor. The small shift of the conductance baseline is caused by the different configurations of the measurement systems. But this shift does not influence the resonance evaluation.....	72
Figure 39 shows the susceptance curves of the QV-shear measurement in acetone. The shift of the Agilent 4395A curve is again caused by the parallel capacitance of the sensor cable. This shift has no effect on the evaluation of the locus of admittance but it decreases the signal-to-noise ratio. In the <i>QxSens</i> system the cable compensation compensates the effects of the cable and therefore improves the S/N ratio. ....	73
Figure 40: The conductance spectra of the QV-shear sensor, with a series resonance frequency of 2.7 MHz, immersed in oil. At this very small admittance level the spurious effects of the parallel capacitance can be observed clearly. The Agilent 4395A, which has no cable compensation, shows a very noisy signal. In contrast to this, the <i>QxSens</i> system with the cable compensation shows a much smoother conductance curve. Besides the noise, both systems give essentially the same results for the series resonance frequency and the quality factor. The small shift between the conductance spectra is caused by different system configurations and does not influence the resonance evaluation.....	74
Figure 41: Comparison of the conductance spectra of a QV-shear sensor in air and in oil, respectively. Both measurements were done with the same hardware setup. The graph shows the big change of half width and conductance with increasing viscosity. It also shows the impressive ability of the <i>QxSens</i> system to measure a big dynamic range concerning frequency resolution and admittance with just one hardware setup. ....	75
Figure 42 shows an excellent overlap of the conductance curves obtained with the Agilent 4395A and the <i>QxSens</i> system, respectively. The range of 6 MHz is an optimal frequency range for both measurement systems. This is also the reason for the almost noise-free measurement results. The zoom shows the exact matching of both measurement systems near the series resonance frequency.....	76
Figure 43: The conductance spectrum of a QV-shear sensor at 6 MHz immersed in oil. The Agilent 4395A curve shows a worse S/N ratio than the <i>QxSens</i> curve. This is due to the cable compensation that is only available for the <i>QxSens</i> system. The high damping of the oil decreases the admittance level so much that the spurious effects of the cable capacitance become noticeable.....	77
Figure 44: Comparison of the conductance spectra of a standard oscillating quartz crystal with a nominal series resonance frequency of 15 MHz. Both measurement systems give clear measurement results. The difference in the series resonance frequency and the height of the conductance peak comes from the absolute error of the <i>QxSens</i> synthesizer and from the fact, that the sensor was connected directly to the Agilent 4395A, but with a cable to the <i>QxSens</i> system. ....	78
Figure 45: Comparison of the Agilent 4395A with the <i>QxSens</i> system measuring a QT sensor at 29 MHz. Both measurement systems show a very high signal-to-noise ratio and a good match of the measured half width. The absolute error of the synthesizer and the influence of the cable, that is only used with the <i>QxSens</i> system, are the reasons for the small frequency difference and the different heights of the conductance peaks. ....	79

Figure 46: Nassi-Shneiderman diagram of the Peak Tracking Measurement. The PTM first searches a peak in the whole frequency range. Once the peak was found, the system tracks the peak.....	82
Figure 47: Nassi-Shneiderman diagram of the Auto Ranging Procedure. The ARP calculates the frequency interval that must be measured in order to keep track of a moving resonance peak. ....	86
Figure 48: Nassi-Shneiderman diagram of the Optimized Peak Search. The OPS finds a resonance peak by means of a pendulum search starting at the last known series resonance frequency. ....	88
Figure 49: Example, showing how the Peak Search works. On top of the picture the whole frequency range is shown, limited by $f_{min}$ and $f_{max}$ . The last measured series resonance frequency $f_{s\ meas}$ and the current series resonance frequency $f_{s\ curr}$ are marked. The Peak Search starts the search at $f_{s\ meas}-3HW$ , where $HW$ is the half width of the peak. The 3 $HW$ are needed for the peak to be detected when it is exactly at $f_{s\ meas}$ . The Peak Search scans the tenth part of the whole measurement range in one scan. After the first scan the search jumps back to the minimum of the already searched frequency range $f_{meas\ min}$ . In addition to the 3 $HW$ the maximum change of the measurand during the 1 <sup>st</sup> scan is also factored in the start frequency of the 2 <sup>nd</sup> scan $f_{meas\ min}+S\cdot T_s\cdot t_{passed}+3HW$ , where $S$ is the sensitivity in [Hz/unit], $T_s$ is the maximum time slope of the measurand in [unit/s] and $t_{passed}$ is the time that one scan takes. The scan is done in the other direction and as no resonance is found, the search jumps to the maximum of the already measured frequency range regarding the same factors as in the 2 <sup>nd</sup> scan, now $f_{meas\ max}-S\cdot T_s\cdot t_{passed}-3HW$ . In this example the resonance is found in the 3 <sup>rd</sup> scan. The Peak Search was successful and is terminated. .	92
Figure 50: Schematic drawing of the temperature measurement process. ....	96
Figure 51: User interface of the QT Measurement program. ....	99
Figure 52: Exemplary temperature measurement result obtained with a 29 MHz quartz crystal sensor (QT) and a 6 MHz gallium-orthophosphate crystal sensor (GT). The blue line shows the temperature step function that was applied to the sensors. The responses of the sensors show different time-constants, that are due to the different sensor constructions.....	100
Figure 53: Flow between two parallel plates. The plate on top is moving parallel relative to the bottom plate. Between the two plates there is the liquid, whose viscosity should be measured. ....	101
Figure 54: Schematic overview of the QV sensor calibration. ....	103
Figure 55: Continuous functions for the density and viscosity are calculated out of the discrete density and viscosity data of the calibration oils. A linear function is fit into the density data and a fit in Vogel's equation is used for viscosity. The fit results for the calibration oil S200 are displayed in this graph. ...	104
Figure 56: The measurement results of two calibration measurements with the KN334 QV sensor from Flucon in an S20 (red) and an S200 (cyan) calibration oil. The overall calibration function (blue) was calculated using (58). In the zoomed window the transfer from one calibration function to the other can be seen in more detail. ....	106
Figure 57: Three sensors mounted in a specially developed metal housing, that is put in a water bath. This measurement system is used for calibration of QV sensors.....	107
Figure 58: User interface of the QV Calibration software. ....	107
Figure 59: Time behaviour of the oil temperature in a calibration measurement in temperature scan mode. The temperature scan goes from 20 to 80°C in steps of 10°C. At each temperature step, calibration measurements are done. The detailed view at 40°C shows the stability of the oil temperature during the calibration measurement. ....	109
Figure 60: Measurement result of a temperature compensation measurement in air. The QV sensor KN334 was put in an oven at 100°C. The series resonance frequency was measured during the cooling phase using the QV calibration software in continuous mode. ....	110
Figure 61: Measurement results of calibration measurements with a KN334 QV sensor in S200 calibration oil. First the oil was heated up in a temperature scan. Calibration measurement have been done every 10°C from 10 to 90°C. Then the heating was turned off and the calibration software was used in continuous mode during the cooling. ....	111
Figure 62: User interface of the VogelGleichung&SensCalib application. ....	112
Figure 63: User interface of the Functionstep program. ....	115
Figure 64: Schematic overview of the viscosity measurement process. ....	116

Figure 65: Schematic drawing of the viscosity measurement process with one QV sensor .....	117
Figure 66: User interface of the QV measurement program .....	120
Figure 67: Viscosity measurement result for Castrol SAE 15W40 motor oil measured with a KN334 QV-torsion sensor from Flucon. The oil was heated up to 83°C. During the cooling phase, down to 20°C, the viscosity-density product was measured continuously. ....	122
Figure 68: Viscosity measurement result for viscose from Lenzing AG, Austria, measured with a KN370 QV-torsion sensor from Flucon. The viscose was heated up to 45°C. During the cooling phase, down to 20°C, the viscosity-density product was measured continuously. ....	123

# List of tables

Table 1: Device names used in the automatic NI DAQ device detection. ....	41
Table 2: Analog Input channels (AI) .....	43
Table 3: Error messages that can occur in the resonance measurement program. ....	64
Table 4: Comparison of the measurement results of a QV-torsion sensor at 55 kHz measured with the <i>QxSens</i> measurement system and the Agilent 4395 A device. ....	67
Table 5: Possible status messages of the QV Calibration software. ....	110
Table 6: Possible status messages of the QV measurement software. ....	121

# List of references

- [1] E. Benes and M. Gröschl, "Piezoelektrische Resonatoren als Sensorelemente," *e&i Elektrotechnik und Informationstechnik*, vol. 112, pp. 471-483, 1995.
- [2] "Fifth Framework Programme - 1386. Multi-channel measurement and control system based on resonant piezoelectric crystal sensors (QXSENS)," Office for Official Publications of the European Communities, 6.8.2007, <[http://cordis.europa.eu/data/PROJ\\_FP5/ACTIONeqDndSESSIONeq112242005919ndDOCEq1386ndTBLeqEN\\_PROJ.htm](http://cordis.europa.eu/data/PROJ_FP5/ACTIONeqDndSESSIONeq112242005919ndDOCEq1386ndTBLeqEN_PROJ.htm)>
- [3] K. S. Van Dyke, "The electric network equivalent of a piezo-electric resonator," *Phys. Rev.*, vol. 25, pp. 895, 1925.
- [4] "Measurement of quartz crystal unit parameters - Part 5: Methods for the determination of equivalent electrical parameters using automatic network analyzer techniques and error correction," CEI/IEC Standard No. 444-5, 1995.
- [5] R. J. Williamson, "An improved method for measuring quartz crystal parameters," *IEEE Transactions on Ultrasonics, Ferroelectrics, and Frequency Control*, vol. 34, pp. 681-689, 1987.
- [6] M. Schmid, E. Benes, and R. Sedlaczek, "A computer-controlled system for the measurement of complete admittance spectra of piezoelectric resonators," *Meas. Sci. Technol.*, vol. 1, pp. 970-975, 1990.
- [7] "Dithering," National Instruments Knowledge Base, 6.8.2007, <<http://zone.ni.com/devzone/cda/tut/p/id/5355#toc5>>
- [8] "Can I Enable Dithering On a 16-bit E Series DAQ Device?," National Instruments Knowledge Base, 6.8.2007, <<http://digital.ni.com/public.nsf/allkb/41B0890ABC09B0CB86256B92007E64F5>>
- [9] L. Spassov, V. Georgiev, L. Vergov, N. Vladimirova, V. Drobin, and N. Agapov, "Thermosensitive quartz resonators at cryogenic temperatures," *Sensors and Actuators A*, vol. 62, pp. 484-487, 1997.
- [10] P. W. Krempf, C. Reiter, W. Wallnöfer, and J. Neubing, "Temperature sensors based on GaPO<sub>4</sub>," presented at IEEE Ultrasonics Symposium 2002, München, Germany, 2002.
- [11] E. Benes, R. Thalhammer, M. Gröschl, H. Nowotny, and S. Jary, "Viscosity sensor based on a symmetric dual quartz thickness shear resonator," presented at 2003 IEEE International Frequency Control Symposium / 17th European Frequency and Time Forum, Tampa, Florida, USA, 2003.
- [12] "IEEE Standard on Piezoelectricity," ANSI/IEEE Standard No. 176, 1987.
- [13] R. Thalhammer, S. Braun, B. Devcic-Kuhar, M. Gröschl, F. Trampler, E. Benes, H. Nowotny, and M. Kostal, "Viscosity sensor utilizing a piezoelectric thickness shear sandwich resonator," *IEEE Transactions on Ultrasonics, Ferroelectrics, and Frequency Control*, vol. 45, pp. 1331-1340, 1998.
- [14] R. Schnitzer, "Development of a microprocessor controlled multi-channel measurement system for resonant piezoelectric sensors," Doctoral Thesis, Vienna University of Technology, 2006.
- [15] W. P. Mason, "Measurement of the viscosity and shear elasticity of liquids by means of a torsionally vibrating crystal," presented at Trans Am. Soc. Mech. Eng., 1947.
- [16] A. J. Matheson, *Molecular Acoustics*. London, Toronto, New York, Sydney: Wiley-Interscience, 1971.
- [17] B. Bode, "Entwicklung eines Quarzviskosimeters für Messungen bei hohen Drücken," Doctoral Thesis, Technischen Universität Clausthal, 1984, pp. 120.
- [18] "LEMO - special cables and fibre optic cables," LEMO Elektronik GmbH, Munich 2000.

- [19] "TE5100 Programming Manual," Team Solutions., 8.8.2007, <<http://www.team-solutions.com/Products/PXIcPCI/TE5100/TE5100%20Programming%20Manual.pdf>>
- [20] "Ground Loops and Returns," National Instruments Knowledge Base, 6.8.2007, <<http://zone.ni.com/cms/images/devzone/tut/a/7f48553b915.gif>>
- [21] R. Schnitzer, M. Gröschl, L. Spassov, K. Paskalev, and E. Benes, "Temperature sensitive quartz crystals for high precision dew point hygrometry," presented at 2nd Congress of Alps-Adria Acoustics Association and 1st Congress of Acoustical Society of Croatia, Opatija, Croatia, 2005.
- [22] R. A. Baeza- Yates, J. C. Culberson, and G. J. E. Rawlins, "Searching in the plane," *Information and Computation*, vol. 106, pp. 234-252, 1993.
- [23] A. Cameron and C. Ettles, *Basic lubrication theory*. 3rd edition, Chichester, UK: Ellis Horwood, 1981.

# Curriculum vitae

**Name:** Thomas Kliche  
**Date of birth:** 25.12.1975  
**Place of birth:** Vienna, Austria



## **Education:**

1982-1985 Elementary school in Biedermannsdorf  
1986-1994 Secondary school in Moedling  
1994-2008 Study of technical physics at the Vienna University of Technology

## **Employment:**

06/1994-12/1999 Part time work as software developer at Erste Bank, Vienna  
since 01/2000 Software developer and project manager at s IT Solutions, Vienna